7 SIMPLE THIN LENS OPTICAL SYSTEMS

7.1 INTRODUCTION

7.1.1 Thin lens solution. The first two steps in designing optical systems, which will be discussed further in Section 9 , are (1) selecting lens types for the various elements, and (2) finding a first order solution assuming thin lenses. The methods and procedures used in step (2) were developed in Section 6. In Section 7 the optics of several thin lens optical systems will be described to illustrate the usefulness of the paraxial equations and to indicate the reasoning a designer uses in following step (1). With information obtainable from only paraxial ray data, a designer can conclude many of the important features needed for a final design. There are numerous discussions in text books of simple optical systems such as the microscope and the telescope. The following discussion, assuming that the reader has read some explanation of these systems, will concentrate on the numerical analysis.

7.1.2 Optical systems used with the eye. The optical systems considered in this section are all used with the human eye. Because of this the eye is an integral part of the system and must be considered in the design. There are four basic types of lenses: (1) microscope objectives, (2) telescope objectives, (3) eyepieces and (4) photographic objectives. The first three are used with the human eye and systems employing these types are discussed in Section 7.

7.2 THE SIMPLE MAGNIFIER

7.2.1 A single lens. One of the simplest of optical devices is the simple magnifier. A single positive lens works as a magnifier because it makes an object appear to subtend a larger angle at an observer's eye than is possible with the unaided eye. Without a magnifier, an observer can make an object appear larger only by bringing it close to his eye. As an object is moved closer and closer to an observer's eye it is necessary for the eye to increase its refractive power in order to continue to focus the image on the retina. There is a minimum distance V at which the eye has increased its refractive power to its maximum capability. For object to eye distances less than V the image will no longer be sharply focussed on the retina. For the standard observer this distance V is approximately 10 inches or 250 mm (V is always considered positive). Therefore, in order to make the object appear still larger, it is necessary to add refractive power to the eye, so that the object may in effect be brought closer. The magnifier provides the extra refractive power required.

7.2.2 Magnifying power. The magnifying power of a visual instrument may be defined as

$$MP = \frac{\text{size of retinal image obtained with instrument}}{\text{size of retinal image obtained with the unaided eye}}$$

In the region of the paraxial approximation this is equivalent to the definition, $MP = \beta/\alpha$ where β equals one half the angle subtended by the object as seen through the instrument, and α equals one half the angle subtended by the object as seen by the naked eye. (These particular definitions of α and β assume that the object and image are centered with respect to the optical axis. This is usually the case with visual instruments. According to this assumption, when reference is made to "an object $\bar{y}_o$," the object height is rigorously $2\bar{y}_o$.) β is called the half image field angle, and α is called the half object field angle. Magnifying power, then, is the ratio of the field angles.

7.2.3 Diagram of a single lens magnifier. In Figure 7.1 (a) an object $\bar{y}_o$ is shown viewed with the unaided eye. Figure 7.1 (b) shows the same object viewed by a single lens magnifier. The eye is placed at a distance d from the lens. The object is placed in relation to the lens so that the visual image $\bar{y}_k$ lies to the left of the eye at a distance, A. (A is negative). For the eye to focus on the image, A must be numerically equal to or larger than V. The numerical formulation of this problem may be handled with simplicity by the usual methods adequately covered in most text books. In the following analysis, it will be handled formally using the ray trace format in order to illustrate a method of analysis which can be used for any system, regardless of its complication.

7.2.4 Ray trace format.

7.2.4.1 The system consists of an object plane, an entrance pupil plane, a thin lens, an aperture stop and exit pupil, and a final image plane. Table 7.1 contains a layout of a computation sheet for this simple magnifier system. The data may be filled in as follows. First, all the ϕ values are zero except that of the lens. We also know that $y_o = 0$ and we may choose to trace a paraxial ray at any angle from the point $y_o = 0$.

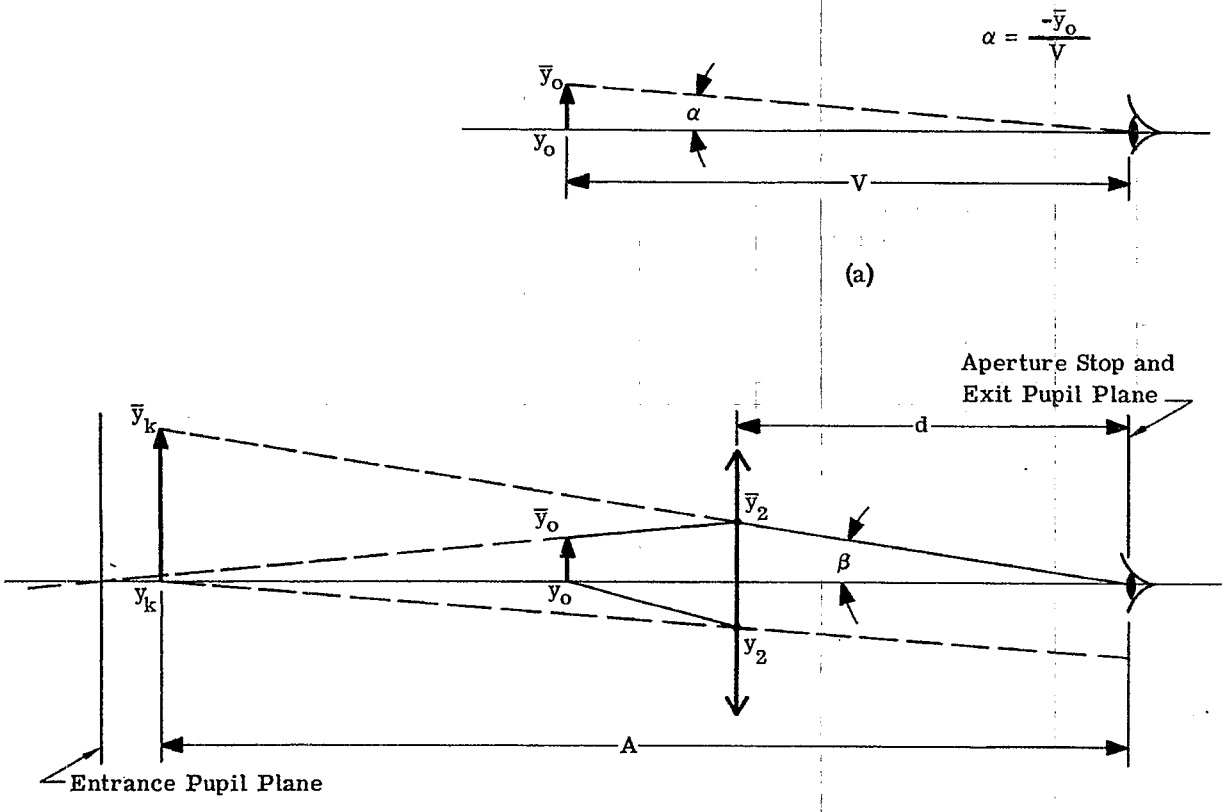

Figure 7.1 - Diagrammatic illustration of a single lens magnifier.

	Object	Entrance Pupil Plane	Lens	Exit Pupil Plane	Image Plane
Surface	0	1	2	3	4
$-\phi$	0	0	$-\phi$	0	0
t		$-\bar{y}_o/\beta(1-d\phi)$	$-d/(1-d\phi)$	d	A
y	0	$A/(1-d\phi)(d+A)$	1	$A/(d+A)$	0
u		$\left[\phi - \frac{1}{d+A}\right]$	$\left[\phi - \frac{1}{d+A}\right]$	$-1/(d+A)$	$-1/(d+A)$
$\bar{y}$	$\bar{y}_o$	0	$-d\beta$	0	$\bar{y}_k$
$\bar{u}$		$\beta(1-d\phi)$	$\beta(1-d\phi)$	β	β

Table 7.1 - Computation sheet for a simple magnifier

Therefore, we elect to make $y_2 = 1$. (Figure 7.1 (b) shows y_2 negative; this has been so done for pictorial clarity). The system has only two physical stops, the lens and the eye pupil. One of these is the aperture stop. To find which one, we can image each stop in the system preceding it, and see which image subtends the smallest angle at the base of the object, $y_o = 0$. The image of the lens in the lens is of magnification unity and is at the lens; hence if the size of the lens and its distance from the object is known, the angle subtended can be found. Likewise if the eye pupil size and location is known, its image in the lens can be determined, and the angle subtended by this image compared with the previous angle. We see, therefore, that which of the two stops is the aperture stop depends on the size and location of the two elements, i.e. on the design of the system. In such systems it is usual to assume that the lens is so much larger than the eye pupil that the latter is the aperture stop. Hence it is also the exit pupil. Therefore we can fill in d, the distance from the lens to the aperture stop plane, and A the distance from the aperture stop plane to the final virtual image plane. Since $y_k = 0$ and $u_2 = u_3$ (no refraction occurs at surface 3), it can be concluded that $u_2 = u_3 = -1/(d + A)$. With y_2 and u_2 known it is possible to calculate u_1 from equation 6-(24). Then $u_1 = \phi - 1/(d + A)$. Also $u_o = u_1$.

7.2.4.2 The oblique principal ray may now be traced backward through the system from the center of the exit pupil. Let this go back at the angle β with the optical axis. $\bar{y}_2$ is now determined as $-\beta d$. $\bar{u}_1$ and $\bar{u}_o$ are also determined. Knowing $\bar{y}_o$, $\bar{y}_1$, $\bar{y}_2$, $\bar{u}_o$ and $\bar{u}_1$, t_o and t_1 may be computed. Since all the spaces are now determined y and u are known on every surface for each ray.

From Equation 6-(7),

$$\bar{y}_k = \bar{y}_o \frac{u_o}{u_{k-1}} .$$

Therefore,

$$\bar{y}_k = \bar{y}_o \left[1 - \phi (d + A) \right] .$$

Since

$$\beta = \frac{\bar{y}_k}{A} \quad \text{and} \quad \alpha = - \frac{\bar{y}_o}{V} ,$$

$$MP = - \frac{V}{A} \left[1 - \phi (d + A) \right] . \qquad (1)$$

7.2.5 Analysis of magnifying power equation. There are several cases of special interest which should be noted.

a) If $A = - \infty$

$MP = V \phi$

b) If $d = f' = \frac{1}{\phi}$

$MP = V \phi$

c) If $A = - V$ with $d = 0$

$MP = 1 + V \phi$.

One can see by inspection of these equations, that $MP = V/f'$ is the minimum magnifying power and $MP = (V/f') + 1$ is the maximum. Hence for maximum magnifying power, the final image is at the near point of the eye, a distance V from the eye. Therefore the eye has maximum refractive power. For the relaxed eye, the image is at the far point; this is ∞ for the normal eye and results in a minimum magnifying power. The relative increase in magnifying power, as the eye accommodates for smaller A, is small and offset by the greater likelihood of eye strain. (For a typical magnifier of 1 inch focal length, the maximum magnifying power is only 10% higher than the minimum). Therefore simple magnifiers should be designed and used so that the final image is at infinity, or at the far point of the eye, if these cases differ.

7.3 THE MICROSCOPE

7.3.1 Limitations of a simple magnifier. It is clear from Section 7.2.5, that for large magnifying power, ϕ must be large, hence the focal length, f', must be small. Because the final image is to be at infinity, the object must be at F_1. Therefore for large magnifying power, the object must be placed very close to the lens. By Equation 6-(22) we see that the lens surfaces must have very short radii, and therefore the diameter of the lens will be small. Because it was assumed that the eye pupil was the aperture stop, for the case of the simple magnifier, the only other stop in the system, namely the lens, is the field stop. Whereas the aperture stop limits the bundle of rays traversing the system, the field stop (a physical stop) limits the field of view. Hence a small diameter magnifying lens means a small object field.

7.3.2 The simple microscope. A practical method of overcoming the limitations of the simple magnifier is to use a relay lens as shown in Figure 7.2. While the object is being relayed it may also be magnified. The magnifying power of the microscope is then the product of the lateral magnification of the objective and the magnifying power of the eyepiece. As with the magnifier, it is advisable to adjust the microscope so that the final virtual image is at ∞; the microscope is then in afocal adjustment. In this case the eyepiece magnifying power is $MP_e = V/f'_e$, and the magnifying power of the microscope may be written

$$MP = m_o \frac{V}{f'_e} \qquad (2)$$

where m_o is the lateral magnification of the objective. The focal length of the objective can, in principle, have any value. If the focal length is made long, the overall length of the system will also be long.

7.3.3 Paraxial ray trace. Table 7.2 contains the paraxial ray trace for a microscope with an objective focal length of 16 mm and an eyepiece focal length of 25 mm. In order to use the objective lens symmetrically, i.e. in order that the chief ray pass through the center of the lens, the entrance pupil is placed in contact with the objective. The axial ray is traced from the object at an angle of 0.25. This corresponds to the sine of the angle of the actual ray to be traced through the system. This paraxial ray then passes through the optical system at very nearly the same heights as an actual true ray. As discussed in Section 23, the resolving power of a microscope depends on the wavelength and a quantity called the numerical aperture, or N.A. The numerical aperture $= n_o \sin U_o$. Since the object space has an index of $n_o = 1$, the system, as laid out, has a numerical aperture of 0.25. The chief ray was traced through the entrance pupil from an object height $\bar{y}_o = 1.0$. From this trace the exit pupil is found to lie 28.55 to the right of the lens (b).

7.3.4 Aperture stop and pupils. It is now possible to gather information about the pupils of this system from these paraxial rays. One can read directly from the table that the radius of the exit pupil is 0.625. Since the calculations are made in millimeters, the exit pupil is therefore 1.25 mm. In order that this exit pupil be the true exit pupil of the system, it is necessary to have the pupil of the observer's eye located fairly centrally in this exit pupil plane. Since the normal eye pupil is approximately 2 mm in diameter, the microscope exit pupil will definitely be the exit pupil of the entire microscope - eye system. The objective is the aperture stop and the entrance pupil of the system.

7.3.5 The f - number. The f - number of a lens (always considered positive) is defined as f/D where D is the diameter of the lens. It is very useful to calculate this quantity because from it one can estimate the difficulty of optically correcting the lens for image errors. Equation 6-(24) gives a relation between f and y for a thin lens. From this equation then, assuming $y = D/2$,

$$f \text{ - number} = 0.5/|\Delta u| .$$

In Table 7.3 the f - numbers for the objective and eyelens are listed for both the axial and oblique rays.

7.3.6 Difficulties in designing the eyepiece. The lenses should have sufficient diameter for the smallest f - number in each case. Therefore the objective should have an f - number of 1.82 and the eyepiece an f - number of 1.09. Figure 7.3 (a) shows a picture of an $f/1$ lens. This is an extremely fat lens and the chief ray would strike the curved surfaces at very large angles of incidence. The large angles of incidence introduce appreciable aberrations and the paraxial assumptions no longer hold. Hence the image at $\bar{y}_k$ would not be near the position predicted by first order theory. This lens is also uncorrected for color. Since correcting for color has the effect of approximately doubling the power of the positive element if the total power is to remain constant - because of the necessary addition of a negative element - one can see that it would be out of the question to color correct this lens. Therefore, it is clear that it will not be practical to use a single lens eyepiece. Either the size of the object will have to be reduced considerably, thereby reducing $\bar{u}_4$ and hence increasing the f - number, or several lenses will have to be used for the eyepiece.

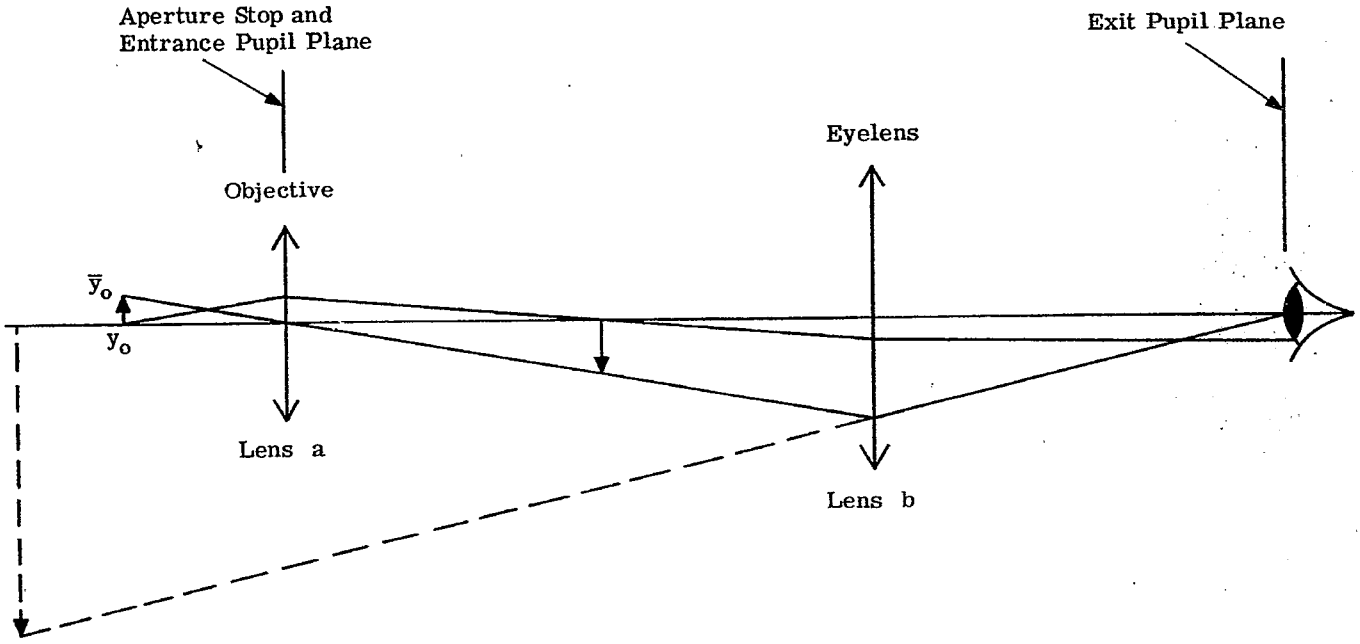

Figure 7.2 - The simple microscope. Lens (a) is the relay lens.

Surface	Object Plane 0	Entrance Pupil 1	Objective (a) 2	First Image Plane 3	Eyelens (b) 4	Exit Pupil Plane 5
$-\phi$	0	0	-0.0625	0	-0.04	
t	17.6	0	176.0	25.0	28.55	
y	0	4.4	4.4	0	-0.625	-0.625
u	0.25	0.25	-0.025	-0.025	0	
$\bar{y}$	1.0	0	0	-10.00	-11.42	0
$\bar{u}$	-0.0568	-0.0568	-0.0568	-0.0568	0.400	
ν_{F-C}	∞	∞	60	∞	60	
a	0	0	-0.02017	0	-0.00026	Σ a = -0.02043
b	0	0	0	0	-0.00476	Σ b = -0.00476
α TAch						= 0.0327
α Tch						= 0.0076

Table 7.2 - Calculations on a simple afocal microscope. All lengths are in mm.

	Axial Ray	Oblique Ray
Objective Lens	1.82	∞
Eyelens	20	1.09

Table 7.3 - f - numbers of lenses shown in Table 7.2.

7.3.7 Chromatic aberrations of a simple afocal microscope.

7.3.7.1 Before deciding which of these alternatives is preferable, consider the calculation for axial and lateral color for the system shown in Table 7.2. Since this is an afocal system, the axial beam emerges parallel to the axis, and $u_{k-1} = 0$. Under this condition, it is not possible to use Equations 6-(37) and 6-(38), for the color surface contributions. When $u_{k-1} = 0$ it is necessary to substitute the differential du from Paragraph 6.10.2.2 into Equation 6-(33) and obtain the following equations for the angular chromatic aberrations,

$$d u_{k-1} = \alpha \; TAch = \frac{1}{y_k \; n_{k-1}} \sum_{j=1}^{j=k-1} a \qquad (3)$$

and

$$d\bar{u}_{k-1} = \alpha \; Tch = \frac{1}{y_k \; n_{k-1}} \sum_{j=1}^{j=k-1} b \qquad (4)$$

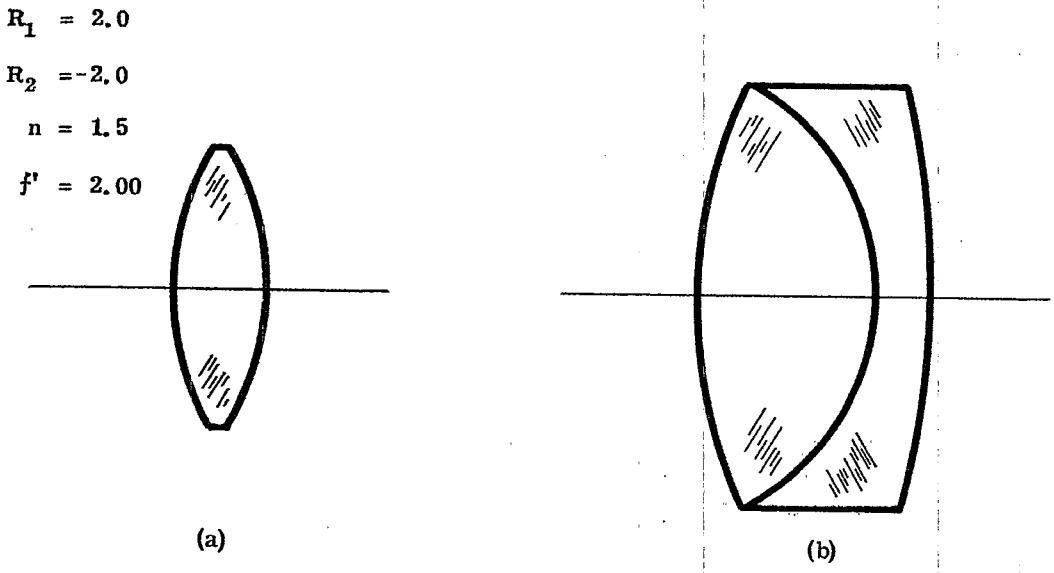

Figure 7.3 - (a) is an $f/1$ single lens; (b) is an $f/1.8$ achromatic doublet.

	Object Plane	Entrance Pupil Plane	Lens (a) Objective	Lens (c)	Lens (b)	Exit Pupil Plane
Surface	0	1	2	3	4	5
$-\phi$	0	0	-0.0625	-0.02662	-0.06662	0
t	17.6	0	151	30.02	8.571	
y	0	4.4	4.4	0.625	-0.625	-0.625
u	0.25	0.25	-0.025	-0.04164	0	
$\bar{y}$	1.0	0	0	-8.580	-3.428	0
$\bar{u}$	-0.0568	-0.0568	-0.0568	0.1716	0.400	
ν_{F-C}	∞	∞	60	60	60	
a	0	0	-0.02017	-0.00017	-0.00043	Σ a = -0.0208
b	0	0	0	0.00238	-0.00238	Σ b = 0
α TAch						0.0332
α Tch						0

Table 7.4 - Calculations on an afocal microscope with a double lens eyepiece. All lengths are in mm.

These equations are analogous to Equations 6-(37) and 6-(38). The results show that the simple microscope is afflicted with 0.0327 radians of axial color and 0.0076 radians of lateral color. Almost all the axial color is due to the objective. The lateral color is due entirely to the eyelens. The normal observer can detect as little as 0.0003 radians of color fringing assuming that the minimum angle of resolution is about 1' of arc. It is then clear that both the axial and lateral color exceed noticeable amounts of chromatic aberration.

7.3.7.2 The objective lens can be corrected for axial color by making it a doublet. Equations 6-(44) and 6-(45) are used to compute the powers of the separate components. Figure 7.3 (b) shows an $f' = 10$ objective with an f - number of 1.82. It turns out that these curves are again too sharp and the monochromatic aberrations will be difficult to correct. In order to correct the monochromatic aberrations then, it is necessary to flatten the surfaces by dividing the lens into two doublets, each working at $f/3.64$. To do this we divide the entire $|\Delta u| = 0.275$ into two equal parts, each of 0.1375. Each doublet will now work at the same f - number. This value of the f - number ($= 0.5/|\Delta u|$) will not necessarily equal the value for an infinite object ($= f'/D$).

7.3.7.3 The chromatic aberration in the eyelens can be corrected in the same way by splitting this lens into two lenses each working at $f/2.18$ and then by achromatizing each part. There is, however, another method which is sometimes used in eyepiece design. A single positive lens may be placed in front of the image plane 3 and adjusted to help refract the chief ray. For such a lens $\bar{y}$ and y will have opposite signs so according to Equation 6-(41) the lens should give a positive lateral color contribution. A lens such as this has been worked out in Table 7.4. The procedure for designing this system was as follows. The extra lens (c) was inserted to the left of the image plane at a position where $y_3 = 0.625$, the same value as the final height of the axial ray but of opposite sign. The chief ray was then traced to the (c) lens intersecting it at $\bar{y} = -8.580$.

7.3.7.4 Since this extra lens is to be used, it should help bend the chief ray. In Table 7.2 the chief ray was bent from -0.0568 to 0.400 by the (b) lens, a total bending of 0.4568. With the (c) lens added, the (b) and (c) lenses should each bend the chief ray by 0.2284. Therefore $\bar{u}_3$ between the (c) and (b) lenses should be 0.1716. This determines ϕ_3, the power of the (c) lens. With ϕ_3 known, u_3 is determined and then t_3 is set so that $y_4 = -0.625$. Thus ϕ_4 is defined. Now the lateral color contribution of a thin lens is proportional to $y\bar{y}\phi/\nu$. $\bar{y}\phi$ is equal to the bending $|\Delta\bar{u}|$ experienced by the chief ray. By making the (b) and (c) lenses refract the chief ray equally and by making $y_3 = -y_4$, the lateral color contributions of the (b) and (c) lenses exactly cancel each other since the ν-values are the

same. The axial color of the system is only slightly more under-corrected than the original system in Table 7.2. This chromatic aberration can be eliminated completely by introducing over-correction in the objective lens (a).

7.3.8 Additional effects of adding a field lens.

7.3.8.1 Lens (c) is referred to as a field lens of the eyepiece. (The introduction of a lens near the position of the image due to the objective increases the field of view.) This extra lens (c) has helped the system significantly. The (b) and (c) lenses are $f/2.18$ now and are far more reasonable lenses. There is at this point sufficient reason to expect that this microscope could be corrected to give good imagery. In Section 8 it will be shown that the monochromatic aberrations at an object height of $y_o = 1$ are rather large, so that the final optical design will probably have to have a smaller object field.

7.3.8.2 It should also be noted that the introduction of the (c) lens caused a marked reduction (by a factor of 3) in the distance between the eyelens and the exit pupil. In Table 7.4 this distance is only 8.57 millimeters. This distance, called the eye relief, is too short for comfortable viewing, so some other arrangement of lenses should be found. Without introducing a serious amount of lateral color the (c) lens could be designed with less power. The chief ray would then strike the (b) lens at a larger aperture resulting in an increased distance to the exit pupil. With an eyepiece of this type, the lateral and axial color for the object is fully corrected. However the eyepiece is not color corrected for the plane between the two lenses (b) and (c) where an intermediate image is formed. If cross hairs, or a reticle, is placed in this position it is in effect viewed only by the single eyelens. The reticle will be imaged with lateral color since the single lens is not achromatized. If a reticle is to be used, it is advisable to use an eyepiece that is also color corrected for the intermediate image plane.

7.4 THE TELESCOPE

7.4.1 General. A telescope may be considered as a special case of the microscope, with this slight difference. In the microscope, one compares the visual angle subtended by the image, as viewed through the instrument, with the visual angle subtended by the object at the unaided eye. It is assumed that the observer can place the object at the distance V from the eye. In the telescope it is assumed that the object is inaccessible to the observer. Therefore, in a telescope one compares the visual angles, assuming the observer is always at a fixed distance with respect to the object. This is illustrated in Figure 7.4.

7.4.2 Magnifying power. An object of height $\bar{y}_o$ is located a distance L from an observer. (L is always considered to be positive.) The angle α subtended by the object is $-\bar{y}_o/L$. With the instrument in place, the object is at a distance of z from the first focal point of the objective. A ray from the top of the object, $\bar{y}_o$, passing through the first focal point of the objective strikes the objective at a height $\bar{y}_1 = -\bar{y}_o f_o/z$. This ray then is parallel to the optical axis until it strikes the eyepiece. It then refracts to the second focal point of the eyepiece at an angle with the axis of $\beta = (y_o/z)(f_o/f'_e)$. If the eyepiece is adjusted so that $A = \infty$, or if the eye is located at the second focal point of the eyelens, then β is the apparent angle subtended by the object. Then,

$$MP = -\frac{f_o}{f'_e}\frac{L}{z} = m_o\frac{L}{f'_e} . \qquad (5)$$

This equation actually applies to the microscope by making $L = V$. If L becomes very large as it does for most applications in which telescopes are used, then L/z approaches 1 and, $MP = -f_o/f'_e$. This is the formula usually given for a telescope. At a value of L where L/z is not unity, the MP is increased. Thus it is possible to obtain a magnifying power greater than unity even if $f_o = f'_e$. This makes an interesting optical device. It has unit MP for objects at infinity but greater than unit MP for objects at finite distances.

7.4.3 Objective and eyepiece design. The optics of the objective and eyepiece for the telescope are similar to that of the microscope. The entrance pupil is usually placed at the objective. The eyepiece is usually split into two or more lenses in order to correct for the lateral color. The extra lenses also allow for a wider field of view than one could achieve with a single lens.

7.5 OPTICAL RELAY SYSTEMS. PERISCOPES

7.5.1 Image orientation.

7.5.1.1 In the case of the afocal magnifier, the expression for the MP is V/f'. Since V is always con-

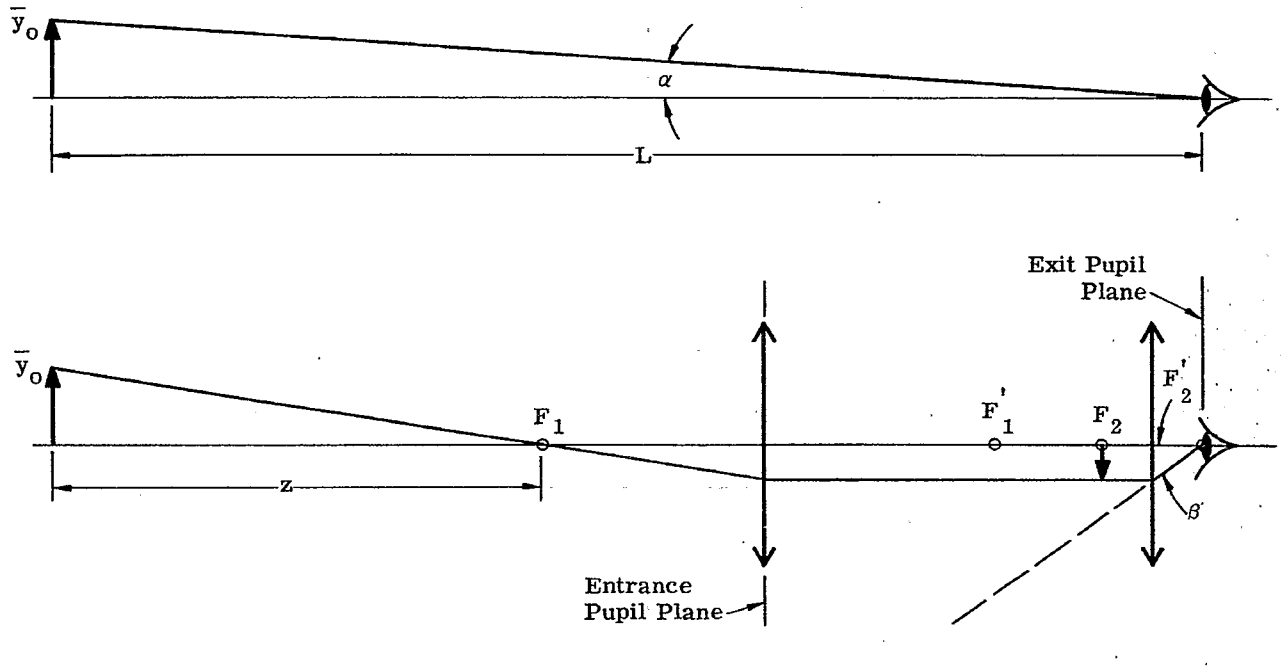

Figure 7.4. The optics of a simple telescope

sidered to be a positive number, the formula indicates that the MP is positive for a positive lens. Positive MP means that the virtual image is in the same orientation as the object.

7.5.1.2 Negative MP or negative magnification means that the image $\bar{y}_k$ is the negative of the object $\bar{y}_o$, in other words the object is inverted; if the optical system is a centered spherical optical system $\bar{x}_k$ will be the negative of $\bar{x}_o$. This means that the object $\bar{y}_o$ $\bar{x}_o$ appears as $\bar{x}_k$ $\bar{y}_k$. Or a letter R will appear as Я. The image is said to be inverted but right handed. This means it is upside down but readable. It appears as a normal R by turning the paper through 180° in its plane.

7.5.1.3 An erect, left-handed image, such as occurs in plane mirrors, would appear as Я. All left-handed images, whether erect or inverted, are unreadable by rotation in the plane only. Left-handed images are sometimes referred to as perverted images. Also see Section 13.

7.5.2 Image inversion for microscopes and telescopes. From Equations (2) and (5) it is seen that a simple microscope and telescope give a negative MP because m_o for an objective is negative. Therefore, these instruments provide a right-handed inverted image. In the microscope it seldom matters if the object is inverted, but in telescopes it is very disturbing to see turned upside down, objects which we are used to seeing erect. Therefore, for telescopes, some means for erecting the image is usually provided. This can be done using prisms or extra lenses. The use of prisms will be described in Section 13. A brief analysis of methods of image erection by lenses will be discussed in the next paragraph.

7.5.3 Image erection by lenses. It is possible to use a second objective in a microscope or telescope to re-image the first image before it is viewed by the eyepiece. This is illustrated in Figure 7.5. The magnifying power for such a system is given by the expression, $MP = m_1 \; m_2 \; L/f'_e$. This procedure can, of course, be carried on with several re-imaging stages if it is desirable to have a long system as in periscopic designs. Since L/f'_e is positive, and each m due to the relaying objectives is negative, it is clear then that if there are an odd number of real images, the MP is negative, while for an even number of real images the MP is positive. A positive overall MP means the image is erect and right-handed.

7.5.4 Field lenses for periscopes. Inspection of Figure 7.5 shows that the size of the object which may be seen through the instrument is definitely limited by the size and permissible f - number of the second

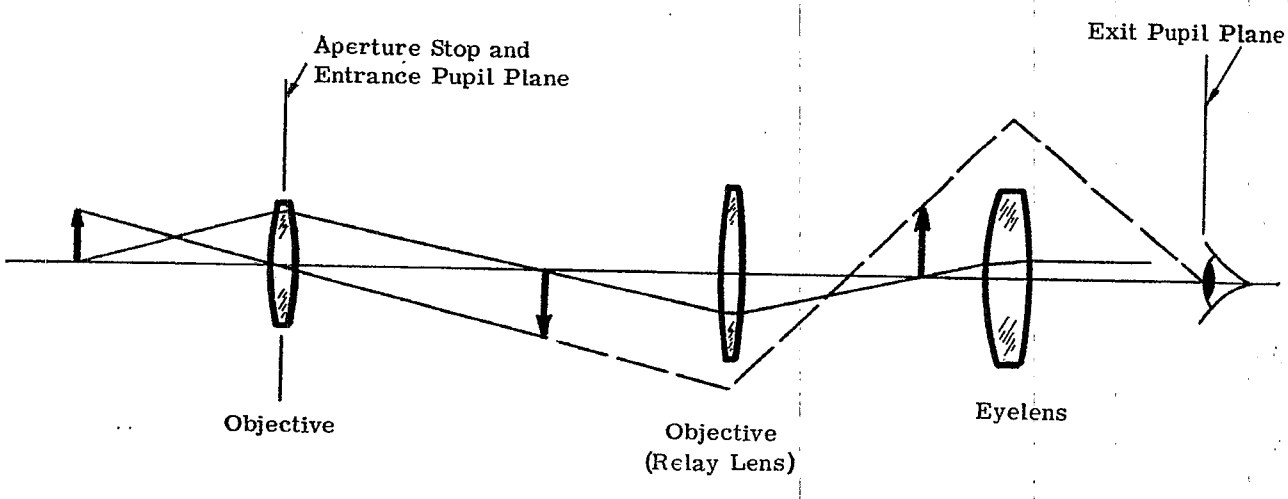

Figure 7.5 - An optical relay system or periscope.

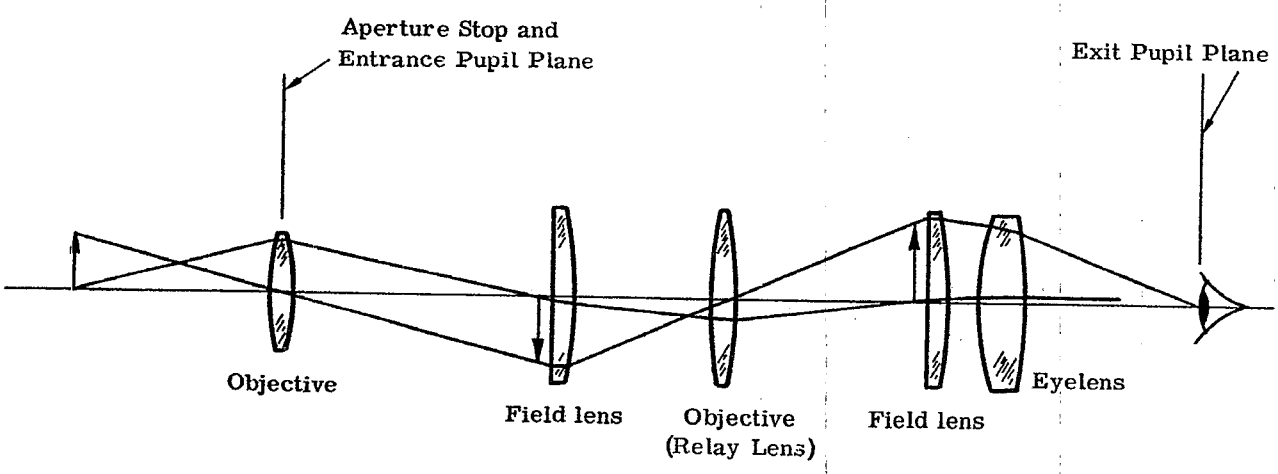

Figure 7.6 - A periscope with field lenses.

objective. The field of view can be increased significantly by introducing extra lenses to help refract the chief ray. This is the same situation described with the eyepiece in Table 7.4. Extra lenses can be introduced at the position of the objective or, if it is desirable to keep the diameter of the system small, the extra lenses can be added near the intermediate images. If the lenses are added near the intermediate images, and therefore referred to as field lenses, they act principally on the chief rays and their primary purpose is to help increase the field of view. Figure 7.6 shows an erecting telescope using field lenses to help increase the field of view.

7.5.5 Position of the aperture stop. The drawing (Figure 7.6) indicates that the first objective is the aperture stop. As drawn, the second objective (relay lens) is larger in diameter than necessary. It could be reduced until the axial ray passed through the margin of the lens, as it does at the first objective. If the diameter of the relay lens were further reduced, this lens would become the aperture stop and the first objective would be too large. In practice the diameters are adjusted so that both objectives are aperture stops.

7.6 THE GALILEAN TELESCOPE

7.6.1 Use of negative eyepiece. In the telescope with $f'_o \geq |f_e|$ it is possible to have a positive or negative focal length eyepiece. If the eyepiece focal length is negative, Equation (5) shows that the MP is positive. The image would therefore be erect. Such a system has very interesting possibilities. A sketch of a telescope of this type is shown in Figure 7.7.

7.6.2 Analysis of the simple Galilean telescope.

7.6.2.1 The exit pupil and aperture stop of this system is usually the pupil of the eye. The entrance pupil is actually located behind the observer's eye, and the size of the objective determines the size of the field of view. The objective is therefore the field stop. A system of this type is worked out in Table 7.5. The table shows the sizes and positions of the entrance and exit pupils. The object field of view (sometimes called the real field) $-\beta\phi_o/\phi_e$ depends on β. In order to obtain an image field of view (sometimes called the apparent field) of β, the $\bar{y}_2$ on the objective lens must be,

$$\bar{y}_2 = \beta \left[\text{MP}\, d - t_2 \right] .$$

Therefore, for a given diameter of objective lens, the field of view is determined.

7.6.2.2 For the case of $d = 0$, we have $\bar{y}_2 = -\beta t_2$. Since $f'_o/2\bar{y}_2 = (f\text{-number})_o$ at which the objective is working for the chief ray,

$$\beta = -\frac{f'_o}{2t_2\,(f\text{-number})_o}$$

and

$$\alpha = \frac{\beta}{\text{MP}} = -\frac{f'_o}{2\,\text{MP}\,t_2\,(f\text{-number})_o} .$$

For MP large compared to unity, the focal length of the objective is large compared to the focal length of the eyepiece. Assuming that $f'_o + f_e = t_2$ can be replaced by f'_o, we have

$$\beta = \frac{1}{2\,(f\text{-number})_o}$$

and

$$\alpha = \frac{1}{\text{MP}\,2\,(f\text{-number})_o} .$$

These equations show that for a large MP the field of view can be made large only by decreasing $(f\text{-number})_o$. For example, if MP = 10, then $\alpha = 0.05$ radian if the objective is $f/1$. An $f/1$ lens is very difficult to make. The usual doublet achromat would have only an $f/3$ aperture. For such a doublet objective $\alpha = 0.017$ radian or 0.95°. Then $\beta = 9.5°$, which is a very small apparent field of view.

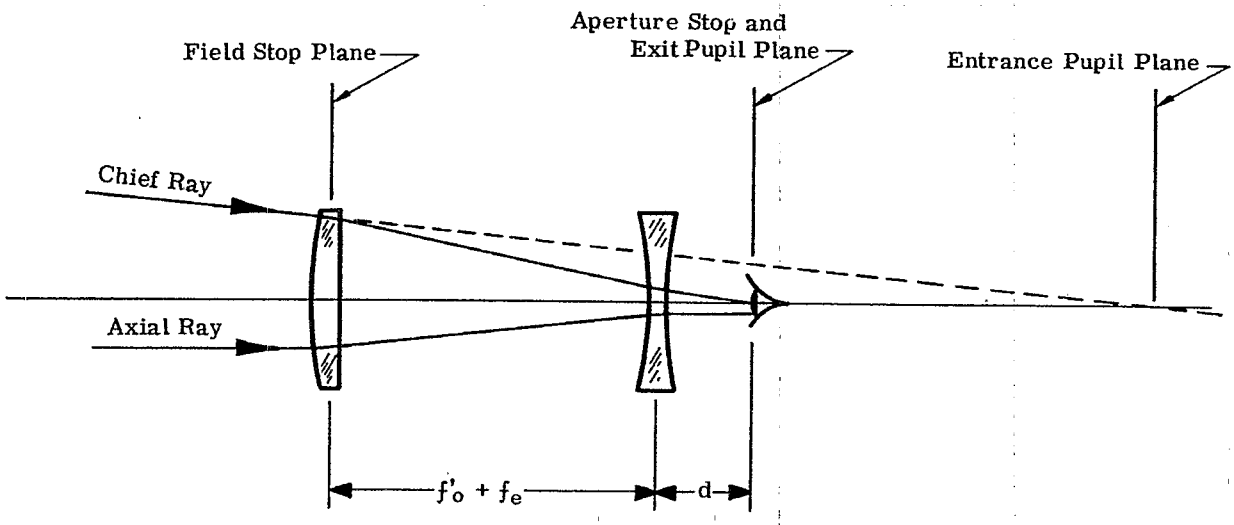

Figure 7.7 - The Galilean telescope

Surface	Object 0	Entrance Pupil 1	Objective 2	Eyepiece 3	Exit Pupil 4
$-\phi$	0	0	$-\phi_o$	$-\phi_e$	0
t		∞	$-MP\left[dMP - t_2\right]$	$(f'_o + f_e)$	d
y	0	$-r\,\frac{\phi_e}{\phi_o}$	$-r\,\frac{\phi_e}{\phi_o}$	r	r
u		0	0	$r\phi_e$	0
$\bar{y}$	∞	0	$\beta\left[dMP - t_2\right]$	$-d\beta$	0
$\bar{u}$		$-\beta\,\frac{\phi_o}{\phi_e}$	$-\beta\,\frac{\phi_o}{\phi_e}$	$\beta - \phi_e d\beta$	β

Table 7.5 - Calculations for a Galilean telescope.

8 ABERRATION ANALYSIS AND THIRD ORDER THEORY

8.1 SIGNIFICANCE OF RAY TRACE DATA

8.1.1 First order system.

8.1.1.1 In Sections 5, 6, and 7, formulae and techniques were presented to enable the designer to set up a first order optical system. As an aid in arriving at a final first order solution, it is customary to trace two paraxial rays. One of these starts from an object point on the optical axis and heads toward the tentative edge of the entrance pupil. The other ray starts from an object point at the tentative edge of the field and heads toward the tentative center of the entrance pupil.

8.1.1.2 The data from these two rays may be used to determine the trace of any other paraxial ray through the system. The magnification, focal length, and chromatic aberration may be calculated. The planes of the paraxial image, entrance pupil, aperture stop, exit pupil, and field stop may be finally located, and the sizes of the pupils and stops can be finally determined. The f - number and fields of view can be calculated.

8.1.1.3 The calculation of the above characteristics of a first order solution has already been discussed. Additional calculations using paraxial ray trace data will be given later in this section where the aberrations of a system will be analyzed, and a third order theory will be developed which will provide understanding of the sources of image errors and suggest methods for correcting these errors.

8.1.2 Skew ray trace. After a first order system has been set up, skew and meridional rays are traced by the methods discussed in Section 5. This tracing of skew rays provides the basic method of investigating lens performance. The paraxial image and the entrance pupil furnish excellent reference planes which are used in the interpretation of non-paraxial ray trace data.

8.2 THE SPOT DIAGRAM

8.2.1 Representation of ray trace data. One way to make a graphical summation of ray trace data is by means of a spot diagram. Such a diagram is a plot of the intersection coordinates in the reference planes of rays traced through the lens or system from a single object point. The two reference planes usually chosen are the entrance pupil plane and the paraxial image plane. The rays traced from the object point are usually chosen so as to form a uniform pattern of intersection with the entrance pupil plane while the resulting image is represented by the ray intersections in the paraxial image plane. Figures 8.1 (a) and 8.1 (b) show typical spot diagrams of this type for rays traced from an object point (object distance not specified) which lies in the YZ (meridional) plane at coordinates $X_o = 0$ and Y_o = an arbitrary value. Thus, the twelve spots at $X_1 = 0$ in Figure 8.1 (a) represent meridional rays; all others are skew rays. In Figure 8.1 (b), the meridional rays are at $X_k = 0$. There is a one to one correspondence between the spots in the two diagrams. In general, the spots at large values of X_1 correspond to the spots at large X_k. The Y_k axis is an axis of symmetry because the Y_1 axis is an axis of symmetry.

8.2.2 Ray distribution in the entrance pupil. The shape of the entrance pupil may be found with sufficient accuracy for most applications from paraxial ray tracing by the method described in Section 6. With automatic high speed computers it is possible to trace a regular grid of rays through the system. If any ray does not pass through every clear aperture the ray is rejected. With a computer program of this type, the shape of the vignetted aperture is automatically found as the boundary of the non-rejected rays.

8.2.3 Ray distribution in the image plane.

8.2.3.1 The spot diagram shown in Figure 8.1 (b) is extremely useful to a designer in evaluating a system. The diagram indicates how well the lens concentrates the energy from the object point into an image point. One can count the number of points in concentric circles in the image plane and obtain what is called an energy distribution curve. In Figure 8.1 (a) there are 192 points in the entrance pupil. If it is assumed that each point represents an equal amount of energy, a given point is equivalent to 1/192 of the total energy from the object point passing through the aperture. Now by drawing concentric circles around what appears to be the center of concentration of spots, and counting the number of spots within each circle one obtains the total energy as a function of (circular) image size. Figure 8.2 is a plot of percent energy versus image size for the spot diagram shown in Figure 8.1 (b). In a theoretically perfect geometrical image all the spots would be concentrated at a point. However, in the case of the image due to a perfect optical system, the geometrical image is only an approximation; the actual image formed would be larger than a point due to diffraction effects.

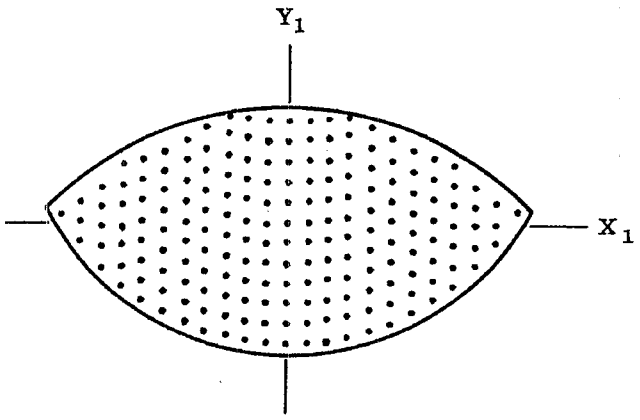

Figure 8.1 (a)- Spot diagram of rays passing through the entrance pupil.

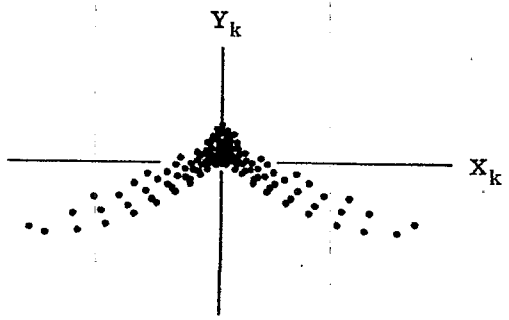

Figure 8.1 (b) - Spot diagram of rays incident on the paraxial image plane.

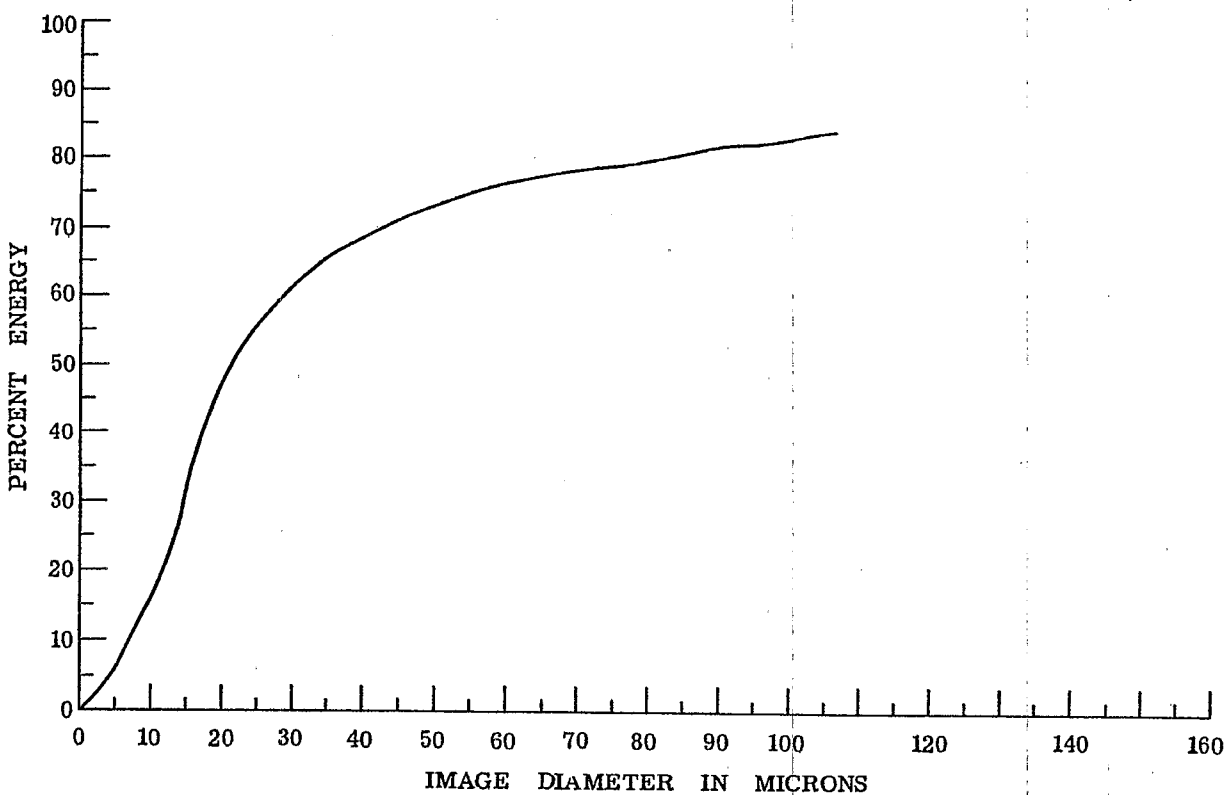

Figure 8.2- Energy distribution for the image shown in Figure 8.1 (b).

8.2.3.2 The spot diagram is useful in evaluating the image performance of a lens but it gives little insight to a designer as to why an image is spread out. In making a spot diagram, no attempt is usually made to identify each ray; therefore the designer usually has no means of visualizing what happens to the ray as it passes through the lens. Of course, it is perfectly possible to program the computer so that each ray in Figure 8.1 (b) is identified with a ray in Figure 8.1 (a), but with the large number of rays usually chosen for energy distribution representation, this would be unnecessarily complex. Instead, in order to understand the reason for image deformation, it is common practice to trace only a few selected rays through the aperture and plot the data in a different manner.

8.3 MERIDIONAL AND SKEW FANS

8.3.1 General method.

8.3.1.1 Instead of using spot diagrams and energy distribution functions, the ray trace data usually may be more conveniently analyzed by the method of meridional and skew ray fans. In using this method a common practice is to trace from a selected object point in the YZ plane, five to seven meridional rays (rays lying in the YZ plane) through the system. These rays, called the meridional ray fan, are chosen to intersect the vignetted entrance pupil in a nearly uniform spread, with upper and lower extremes (the rim rays) as close as possible to the respective vignetted pupil limits. See Figure 8.3. One of these rays is chosen to intersect the entrance pupil at $X_1 = 0$, $Y_1 = 0$ and thus, by definition, is the chief ray. The angle between the chief ray from the given object point and the optical axis is used to identify the meridional ray fan and its associated skew ray fan. The latter is constructed by tracing three to five rays from the same object point, which enter the vignetted entrance pupil at the intersection of the pupil and the XZ plane, i.e., at $Y_1 = 0$. Rays having positive X values only are needed since the object point lies in the meridional plane and the system is therefore symmetrical about the YZ plane. On the other hand, since the object point is not necessarily on the optical axis, rays above and below the Z axis are not symmetrical, so that rays must be traced having both positive and negative Y values at the entrance pupil plane.

8.3.1.2 Since they lie in a plane throughout their passage through the system, the behavior of the meridional rays can be well understood by making a plot of the coordinates of each ray intercept in the image plane (Y_k) versus the corresponding ray intercept in the entrance pupil plane (Y_1). This, in effect, is a similar but much more accurate presentation of the ray height data which could be obtained through graphical ray tracing.

8.3.1.3 Skew rays, on the other hand, do not usually remain in a single plane during their passage through the system. Thus, even though we have simplified the problem by choosing only those that intersect the entrance pupil plane on the X_1 axis ($Y_1 = 0$), they will normally have both X and Y coordinates in the image plane. Thus, for skew rays, it is necessary to make two types of plots: X_k versus X_1, and Y_k versus X_1. For perfect geometrical imagery, these plots would be straight lines of zero slope.

8.3.2 Illustrative example. In the following paragraphs, the arrangement and interpretation of these three curves will be discussed in detail. The example to be used will employ the same lens as shown in Table 6.7, except that in the table, the entrance pupil plane was not included, therefore surface 1 is the first lens surface. However, in the following discussions, surface 1 will be the entrance pupil plane, surface 2 the first lens surface, and so on. This is illustrated in Figure 8.4, which is drawn to scale from Table 6.7. The lens is a typical photographic Taylor triplet. The object surface for the lens is at infinity; the entrance pupil plane is located 2.2 cms to the right of the first surface of the lens. Rays representing fans of obliquities of 0°, 10°, 15°, and 20° have been traced into the system. (Note: with the object at infinity, the term "fan" is somewhat of a misnomer since all rays from a given object point are parallel, a situation which would not exist if the object were at a finite distance). The diagram shows the path of the extreme upper and lower rays for field angles of 10° and 20°. The upper rim ray at 0° is also shown; the lower is similar by symmetry. Notice how the upper and lower rays at 10° and 20° do not pass through the edge of the aperture stop. This is because the designer decided to vignette the oblique rays in order to eliminate some badly aberrated rays. The back focal length (BFL) is the distance between the last surface of the last element (surface 7) and the second focal point. Table 8.1 gives the numerical values for this lens.

8.4 USE OF THIRD ORDER THEORY IN ABERRATION ANALYSIS

8.4.1 Ray trace data. The numerical data used in the following discussions are the results of paraxial, meridional and skew ray traces for the lens shown in Table 8.1 and Figure 8.4. This lens, with very slightly different ν - number, was given in Tables 6.6 and 6.7.

8.4.2 Analysis of data. The curves of ray trace data will be plotted and analyzed in a manner that will be helpful to the designer trying to minimize the aberrations. The plots and analyses will make use of the third order theory to investigate the third order aberrations which, as explained in Section 5.11.3 are the first

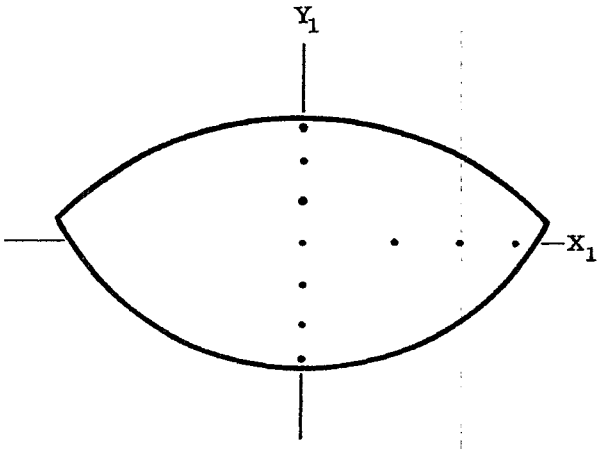

Figure 8.3 - Positions in the entrance pupil of selected meridional rays and skew rays used to analyze images.

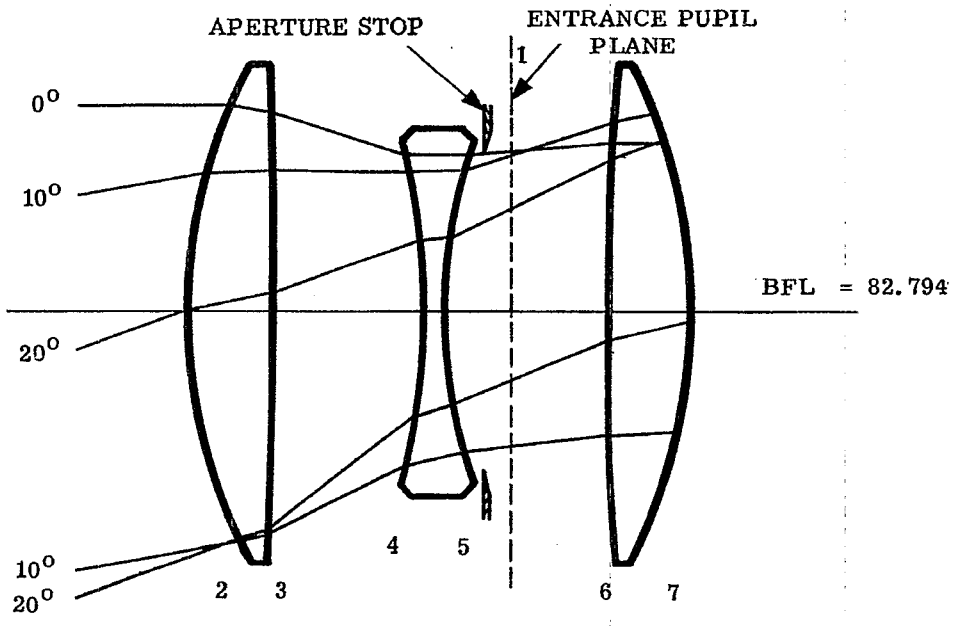

Figure 8.4 - Sample lens used for numerical analysis.

Surface	Radius	Thickness	n_D	ν-no.
2	39.55	6.0	1.620	60.3
3	-678.43	10.654	1.0	
4	-50.15	1.5	1.621	36.2
5	38.50	11.369	1.0	
6	197.43	6.0	1.620	60.3
7	-40.67			

Table 8.1 - Numerical values for lens in Figure 8.4. All lengths in millimeters. The numerical values are exact except for the radii. Exact curvatures are given in Table 8.2.

approximations to the aberrations. The method of plotting differs from that described in Section 8.3 in that only the essential information is shown. That is the difference in the paraxial plane intercepts for the chief ray and the other rays of the fans is plotted since it is this difference, or lack of coincidence, which the designer is trying to overcome.

8.5 THE 0° IMAGE IN D LIGHT

8.5.1 The 0° image polynomial.

8.5.1.1 The image of an axial object point at infinity is studied by tracing three meridional rays with $K_o = 0$, $L_o = 0$, $M_o = 1$ at values of $Y_1 = 1.5$, 1.0 and 0.5. For meridional rays from an axial object point, negative values of Y_j are symmetrical with the positive values. The results are plotted and encircled in Figure 8.5. The vertical scale is labelled $(Y_k - \overline{Y}_k)$. $\overline{Y}_k$ is the height of the chief ray $(\overline{Y}_1 = 0)$ on the final paraxial $(y_k = 0)$ image plane. For these axial rays $\overline{Y}_k = 0$. The circled points, connected by the full curve, can be fitted fairly accurately to a power series of the form

$$Y_k - \overline{Y}_k = b_1 Y_1 + b_3 Y_1^3 + b_5 Y_1^5 + O(7). \qquad (1)$$

The letters b_3, b_5, etc. are called the spherical aberration coefficients. The term $O(7)$ stands for all the terms of order 7 and above, as explained in Paragraph 5.5.2.3.

8.5.1.2 When ray data are plotted in this manner the slope of a line drawn between any two ray points on the curve is proportional to the longitudinal distance from the paraxial image plane to the plane where the two rays focus. That this is true, can be seen from Figure 8.6. This diagram shows two actual rays converging towards the image surface. The image surface, where the two rays focus, will be called the $k+1$ surface. The paraxial image plane is called the kth surface. By placing the paraxial image plane to the left of the intersections of the optical axis with rays (a) and (b), the two Y_k values are positive. Such a diagram would not represent the physical situation of a single converging lens, because for that case, the paraxial image plane is to the right of the intersection points of the optical axis with non-paraxial rays. The situation represented in Figure 8.6 could be attained, for example, by the forming of an image by a diverging system of an unaberrated, virtual object.

8.5.1.3 From the diagram we have

$$Y_{ka} = Y_{(k+1)a} - t_k \tan U_{(k-1)a}$$

and

$$Y_{kb} = Y_{(k+1)b} - t_k \tan U_{(k-1)b}.$$

Since $Y_{(k+1)a} = Y_{(k+1)b}$, subtraction gives

$$t_k = -\frac{Y_{ka} - Y_{kb}}{\tan U_{(k-1)a} - \tan U_{(k-1)b}}.$$

This equation and Figure 8.6 apply to two non-paraxial rays. It will be assumed that the following relation is a valid approximation for either of these rays; namely

$$\frac{Y_1}{\tan U_{k-1}} = \frac{y_1}{u_{k-1}}.$$

If these rays were paraxial, this relation would be exact; assuming it to hold approximately for non-paraxial rays, there results

$$\tan U_{(k-1)a} - \tan U_{(k-1)b} = \frac{Y_{1a}}{y_1 / u_{k-1}} - \frac{Y_{1b}}{y_1 / u_{k-1}},$$

and finally,

$$t_k = -\frac{y_1}{u_{k-1}} \left(\frac{Y_{kb} - Y_{ka}}{Y_{1b} - Y_{1a}} \right). \qquad (2)$$

When the object point is at infinity, then $-y_1 / u_{k-1} = f'$. Equation (2) is only an approximation for non-paraxial rays. But at worst it gives the order of magnitude of t_k; this is all that is needed for

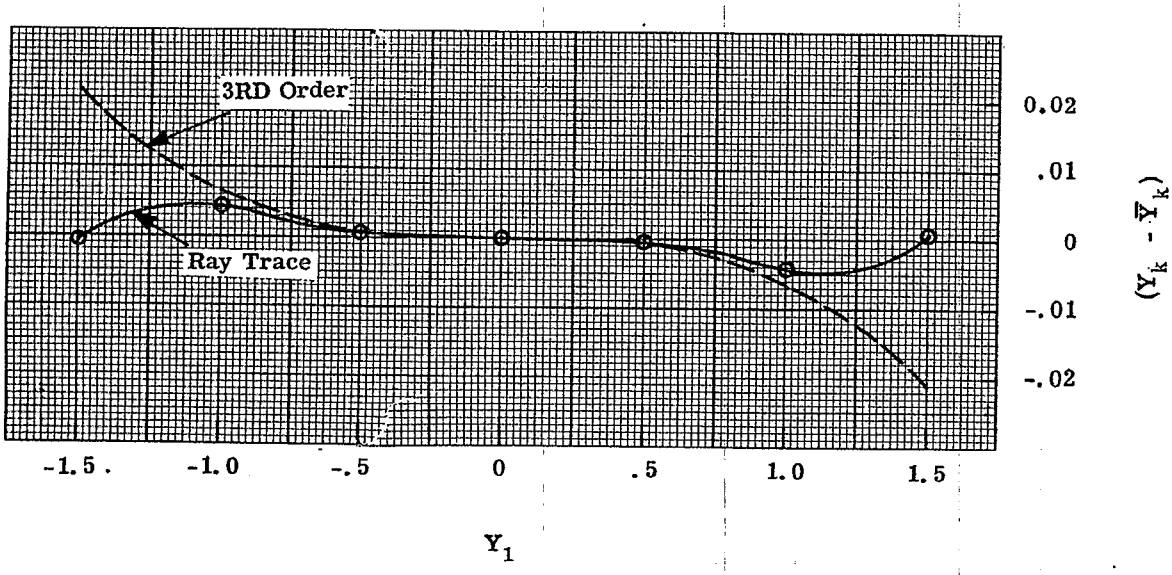

Figure 8.5 - Meridional ray plot at 0^o.

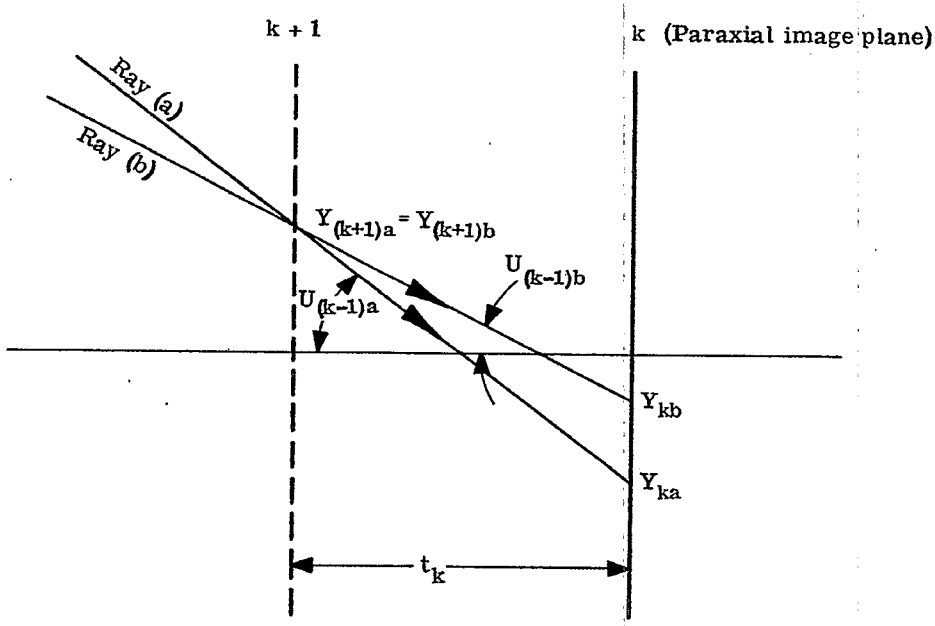

Figure 8.6 - Diagram illustrating shift of focus relationships.

third order design procedure.

8.5.1.4 Since the slope of the line connecting any two points on the $(Y_k - \overline{Y}_k)$ versus Y_1 curve is $\Delta Y_k / \Delta Y_1$, this slope is proportional to the distance from the paraxial image plane to the plane of focus for the two rays. As the two rays approach each other, the two points on the curve do likewise, and the slope of the chord approaches the slope of the curve. Hence the slope of the curve at any point is proportional to the distance from the paraxial image plane to the plane of focus for infinitely close rays. From ray trace data resulting in Figure 8.5, and from paraxial ray trace data giving y_1 / u_{k-1}, we are able to determine the shift (t_k) of the image plane from the paraxial image plane.

8.5.1.5 Now since the ray data shown in Figure 8.5 was obtained in the paraxial image plane the slope of the curve must be zero at $Y_1 = 0$. Therefore b_1 will be zero in Equation (1). The presence of a linear term indicated by a slope different from zero at $Y_1 = 0$, means that the paraxial rays are not focused in the final image plane upon which the ray heights are calculated. This linear term in Equation (1) can be eliminated by shifting the plane upon which the ray heights are calculated. When this has been done, so that the slope of the curve is zero at $Y_1 = 0$, and the linear term is absent, any further deviation, $(Y_k - \overline{Y}_k) \neq 0$, indicates the presence of spherical aberration. Therefore, the first approximation to the spherical aberration, written as $(Y_k - \overline{Y}_k)$, varies as the cube of the entrance pupil radius. This part of the spherical aberration, the third order spherical aberration, would vary with Y_1 as shown by the dashed line in Figure 8.5.

8.5.1.6 Because the slope of the line between any two points on the curve is proportional to the t_k for the two rays considered, Figure 8.5 shows that the rays traced at $Y_1 = 0.5$ and 1.0 are focused closer to the lens than the paraxial image plane, while the ray at $Y_1 = 1.5$ is focused almost exactly on the paraxial image plane. In this system, the third order coefficient, b_3, is negative and the lens is said to be undercorrected for the third order spherical aberration. It is called undercorrected spherical aberration because a single positive lens has spherical aberration of this sign. (See Paragraph 6.10.5.1). The coefficient, b_5, is called the fifth order coefficient. In this case it is positive because the full curve (Figure 8.5) is between the third order curve and $Y_k - \overline{Y}_k = 0$; hence the fifth order term [Equation(1)] has a sign opposite to that of the third order term. The fifth order coefficient is said to be overcorrected.

8.5.2 The third order aberration coefficient.

8.5.2.1 Now a truly remarkable feature of optical systems is that the coefficient, b_3, may be computed from axial paraxial ray data. This is done by calculating B_j, the third order spherical aberration surface contribution, at each surface in the optical system. Then,

$$b_3 = - \left[\frac{1}{2 (n_{k-1} \; u_{(k-1)}) \; y_1^3} \right] \sum_{j=1}^{j=k-1} B_j \; , *$$

where y_1 is the height of the axial paraxial ray in the entrance pupil plane and u_{k-1} is the final angle with the optical axis for this ray. Therefore, since $\overline{Y}_k = 0$ for 0° obliquity, the third order approximation for Y_k is,

$$_3Y_k = - \frac{\Sigma B}{2 (n_{k-1} \; u_{k-1})} \left(\frac{Y_1}{y_1} \right)^3 . \; ** \qquad (3)$$

8.5.2.2 B_j is calculated from the axial paraxial ray data for each surface with the following formulae

$$B = S i^2 , \qquad (4)$$

and

$$S = y \, n_{-1} \left(\frac{n_{-1}}{n} - 1 \right) (u + i) . \qquad (5)$$

In Table 8.2, B_j is calculated for each surface of the sample lens being studied. This is the same lens

* Up to this point in the text an attempt has been made to derive the equations, or to indicate specifically how they may be derived. This practice will no longer be followed; thus, equations may be presented without proof. To do otherwise would necessitate lengthy and complex departures from the main train of thought.

** In later sections the symbol Σ will be used to indicate the summation of all surface contributions. The proper summation limits will be eliminated.

Surface	Object	Entrance Pupil						Image	
	0	1	2	3	4	5	6	7	8	
c		0	0.25285	-0.01474	-0.19942	0.25973	0.05065	-0.24588	0	
t		-2.20000	0.60000	1.06541	0.15000	1.13691	0.60000	8.27937		
n	1.0000	1.00000	1.62000	1.00000	1.62100	1.00000	1.62000	1.00000		
$(n_{-1}/n)-1$			-0.382716	0.62000	-0.383097	0.62100	-0.382716	0.62000		
y		1.50000	1.50000	1.41291	1.14862	1.13883	1.22735	1.24192	0	
u	0	0	-0.145155	-0.24806	-0.065279	0.077866	0.02427	-0.15000		
i		0	0.37928	-0.16598	-0.47712	0.230508	0.14003	-0.281089		
u+i		0	0.23412	-0.41404	-0.54239	0.30837	0.16431	-0.43109		
B			-0.01933	-0.01619	0.05433	0.01878	-0.00151	-0.04249	Σ B = -0.00641	
$\bar{y}$		0	-0.80073	-0.61944	0.09189	-0.04712	0.49425	0.66486	$3Y_k$ = -0.02135	
$\bar{u}$	0.36397	0.36397	0.30216	0.49516	0.29845	0.47618	0.28436	0.35930	3.63966	
$\bar{i}$		0.36397	0.16150	0.31129	0.51348	0.28621	0.50121	0.12088		
F			-0.00823	0.03036	-0.05847	0.02332	-0.00542	0.01827	Σ F = -0.000170	
C			-0.00351	-0.05694	0.06293	0.02896	-0.01939	-0.00786	Σ C = -0.004200	
E			-0.01378	0.10994	-0.09223	0.07278	-0.09008	0.01544	Σ E = -0.002070	
P			-0.09677	-0.00564	0.07640	0.09950	-0.01938	-0.09410	Σ P = -0.04000	
dn/n		0	0.00635	0	0.01058	0	0.00635	0		
Δ (dn/n)			0.00635	-0.00635	0.01058	-0.01058	0.00635	-0.00635		
a			-0.00362	-0.00242	0.00580	0.00450	-0.00109	-0.00361	Σ a = -0.00040	
b			-0.00154	0.00452	-0.00624	0.00559	-0.00390	0.00154	Σ b = -0.000026	

Table 8.2 - Third order calculations on triplet lens in Figure 8.4.

illustrated in Table 6.7. The dotted curve in Figure 8.5 shows the third order curve as predicted by Equation (3). One notes that at $Y_1 = 1.5$, the dotted curve passes through the point $Y_k = -0.0214$. Notice also how the third order curve follows the true aberration curve very closely out to $Y_1 = 0.75$.

8.5.2.3 Returning to Equation (1) it follows that $b_3 = -0.0214/y_1^3 = -0.006341$. Since the actual ray traced at $Y_1 = 1.5$ strikes the final image plane at $Y_k = 0$ it is possible to compute that $b_5 = 0.002818$ if it is assumed that $O(7) = 0$. By using Equation (1) then at $Y_1 = 1.0$, Y_k should equal -0.00352. The actual ray traced point comes out at $Y_k = -0.0041$. This difference, 0.0006, is small compared to the total spherical aberration -0.0041. This means that the spherical aberration curve shown in Figure 8.5 may be approximately obtained by calculating the third order coefficient b_3 from axial paraxial ray data, and tracing one non-paraxial ray. On the other hand, the curve can also be obtained by tracing two non-paraxial rays, and calculating b_3 and b_5. Since the third order coefficient calculation depends on the individual surface contributions, it helps the designer see the source of the aberrations. For the example shown in Table 8.2, we see that the first two, and the last two surfaces of the lens give negative spherical aberration. The two surfaces of the central negative element provide all the positive or over-correction. The contribution on surface number four of the lens has the largest positive value. This coupled with the large angle of incidence on this surface is the main reason that the fifth order coefficient is positive. If one wanted to reduce the fifth order coefficient, it would be necessary to find a solution with a smaller angle of incidence on this surface or a smaller spherical aberration coefficient. If the fifth order coefficient were reduced, the total aberration (full curve) will be closer to the third order. The maximum under-correction, which now occurs at about $Y_1 = 1.1$, would increase and would occur at a larger Y_1. Such a lens would exhibit an increased zonal spherical aberration. The point of zero aberration, now at $Y_1 = 1.5$, would increase towards larger values of Y_1, so that the lens could be used at a larger aperture.

8.5.2.4 The Y_k versus Y_1 curves shown in Figure 8.5 were obtained in D light. Similar calculations could be made in F and C light. The value of b_3 can vary with wavelength, and since the plot is made for the paraxial focal plane in D light, the F and C paraxial rays will focus farther from the lens by approximately $f'/2200$. Therefore b_1 for F and C light, if we have a true (F - C) achromat, will be positive and equal to 1/2200. On this scale this is a negligible amount of aberration amounting to one-tenth of the zonal aberration, 0.0041. The F and C curves, corresponding to Figure 8.5, would have a positive slope at $Y_1 = 0$.

8.5.3 The Seidel spherical aberration.

8.5.3.1 Equations (3), (4) and (5) give the calculation of ${}_3Y_k$, the third order approximation to Y_k. Because $\bar{Y}_k = 0$, and hence for an unaberrated image point $Y_k = 0$, ${}_3Y_k$ is the third order approximation to the spherical aberration, measured in a plane perpendicular to the optical axis. Hence, it is sometimes referred to as the transverse spherical aberration. In the following section the aberrations of an off-axis image point will also be expressed as transverse aberrations.

8.5.3.2 Another measure of spherical aberration, called the longitudinal spherical aberration, is the distance along the optical axis between the paraxial image plane and the non-paraxial ray. The third order approximation to the longitudinal spherical aberration, referred to as the Seidel longitudinal spherical aberration, is numerically equal to ${}_3Y_k / u_{k-1}$. Hence, from an expression for the Seidel aberration, Equations (3), (4) and (5) readily follow.

8.6 IMAGERY FOR AN OFF-AXIS OBJECT POINT

8.6.1 The oblique image polynomial.

8.6.1.1 The solid curve in Figure 8.7 (a) is a plot of meridional rays traced through the sample lens at 10° ($K_o = 0$, $L_o = 0.1736$). The coordinates for the entering rays on the entrance pupil extend from $Y_1 = 1.35$ to $Y_1 = -1.35$. The vertical scale is again $(Y_k - \bar{Y}_k)$. The curve represents the displacement between the ray heights and the chief ray height in the paraxial image plane. This curve may also be represented by a power series. The power series can be expressed in different ways, but the following uses the well known Seidel third order coefficients. The polynomial can be expressed for any ray coordinate (Y_1, X_1) in the entrance pupil for any object height $\bar{Y}_o$ ($\bar{X}_o = 0$). Hence the series are sufficiently general so that they can be used with skew rays. There are two equations, one for $(Y_k - \bar{Y}_k)$,

and the other for X_k . $\overline{X}_k$ is always zero. These equations are

$$Y_k - \overline{Y}_k = - \frac{1}{2\,(n_{k-1}\,u_{k-1})} \left[\Sigma B\,(Y_1^2 + X_1^2)\,\frac{Y_1}{y_1^3} + \Sigma F\,\frac{3Y_1^2 + X_1^2}{y_1^2}\left(\frac{\overline{Y}_o}{\overline{y}_o}\right) + \Sigma(3C + P\Phi^2)\,\frac{Y_1}{y_1}\left(\frac{\overline{Y}_o}{\overline{y}_o}\right)^2 \right] + O(5), \qquad (6)$$

and

$$X_k = - \frac{1}{2\,(n_{k-1}\,u_{k-1})} \left[\Sigma B\,(Y_1^2 + X_1^2)\,\frac{X_1}{y_1^3} + \Sigma F\,\frac{(2Y_1\,X_1)}{y_1^2}\left(\frac{\overline{Y}_o}{\overline{y}_o}\right) + \Sigma(C + P\Phi^2)\left(\frac{X_1}{y_1}\right)\left(\frac{\overline{Y}_o}{\overline{y}_o}\right)^2 \right] + O(5)\,. \qquad (7)$$

8.6.1.2 The expressions ΣB , ΣF , ΣC and ΣP are the sums of the third order surface contributions for spherical aberration, coma, astigmatism and Petzval curvature. (C must not be confused with c , the curvature of a surface.) The terms, y_1 , $\overline{y}_o$, and $n_{k-1}\,u_{k-1}$, are the data from the two paraxial rays traced through the system. $\overline{Y}_o$ is the object point height. Y_1 and X_1 are coordinates for a general ray in the entrance pupil. If the object point is at infinity, as it is in the example being described, then $\overline{Y}_o / \overline{y}_o$ should be replaced by $(\tan \overline{U}_o)/\overline{u}_o$ or $L_o / M_o\,\overline{u}_o$.

8.6.1.3 If ΣB , ΣF , ΣC and ΣP are known, Equations (6) and (7) can be used to predict the position coordinates of any ray in the image surface corresponding to a given point in the object surface. The accuracy of the prediction depends on the magnitude of aberrations higher than third order. According to the first order theory, the chief ray should strike the image plane at $\overline{Y}_k = \overline{Y}_o\,m$ if $\overline{Y}_o$ is finite, or at $\overline{Y}_k = f \tan \overline{U}_o$, if the object is at infinity. However, the actual chief ray is displaced from the ideal image point due to a fifth aberration, distortion. There is also a polynomial to express this displacement.

$$(\overline{Y}_k - \overline{Y}_o\,m) = - \frac{\Sigma E}{2\,(n_{k-1}\,u_{k-1})} \left(\frac{\overline{Y}_o}{\overline{y}_o}\right)^3 + O(5)\,, \qquad (8)$$

where ΣE is the third order contribution for distortion. Equation (8) can be included in Equation (6) but it was not because it is somewhat easier to plot $(Y_k - \overline{Y}_k)$ as has been done in Figure 8.7. The fractional distortion which is defined by the ratio $(\overline{Y}_k - \overline{Y}_o\,m)/\overline{Y}_o\,m$ may be written to read as follows,

$$\text{fractional distortion} = \frac{\overline{Y}_k - \overline{Y}_o\,m}{\overline{Y}_o\,m} \doteq - \frac{\Sigma E}{2\,\Phi} \left(\frac{\overline{Y}_o}{\overline{y}_o}\right)^2 .$$

Note that the fractional distortion varies with the square of the object height ratio $(\overline{Y}_o/\overline{y}_o)$. In Section 8.7 the method for calculating B , F , C , E and P will be described. The actual calculations for the sample problem are shown in Table 8.2.

8.6.2 Examples of third order aberrations.

8.6.2.1 The third order ray predictions for $(Y_k - \overline{Y}_k)$ and X_k are shown by the dotted curves in Figures 8.5 , 8.7 and 8.8 . The solid curves show the actual coordinates for rays traced through the same entrance pupil points. Figures 8.7 (a), (b) and (c) are plots for fans of meridional rays at 10°, 15° and 20° respectively. Figures 8.8 (a) and 8.8 (b) show plots for skew fans with $Y_1 = 0$. Figure 8.9 is a plot of the fractional distortion of the lens as a function of the object field angle. The results show that the actual distortion is slightly more positive than predicted from the third order theory.

8.6.2.2 Finally in Figure 8.10 the slopes of all the curves at the chief ray are indicated. (Slopes are proportional to t_k). Curves of this type are called field curves. The points on the curves show the longitudinal distances from the paraxial image plane to the focus of rays close to the chief ray. The three third order field curves were found from surface contributions. The remaining two, the tangential field curve and the sagittal field curve, were obtained by graphically determining the slope of the meridional and skew ray plots respectively. These are shown in Figure 8.7, and in Figure 8.8. The third order tangential and sagittal field curves may be calculated by differentiating Equations (6) and (7) with respect to Y_1 and X_1

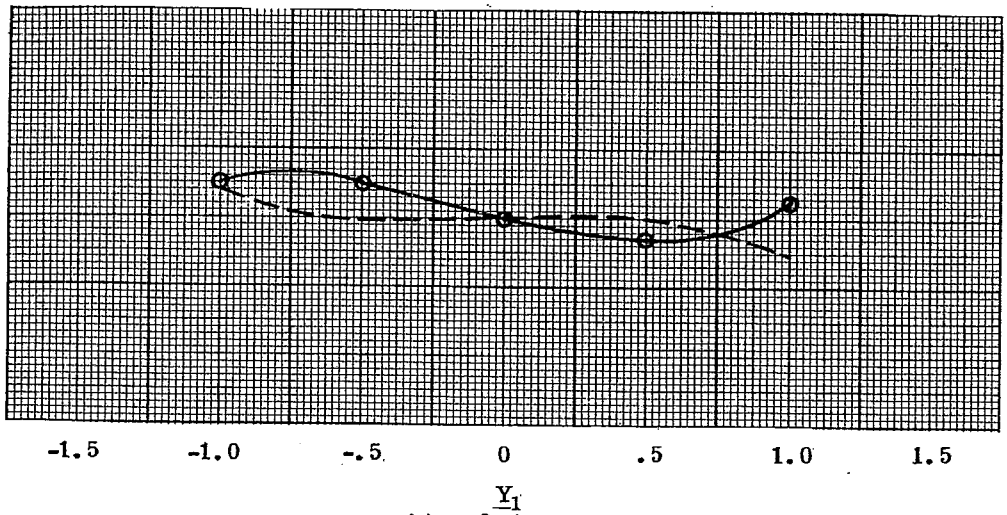

(c) 20° Obliquity

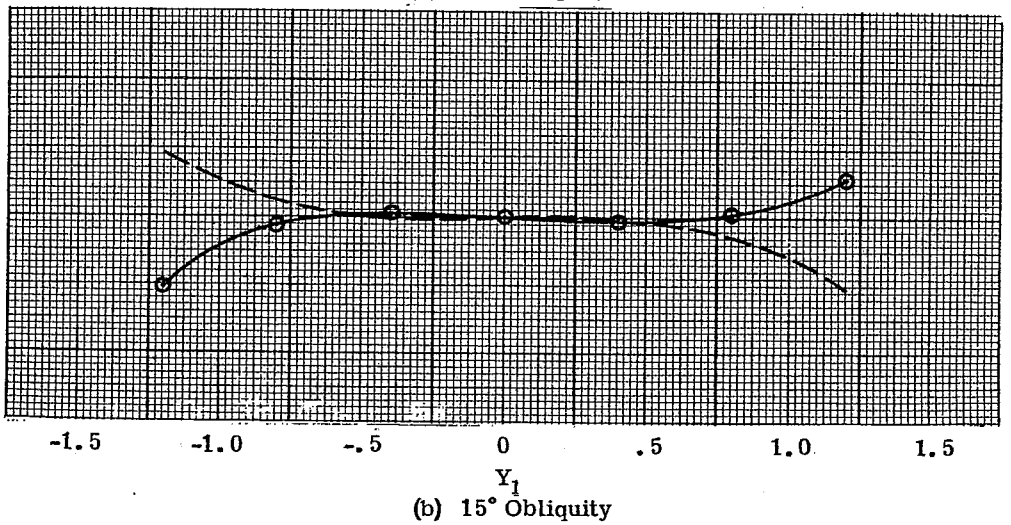

(b) 15° Obliquity

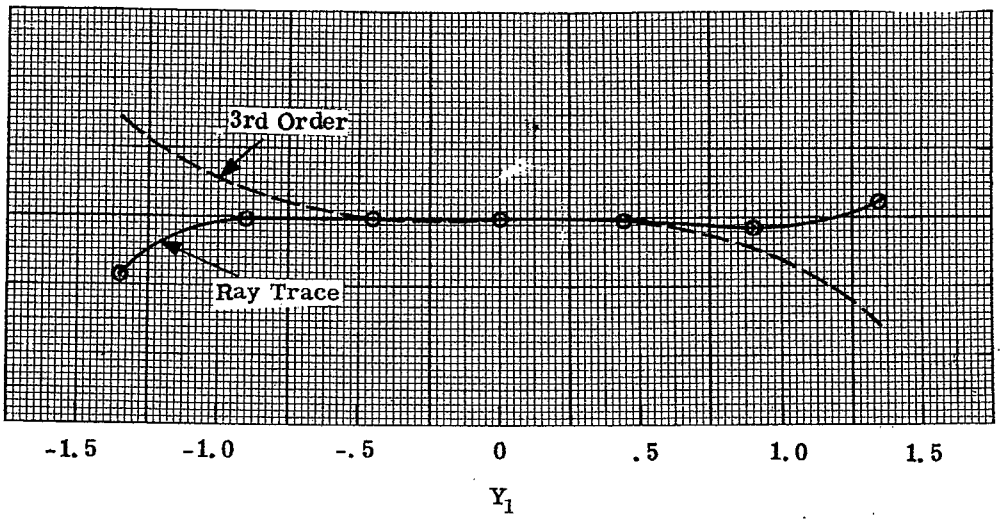

(a) 10° Obliquity

Figure 8.7 - Meridional ray plots.

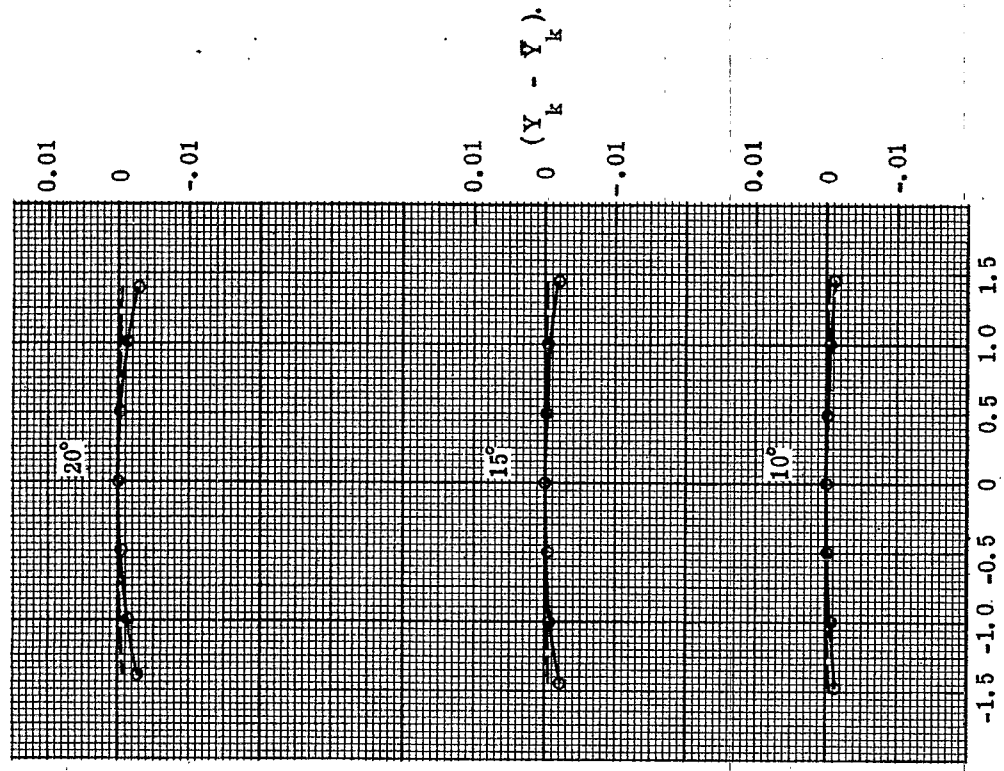

Figure 8.8 (b) - Skew ray image coordinates $(Y_k - \bar{Y}_k)$.

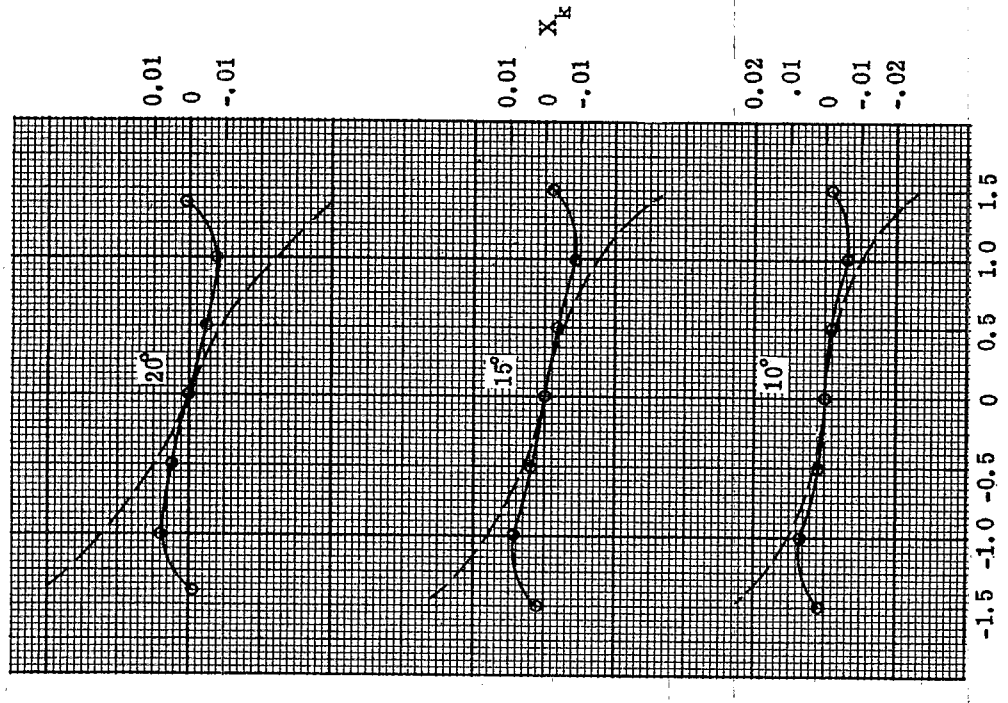

Figure 8.8 (a) - Skew ray image coordinates (X_k).

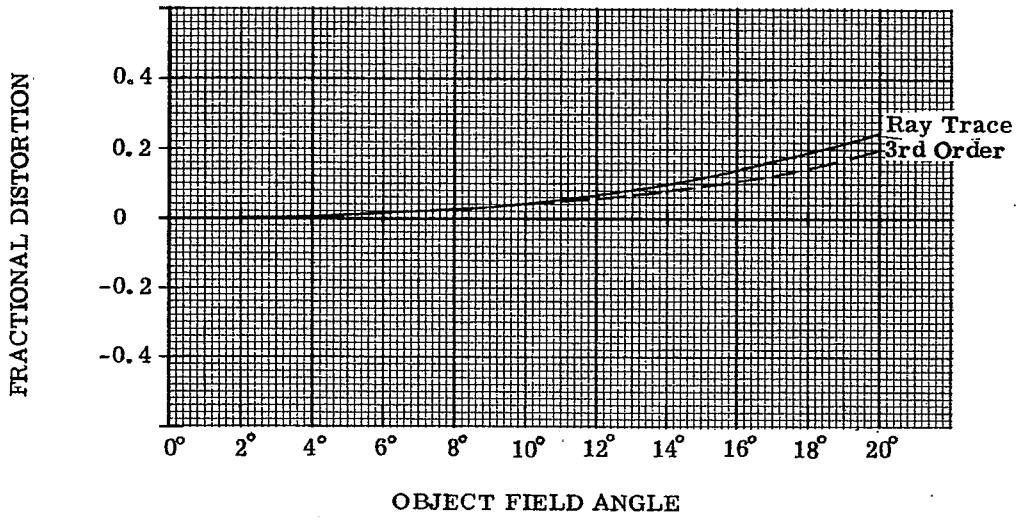

Figure 8.9 - Fractional distortion as a function of field angle.

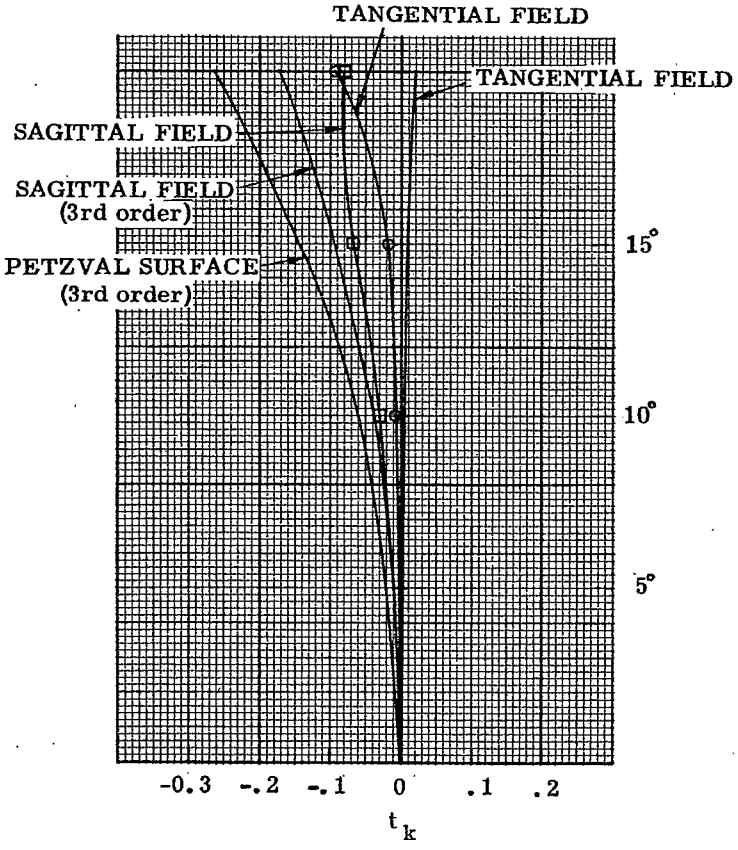

Figure 8.10 - Field curves for a triplet.

respectively and evaluating at $Y_1 = X_1 = 0$. The B and F terms drop out, leaving only the third terms. The final equation for the tangential fan is

$$t_{kT} = \frac{1}{2\,(n_{k-1}\,u_{k-1}{}^2)} \left[\Sigma\,(3C + P\Phi^2) \left(\frac{L_o}{M_o\,\bar{u}_o}\right)^2 \right]. \qquad (9)$$

For the sagittal fan, the equation is

$$t_{kS} = \frac{1}{2\,(n_{k-1}\,u_{k-1}{}^2)} \left[\Sigma\,(C + P\Phi^2) \left(\frac{L_o}{M_o\,\bar{u}_o}\right)^2 \right]. \qquad (10)$$

The Petzval surface curve is determined by the equation

$$t_{kP} = \frac{1}{2}\,(3t_{kS} - t_{kT}) = \frac{1}{2\,(n_{k-1}\,u_{k-1}{}^2)} \left[\Sigma P\Phi^2 \left(\frac{L_o}{M_o\,\bar{u}_o}\right)^2 \right].$$

Comparing this with Equation (9) and (10), it is clear that for $C = 0$, $t_{kP} = t_{kT} = t_{kS}$.

8.7 CALCULATION OF THE THIRD ORDER CONTRIBUTIONS B, F, C, E AND P

8.7.1 Basic formulae. The method for calculating B, surface by surface, was explained in Paragraph 8.5.2.2, and a sample calculation was given in Table 8.2. The coefficients F, C and E are calculated, surface by surface, by using the data of both the axial and chief paraxial rays. The formulae are:

$$B = S\,i^2 \qquad (4)$$

$$F = S\,i\,\bar{i} \qquad (11)$$

$$C = S\,\bar{i}^2 \qquad (12)$$

$$E = \bar{S}\,i\,\bar{i} + \Phi(\bar{u}_{-1}{}^2 - \bar{u}^2)\,*. \qquad (13)$$

P is calculated for each surface from the equation

$$P = \frac{c\,(n_{-1} - n)}{n_{-1}\,n}. \qquad (14)$$

As in the case of Equations (3), (4) and (5), Equations (6), (7), (8), (11), (12), (13) and (14) are derived from the Seidel expressions for coma, astigmatism, distortion and Petzval curvature.

8.7.2 Calculation of aberrations. These surface contributions have been worked out, surface by surface, in the sample problem shown in Table 8.2. The individual surface contributions, when summed up for all the surfaces, may be inserted in Equations (6) and (7) to evaluate the third order polynomials.

8.7.3 Fourth order aspheric effects. A fourth order aspheric deformation term on a surface introduces the following amounts of third order aberrations,

$$B = 8\,(n_{-1} - n)\,e\,y^4 \qquad (4a)$$

$$F = B\,\bar{y}/y \qquad (11a)$$

$$C = B\,(\bar{y}/y)^2 \qquad (12a)$$

$$E = B\,(\bar{y}/y)^3. \qquad (13a)$$

Note that the aspheric deformation term introduces aberrations independent of the curvature of the surface. It introduces no first order chromatic effects or Petzval contribution.

---

* $\bar{S}$ is calculated from Equation (5) using data from the chief ray.

8.7.4 The value of using third order aberration coefficients.

8.7.4.1 Inspection of the ray tracing data in Figures 8.5, 8.7 and 8.8 shows that the third order aberration polynomial does not predict the true aberration accurately for large apertures or field angles. However, third order aberration theory is extremely valuable. Even with present day computers, it is almost essential for a designer to calculate the third order aberrations of a system under consideration. Third order aberration theory provides target values for the designer; the third order aberrations must be within fairly narrow regions in order to obtain a satisfactory design. It is then up to the designer to find a layout which will lie within this third order region, but which will either balance or reduce the higher order aberrations.

8.7.4.2 Third order surface contributions provide the designer with a means for understanding a lens. He knows that the aberrations should be corrected with evenly balanced third order contributions. In other words, the third order contributions of a single aberration should be approximately equal numerically, but have alternating signs so that the sum is small. A large third order aberration on a surface will introduce a large higher order aberration of the same sign. Hence, the third order aberrations should be kept small. It is surprising how well one can control higher order aberrations through the use of third order calculations by remembering the following recommendations.

(1) Try to find the required third order solution with small, evenly distributed aberration contributions. It is seldom advisable to introduce a large contribution on one surface to cancel out several small ones due to other surfaces.

(2) Try to avoid large angles of incidence. The angle of incidence strongly affects the magnitude of higher order aberration contributions.

(3) If a given surface introduces a large amount of any third order aberration, try to correct this by another surface as nearby as possible. The reason for this is that a surface introducing large amounts of third order aberrations also introduces a series of higher order aberrations. If the third order aberrations are corrected by a neighboring surface, the higher order aberrations tend to cancel one another, but if correction is done at some other part of the optical system, the higher order aberrations will not necessarily cancel. For example, if a large amount of spherical aberration is introduced at a position in the system where $\bar{y}/y = k$, then this aberration should be corrected at a surface as close as possible to the position where $\bar{y}/y = k$. It may often be impossible, in a given design, to make the ideal correction, but it is an important step in design procedure to make the attempt. One of the main reasons that aspheric surfaces are so valuable, is that they do allow the introduction of aberration at nearly any place in the optical system, without upsetting the distribution of focal lengths of the different elements needed to correct for color and Petzval field curvature.

8.8 AFOCAL OPTICAL SYSTEMS

8.8.1 Third order polynomial. In telescopic systems, where both the object and image are at infinity, it is convenient to plot the tangents of the angles which the emerging rays make with the optical axis, versus the coordinates (X_1, Y_1) of the entering rays. The meridional ray ($X_1 = 0$ and Y_1 arbitrary) data are plotted as $\left(\frac{L_{k-1}}{M_{k-1}} - \frac{\bar{L}_{k-1}}{\bar{M}_{k-1}}\right)$ versus Y_1. The skew ray ($Y_1 = 0$ and X_1 arbitrary) data are plotted as two curves:

$$\frac{K_{k-1}}{M_{k-1}} \quad \text{versus} \quad X_1 ,$$

and

$$\left(\frac{L_{k-1}}{M_{k-1}} - \frac{\bar{L}_{k-1}}{\bar{M}_{k-1}}\right) \quad \text{versus} \quad X_1 .$$

The third order polynomial may then be written as in Equations (6) and (7) by making the following substitutions:

$$Y_k = -\frac{y_{k-1}}{u_{k-1}} \tan U_{k-1} \qquad X_k = -\frac{y_{k-1}}{u_{k-1}} \frac{K_{k-1}}{M_{k-1}}$$

and

$$\bar{Y}_k = -\frac{y_{k-1}}{u_{k-1}} \tan \bar{U}_{k-1} .$$

Equations (6) and (7) then become

$$\left(\frac{L_{k-1}}{M_{k-1}} - \frac{\bar{L}_{k-1}}{\bar{M}_{k-1}}\right) = \frac{1}{2(n_{k-1}\, y_{k-1})}\left[\Sigma B\,(Y_1^2 + X_1^2)\,\frac{Y_1}{y_1^3} + \Sigma F\,\frac{(3Y_1^2 + X_1^2)}{y_1^2}\left(\frac{\bar{Y}_o}{\bar{y}_o}\right)\right.$$

$$\left. + \Sigma(3C + P\Phi^2)\,\frac{Y_1}{y_1}\left(\frac{\bar{Y}_o}{\bar{y}_o}\right)^2\right] + O(5)\,, \qquad (15)$$

and

$$\frac{K_{k-1}}{M_{k-1}} = \frac{1}{2(n_{k-1}\, y_{k-1})}\left[\Sigma B\,(Y_1^2 + X_1^2)\left(\frac{X_1}{y_1^3}\right) + \Sigma F\,\frac{(2\,Y_1\,X_1)}{y_1^2}\left(\frac{\bar{Y}_o}{\bar{y}_o}\right)\right.$$

$$\left. + \Sigma(C + P\Phi^2)\left(\frac{X_1}{y_1}\right)\left(\frac{\bar{Y}_o}{\bar{y}_o}\right)^2\right] + O(5)\,. \qquad (16)$$

8.8.2 Spot diagram.

8.8.2.1 In an ideal, aberration-free afocal system, the emergent rays from the $k - 1$ surface are parallel. In a real afocal system these rays are almost parallel. The intersection of these rays with a plane would give a series of points more or less evenly spaced; the points would not be concentrated, as in a spot diagram (see Figure 8.1 (b)), and it would be difficult to interpret the diagram in the same way as in the case of the spot diagram.

8.8.2.2 It is possible to concentrate these almost parallel emergent rays and make a spot diagram for an afocal system by adding a hypothetical aberration-free thin lens at the rear of the system with any desired focal length. This is effectively done simply by changing the coordinates for each ray on the last surface of the system to zero. The rays then proceed to the final focal plane of the aberration-free lens from this point at the same angles because they pass through the center (coinciding nodal points) of the thin lens. The distance to the image plane is the arbitrary focal length of this lens. The spread of the points from a single, concentrated spot, is an indication of the non-parallelism of the emergent rays. This in turn is an indication of the aberrations of the afocal system.

8.9 STOP SHIFT EQUATIONS

8.9.1 General. The aim of a lens designer is to minimize the aberrations of the optical system within the specifications of f - number and field of view. It is clear by Equations (4), (5), (11), (12), (13) and (14) that the third order coefficients depend on index, curvature, and thickness. By Equations 6-(34) and 6-(35), the first order chromatic coefficients also depend on these parameters. But the occurrence of $\bar{i}$, $\bar{S}$, and $\bar{u}_{-1}$, in Equations (11), (12), (13) and 6-(35), show that the oblique aberrations (coma, astigmatism, distortion, and lateral color) depend on the position of the aperture stop as well. Hence it is necessary for the designer to know the effect of the stop position on these aberrations.

8.9.2 Aberration polynomial for a shifted chief ray.

8.9.2.1 The aberration polynomials shown in Equations (6) and (7) are calculated from the coefficients B, F, C and E which are determined by tracing an axial and an oblique chief paraxial ray. It is possible to compute the aberration polynomial for any other paraxial chief ray. The term other paraxial chief ray, or shifted chief ray, refers to another ray which crosses the optical axis at the new pupil points. Hence shifting the aperture stop results in a new ray becoming the (shifted) chief ray. Suppose we wish to write down the aberration polynomial for a paraxial chief ray which passes through the original entrance pupil at a height of $\bar{y}^*$. A ray from object point $\bar{Y}_o$ passing through the original entrance pupil at a height of Y_1 will be at a height of Y_1' in the original entrance pupil above the new chief ray. Figure 8.11 shows that $Y_1 = Y_1' + \bar{Y}_1^*$.

8.9.2.2 Equation (6) may be written now in terms of Y_1'. The distortion term in Equation (8) is added to Equation (6) to give the aberration $Y_k - \bar{Y}_o\, m$. For an object of height $\bar{Y}_o$, it can be seen by similar triangles that $\bar{Y}_1^*$ is given by

$$\bar{Y}_1^* = \bar{y}_1^*\left(\frac{\bar{Y}_o}{\bar{y}_o}\right).$$

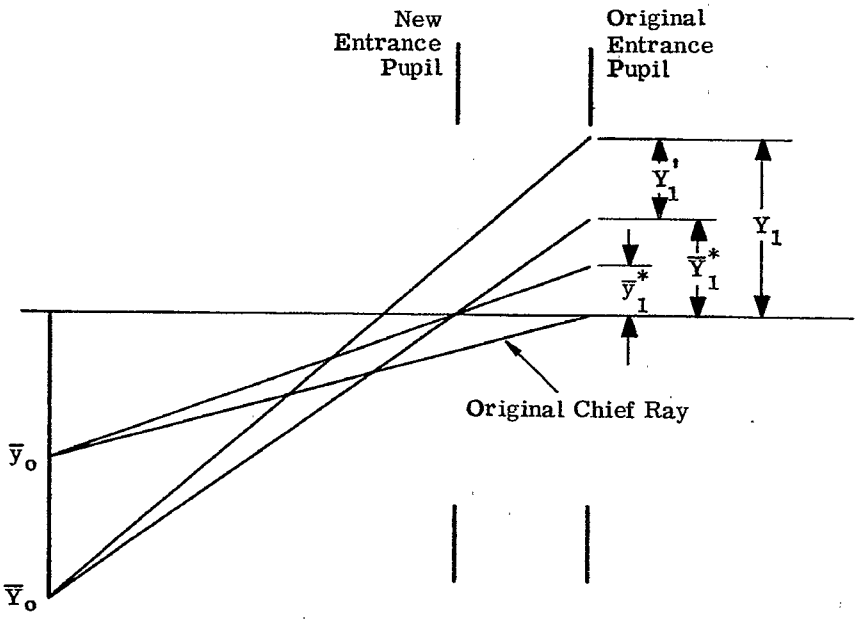

Figure 8.11 - Application of stop shift equations.

Then the height Y_1' of the ray above the new chief ray is

$$Y_1' = Y_1 - \bar{Y}_1^* = Y_1 - \bar{y}_1^* \left(\frac{\bar{Y}_o}{\bar{y}_o}\right) .$$

By substituting this expression into the sum of Equations (6) and (8), and by using the relation,

$$Q = \bar{y}_1^* / y_1 ,$$

it is possible to arrive at the equation

$$(Y_k - \bar{Y}_o\, m) = -\frac{1}{2(n_{k-1}\, u_{k-1})} \left[\Sigma B (Y_1'^2 + X_1^2) \left(\frac{Y_1'}{y_1^3}\right) + (Q\Sigma B + \Sigma F)\left(\frac{3Y_1'^2 + X_1^2}{y_1^2}\right)\left(\frac{\bar{Y}_o}{\bar{y}_o}\right) + \right.$$

$$\left[3Q^2\Sigma B + 6Q\,\Sigma F + \Sigma(3C + P\Phi^2)\right] \left(\frac{Y_1'}{y_1}\right) \left(\frac{\bar{Y}_o}{\bar{y}_o}\right)^2 +$$

$$\left. \left[Q^3\Sigma B + 3Q^2\Sigma F + Q\Sigma(3C + P\Phi^2) + \Sigma E\right]\left(\frac{\bar{Y}_o}{\bar{y}_o}\right)^3 \right] . \qquad (17)$$

8.9.3 Third order aberration coefficients. Equation (17) is the aberration polynomial with a shifted chief ray and therefore a shifted entrance pupil. If this equation is compared with the sum of Equations (6) and (8) it has a similar form. In Equation (17) the original aberration coefficients ΣB, ΣF, ΣC, ΣE and ΣP have been replaced by linear combinations of these coefficients. Since the aberration polynomial has the same form it can be said that the third order coefficients have changed to new values. The new third order coefficients will be indicated with a superscript *. By comparing Equation (17) with Equations

(6) and (8) it follows that

$$\Sigma B^* = \Sigma B , \tag{18}$$

$$\Sigma F^* = Q\Sigma B + \Sigma F , \tag{19}$$

$$\Sigma C^* = Q^2 \Sigma B + 2Q\Sigma F + \Sigma C , \tag{20}$$

$$\Sigma E^* = Q^3 \Sigma B + 3Q^2 \Sigma F + Q\Sigma(3C + P\Phi^2) + \Sigma E , \tag{21}$$

and

$$\Sigma P^* = \Sigma P . \tag{21a}$$

8.9.4 First order aberration coefficients. Using Equation 6-(39), to complete the list of changes of the aberration coefficients as the chief ray is changed, the chromatic coefficients then become

$$a^* = a , \tag{22}$$

and

$$b^* = Q a + b . \tag{23}$$

8.9.5 Use of the stop shift equations.

8.9.5.1 These equations, (18-23), are often called the stop shift equations. They are extremely useful and will be referred to many times in later sections. They enable the designer to predict how the third order coefficients change with the choice of the chief ray. Again we see that any two paraxial rays traced through the lens are sufficient for all third order calculations on the system. If the oblique chief ray traced through the system turns out not to pass through the center of the new aperture stop, it is possible to use the stop shift formulae to compute the third order coefficients for the chief ray that does pass through.

8.9.5.2 The designer should note that Equation (17) uses the aperture variable Y_1' . As shown in Figure 8.11, Y_1' is the height of a general ray above the new chief ray in the original entrance pupil. The height of this general ray above the chief ray in the new entrance pupil will not be Y_1' if the object is at a finite distance. In order to write the polynomial in terms of Y_1 one must account for the magnification between the original and the new entrance pupil. Now it should be noted that the polynomial involves the ratio of Y_1' / y_1 . It turns out that the corresponding ratio for the new entrance pupil has the same value. Therefore the aberration polynomial, Equation (17), can be used with Y_1' and y_1 as coordinates in the new entrance pupil.

8.10 THIN LENS ABERRATION THEORY

8.10.1 Third order coefficients. It is possible to combine the two surface contributions of a thin lens in air and obtain simple expressions for the third order aberrations. By assuming that the lens is thin, the values of y for the axial paraxial ray are the same on the two surfaces. If it is further assumed that the lens is the aperture stop (and hence the entrance and exit pupils), the oblique paraxial chief ray passes through the center of the thin lens at $\bar{y} = 0$. The third order aberration coefficients of the thin lens are then

$$B = \alpha_1 + \alpha_2 c_1 + \alpha_3 c_1^2 , \tag{24}$$

$$F = \beta_1 + \beta_2 c_1 , \tag{25}$$

$$C = -\phi\Phi^2 , \tag{26}$$

$$E = 0 , \tag{27}$$

and

$$P = -\frac{\phi}{n} . \tag{28}$$

The constants of the new equations are:

$$\alpha_1 = -\frac{\phi y^4}{n}\left[(3n+2)\left(\frac{u_{-1}}{y}\right)^2 + \left(\frac{\phi n}{n-1}\right)^2 n - \frac{\phi n}{n-1}(3n+1)\frac{u_{-1}}{y}\right], \quad (29)$$

$$\alpha_2 = -\frac{\phi y^4}{n}\left[(4n+4)\left(\frac{u_{-1}}{y}\right) - \left(\frac{\phi n}{n-1}\right)(2n+1)\right], \quad (30)$$

$$\alpha_3 = -\frac{\phi y^4}{n}(n+2), \quad (31)$$

$$\beta_1 = \frac{\phi \Phi y^2}{n}\left[(2n+1)\frac{u_{-1}}{y} - \left(\frac{\phi n}{n-1}\right) n\right], \quad (32)$$

$$\beta_2 = \frac{\phi \Phi y^2}{n}(n+1), \quad (33)$$

$$\phi = \frac{(u_{-1} - u)}{y} = \frac{1}{f} \text{ (from Equation 6-(24))}, \quad (34)$$

and

$$\Phi = \bar{y}\, u_{-1} - y\, \bar{u}_{-1} = \bar{y} u - y \bar{u}, \quad (35)$$

where u_{-1} is the angle of the axial paraxial ray in air on the left hand side of the thin lens and u is the angle of this ray in air on the right hand side, n is the index of the lens, and c_1 is the curvature of the first surface.

8.10.2 Limitations; comparison with thick lens results.

8.10.2.1 Equations (24) through (28) are valid for any thin lens in air at any position in a system provided $\bar{y} = 0$ at the lens. If the value of $\bar{y}$ is not zero it is necessary to calculate B^*, F^*, C^*, E^*, and P^* from the stop shift equations (18) through (21a). With the proper substitution it can be shown that,

$$B^* = \alpha_1^* + \alpha_2^* c_1 + \alpha_3^* c_1^2, \quad (36)$$

$$F^* = \beta_1^* + \beta_2^* c_1 + \beta_3^* c_1^2, \quad (37)$$

$$C^* = \gamma_1^* + \gamma_2^* c_1 + \gamma_3^* c_1^2, \quad (38)$$

$$E^* = \delta_1^* + \delta_2^* c_1 + \delta_3^* c_1^2. \quad (39)$$

The coefficients of these quadratic equations are as follows:

$$\alpha_1^* = \alpha_1, \quad \alpha_2^* = \alpha_2, \quad \alpha_3^* = \alpha_3, \quad (40)$$

$$\beta_1^* = Q\alpha_1 + \beta_1, \quad (41)$$

$$\beta_2^* = Q\alpha_2 + \beta_2, \quad (42)$$

$$\beta_3^* = Q\alpha_3, \quad (43)$$

$$\gamma_1^* = Q^2 \alpha_1 + 2Q\beta_1 - \phi\Phi^2, \quad (44)$$

$$\gamma_2^* = Q^2 \alpha_2 + 2Q\beta_2, \quad (45)$$

$$\gamma_3^* = Q^2 \alpha_3, \quad (46)$$

$$\delta_1^* = Q^3 \alpha_1 + 3Q^2 \beta_1 - Q(3n+1)\frac{\phi\Phi^2}{n}, \quad (47)$$

$$\delta_2^* = Q^3 \alpha_2 + 3Q^2 \beta_2, \quad (48)$$

and

$$\delta_3^* = Q^3 \alpha_3. \quad (49)$$

8.10.2.2 To illustrate the use of these equations a sample calculation for all the thin lens coefficients is presented in Table 8.4. In this example, the calculations were made on the thin lens illustrated in Table 6.13. Table 8.2 shows the same lens system with thickness added. The thin lens equations were used with

$c_1 = 0.253$ for lens (a),

$c_1 = -0.200$ for lens (b),

and

$c_1 = 0.050$ for lens (c).

8.10.2.3 Table 8.3 lists a comparison between the third order aberration coefficients calculated from the thin lens equations and those calculated from the surface contributions of the thick lens. The differences between the coefficients is due to the thicknesses introduced in the sample shown in Table 8.2. Slight differences are also due to the differences in c_1.

8.10.2.4 In the following sections it will be demonstrated how the thin lens equations are used in the preliminary design of a lens system.

Lens and Coefficient		Thin Lens Formula	Thick Lens Formula
Lens (a) $C_1 = 0.253$	B	-0.0365	-0.0355
	F	0.0241	0.0221
	C	-0.0647	-0.0604
	E	0.1046	0.0962
	P	-0.1021	-0.1024
Lens (b) $C_1 = -0.200$	B	0.0722	0.0731
	F	-0.0340	-0.0352
	C	0.0895	0.0919
	E	-0.0182	-0.0195
	P	0.1770	0.1759
Lens (c) $C_1 = 0.050$	B	-0.0443	-0.0440
	F	0.0136	0.1029
	C	-0.0290	-0.0272
	E	-0.0776	-0.0746
	P	-0.1124	-0.1135

Table 8.3 - Comparison between third order aberrations calculated from thin lens equations and from individual surface contributions of a thick lens.

Quantity	Lens (a)	Lens (b)	Lens (c)
y^2	2.25000	1.28989	1.56630
y^4	5.06250	1.66380	2.45329
$-\phi y^4/n$	-0.51678	0.29456	-0.27574
$\phi\Phi$	-0.09029	0.15669	-0.09942
$\phi\Phi y^2/n$	-0.12541	0.12468	-0.09612
$-\phi\Phi^2$	-0.04930	0.08555	-0.05428
n+1	2.6200	2.6210	2.6200
n+2	3.6200	3.6210	3.6200
2n+1	4.2400	4.2420	4.2400
3n+1	5.8600	5.8630	5.8600
3n+2	6.8600	6.8630	6.8600
4n+4	10.4800	10.4840	10.4800
u_{-1}/y	0	-0.21841	0.06223
$\phi n/n-1$	0.43210	-0.74911	0.47576
$(3n+2)\left(\frac{u_{-1}}{y}\right)^2$	0	0.32739	0.02656
$\left(\frac{\phi n}{n-1}\right)^2 n$	0.30246	0.90964	0.36668
$-\frac{\phi n}{n-1}(3n+1)\frac{u_{-1}}{y}$	0	-0.95926	-0.17348
α_1	-0.15631	0.08182	-0.06060
$(4n+4)\frac{u_{-1}}{y}$	0	-2.28981	0.65213
$-\frac{\phi n}{n-1}(2n+1)$	-1.83209	3.17771	-2.01721
α_2	0.94679	0.26153	0.37641
α_3	-1.87075	1.06659	-0.99817
$(2n+1)u_{-1}/y$	0	-0.92650	0.26384
$-\left(\frac{\phi n}{n-1}\right)n$	-0.70000	1.21430	-0.77073
β_1	0.08778	0.03588	0.04872
β_2	-0.32856	0.32680	-0.25183
Q	-0.53333	-0.06268	0.50844
β_1^*	0.17115	0.03076	0.01791
β_2^*	-0.83352	0.31040	-0.06045
β_3^*	0.99773	-0.06686	-0.50752
γ_1^*	-0.18740	0.08138	-0.02040
γ_2^*	0.61978	-0.03994	-0.15878
γ_3^*	-0.53212	0.00419	-0.25804
δ_1^*	0.19373	-0.01899	-0.07001
δ_2^*	-0.42400	-0.00379	-0.14584
δ_3^*	0.28380	-0.00026	-0.13120

Table 8.4 - Calculation of the thin lens coefficients for the thin lens shown in Table 6.13.

9 METHOD OF LENS DESIGN

9.1 THE PROCESS OF DESIGNING A LENS SYSTEM

9.1.1 Introduction. The formulae used to design a lens system have now been presented. Ray trace equations were derived in Section 5. Their use in first order design and in aberration analysis were discussed in Sections 6 and 8. In the present section a systematic method for the design of lens systems will be described, and this method will be illustrated with the design of a triplet flat field lens in Section 10.

9.1.2 Approach. The design of a lens system at the present state of the art is an iterative procedure. Certain steps in the procedure are repeated until a satisfactory design is attained. In this sense, lens design involves a trial and error procedure. At present (1962), direct methods of design, proceeding from the desired specifications to the specific lens, do not exist. The following steps are the basic elements of the iterative procedure.

(1) Select a lens type.

(2) Find a first order thin lens solution.

(3) Find a third order thin lens solution.

(4) Find a thick lens solution, and calculate first order and third order aberrations.

(5) Trace a few selected meridional and skew fans.

(6) Adjust third order coefficients to balance higher order aberrations, and repeat steps 5 and 6 until the balance between third and higher order aberrations agrees with desired specifications, or at least is reasonable.

(7) Trace additional fans of skew rays; make spot diagrams and calculate the energy distribution.

(8) Evaluate the image.

(9) Return to a previous step and repeat the process until evaluation indicates desired performance. Which step to return to depends on the problem. The most usual procedure is to return to step (4), but often the designer must return to step (1).

9.2 DESCRIPTION AND ANALYSIS OF THE BASIC PROCEDURE

9.2.1 Step 1 - Selection of a lens type.

9.2.1.1 In order to select the type of lens to be designed, the designer must first survey the complete lens problem. He attempts to equate it to one of the simple basic optical systems. He asks if this is a magnifier problem, a microscope, a telescope or a camera lens. After deciding upon the basic system, he then proceeds to make a layout using simple theory as illustrated in Section 7. This analysis thus generates a possible arrangement picture of how the axial and oblique rays will pass through the system.

9.2.1.2 Suppose, for example, that the system to be designed is a telescope. Given the magnifying power, field of view and over-all instrument length, a designer may conclude that the telescope should consist of an objective, a prism erecting system and an eyepiece. From the preliminary analysis he concludes that the objective must work at $f/3.5$ and the eyepiece must cover a half field of 30°. Looking over objective designs (for example, see Section 11) he may then compute the field curvature for the system and conclude that he will use an objective like the one illustrated in Figure 11.7, and, since the eyepiece must cover a half field of 30°, an Erfle type appears to be a logical choice. Inspection of the eyepieces shown in Section 14 discloses that the Erfle is the simplest design. It represents a good starting point.

9.2.1.3 Other factors may influence the designer's choice. Compatability with other systems, existing hardware, economics or delivery schedule are all valid considerations. Thus, unfortunately for the beginner, this step in the procedure is difficult and requires the most experience. As the process proceeds, the steps become more automatic and less dependent on experience. This means that the beginner finds it difficult to get started and it means that the designer instructing must say in effect at the beginning,

"Let us start with a lens of such and such a type. Later I may be able to show you why I picked this particular type of solution." This approach to a problem does not appeal to the analytic mind but at present there is no other way to approach the problem. It would be nice if one could work from the specifications of the image, back to the design required, but there are only very limited procedures which will enable one to establish what lens type is needed for a particular problem. In Sections 10, 11, 12, 13, and 14 the performance and limitations of several types of lenses will be described which it is hoped will help a beginner select the type of lens.

9.2.1.4 The prime accomplishment of this step is the designer's decision to choose a certain lens type to perform a specified function in the system. Thus a starting point is established from which computation and evaluation can proceed. This step, baffling as it is to the beginner, is really the most creative part of the design, and, as experience is gained, this is the part of the design that intrigues the designer and gives him a chance to exercise judgement, which is what humans usually enjoy.

9.2.2 Step 2 - The first order thin lens solution. Once the lens type has been decided on, the next step is to solve the algebraic equations to determine the individual focal lengths and spacings of the elements. It greatly simplifies the procedure to assume that the lenses are thin. At this stage of the problem, there are usually conditions that must be satisfied in the passage of the axial paraxial ray, and the oblique paraxial ray. The entrance and exit pupils may have to be located at special positions, and their sizes may be given. The focal length and back focal length may be specified. It is also necessary to adjust the axial and lateral color, and Petzval sum to appropriate values. The passage of the oblique chief ray has an effect on the distortion. For simple systems it often is possible to write down algebraic equations relating the parameters of the system (ϕ, t, n) and the required conditions to be satisfied, but very often the algebra becomes so complex that graphical or linear approximations are required to find the solutions. The problem basically amounts to trying to solve a set of non-linear equations. Sometimes there are more equations than variables, in other instances the reverse may be true. One can spend a great deal of time on the algebra at this stage of the design. Often, the most sensible procedure is to resort to a systematic trial and error solution. This method will be illustrated in Section 10.2

9.2.3 Step 3 - The third order thin lens solution. By making the thin lens aberration coefficient calculations illustrated in Table 8.4, it is possible to obtain sets of second degree algebraic equations relating the first curvatures of the lenses and the aberrations. Again, in simple systems these can sometimes be solved algebraically or graphically. As a matter of fact, if these equations cannot be solved algebraically there is little justification for using the thin lens approximations, for one can as readily apply the trial and error methods to thick lenses using the surface contribution calculations shown in Table 8.2. By properly choosing the position of the aperture stop it is possible to greatly simplify the equations. The following reasoning is used in the preliminary design. In the preliminary third order design the aberrations are usually all made equal to zero. Equations 8-(18) through 8-(21) show us, that if B, F, C, E and P are all set to zero, then B*, F*, C*, and E* will all be zero. This tells us that the location of the stop position has no effect on the aberrations. Then it is advisable to choose the chief ray to pass through the center of one of the lenses. By so doing, the aberrations for this lens are given by Equations 8-(24) through 8-(28). This eliminates the calculation of E, the C is constant, and F varies linearly with c_1. In practice, it helps to use this procedure even if small residual aberrations are to be left in the system.

9.2.4 Step 4 - First and third order aberrations of a thick lens.

9.2.4.1 During this step in the design, calculations of the type shown in Table 8.2 are made to determine the first and third order aberrations of the lens with actual thicknesses. If the thin lens theory has been worked out completely, then values for the curvatures and the desired angles of the axial and oblique rays are known. Now, the procedure of introducing thicknesses changes all the first order and third order aberrations. The next problem is to modify the thick lens solution to achieve the desired aberrations.

9.2.4.2 Some designers have procedures for computing the positions of the principal planes of each individual element. Then the thick lens system is set up so that the first curvatures of each of the lenses are the same as for each of the thin lenses, and the angles the axial ray makes with the axis is the same as for the thin lenses. Finally, the spaces between the lenses are adjusted to make the spacings between the image principal plane (P_{2a}) and the next object principal plane (P_{1b}) of the thick lenses equal to the spacing between the thin lenses.

9.2.4.3 The designer should not spend too much time trying to adjust the spacings in this way since there is no direct and easy way to set up a thick lens equivalent of the thin lens. The procedure just described always fails to keep all the aberrations the same as for the thin lens; some changes in the power distribution are necessary.

9.2.4.4 If the designer is setting up for the first time a thick lens from thin lens data, there is really very little point in trying to make the thick lens aberrations exactly equal to the thin lens aberrations. The reason for this is that until one has ray traced a design, and determined the magnitude of the higher order aberrations, it is not possible to tell just what third order aberrations are needed to balance out those of a higher order. Usually, a perfectly satisfactory way to set up a thick lens from thin lens data is to assume the positions of the principal planes, from a simple sketch of the lens, using curvatures from the thin lens solution and thicknesses from 10.4.

9.2.4.5 A major problem in lens design is the problem of adjusting a thick lens to arrive at some definite third order aberrations. This can be done by a trial and error method if some information is known about how the aberrations vary with parameter changes. Sometimes the information in the form of curves for the thin lenses provides indications to the designer which help him decide how to adjust the thick lens to find a solution.

9.2.4.6 The problem of adjusting a thick lens system resolves itself into the problem of solving a set of simultaneous equations. One can systematically change one parameter at a time and recalculate all the total aberrations of the new system. By finding the differences in the total aberrations due to the parameter change, it is possible to compute the parameter differential for all the third and first order aberrations. This method will now be discussed in detail.

9.2.4.7 Since B, F, C, E, P, a, and b are functions of all the system parameters, it is possible to write

$$\Delta\Sigma B = \sum_{j=1}^{j=k-1} \left[\left(\frac{\partial \Sigma B}{\partial c}\right)_j \Delta c_j + \left(\frac{\partial \Sigma B}{\partial t}\right)_j \Delta t_j + \left(\frac{\partial \Sigma B}{\partial n}\right)_j \Delta n_j \right], \quad (1)$$

$$\Delta\Sigma F = \sum_{j=1}^{j=k-1} \left[\left(\frac{\partial \Sigma F}{\partial c}\right)_j \Delta c_j + \left(\frac{\partial \Sigma F}{\partial t}\right)_j \Delta t_j + \left(\frac{\partial \Sigma F}{\partial n}\right)_j \Delta n_j \right], \quad (2)$$

$$\Delta\Sigma C = \sum_{j=1}^{j=k-1} \left[\left(\frac{\partial \Sigma C}{\partial c}\right)_j \Delta c_j + \left(\frac{\partial \Sigma C}{\partial t}\right)_j \Delta t_j + \left(\frac{\partial \Sigma C}{\partial n}\right)_j \Delta n_j \right], \quad (3)$$

$$\Delta\Sigma E = \sum_{j=1}^{j=k-1} \left[\left(\frac{\partial \Sigma E}{\partial c}\right)_j \Delta c_j + \left(\frac{\partial \Sigma E}{\partial t}\right)_j \Delta t_j + \left(\frac{\partial \Sigma E}{\partial n}\right)_j \Delta n_j \right], \quad (4)$$

$$\Delta\Sigma P = \sum_{j=1}^{j=k-1} \left[\left(\frac{\partial \Sigma P}{\partial c}\right)_j \Delta c_j + \left(\frac{\partial \Sigma P}{\partial t}\right)_j \Delta t_j + \left(\frac{\partial \Sigma P}{\partial n}\right)_j \Delta n_j \right], \quad (5)$$

$$\Delta\Sigma a = \sum_{j=1}^{j=k-1} \left[\left(\frac{\partial \Sigma a}{\partial c}\right)_j \Delta c_j + \left(\frac{\partial \Sigma a}{\partial t}\right)_j \Delta t_j + \left(\frac{\partial \Sigma a}{\partial n}\right)_j \Delta n_j + \left(\frac{\partial \Sigma a}{\partial \nu}\right)_j \Delta \nu_j \right], \quad (6)$$

$$\Delta\Sigma b = \sum_{j=1}^{j=k-1} \left[\left(\frac{\partial \Sigma b}{\partial c}\right)_j \Delta c_j + \left(\frac{\partial \Sigma b}{\partial t}\right)_j \Delta t_j + \left(\frac{\partial \Sigma b}{\partial n}\right)_j \Delta n_j + \left(\frac{\partial \Sigma b}{\partial \nu}\right)_j \Delta \nu_j \right]. \quad (7)$$

9.2.4.8 In order to correct a finite thickness lens system to any desired third and first order aberrations, a designer must, in effect, solve this set of simultaneous equations. Now since B, F, C, E, P, a, and b do not change linearly with parameter changes, these equations will not, in general, provide the correct changes, so the process must be repeated for a series of iterations. Without a large computer it was a hopelessly long procedure to systematically correct a system to a given set of third order values. Therefore, designers had to resort to other techniques. They did this by separating the problem into two parts. First, a solution was found which corrected a, b, and P, with some consideration given to E. Second, this solution was corrected for B, F, and C.

9.2.4.9 The first step, correction of a, b, P, and E, was done by adjusting the focal lengths of the lenses and the spacings between the lenses. Sometimes different coefficients were found for the changes of a, b, and P, and simultaneous equations solved, but the index and dispersion of glass were usually not included because glasses are manufactured in finite steps. Usually designers resorted to a simple trial and error method of adjusting focal lengths, spaces, and glasses. It is surprising how rapidly an experienced designer can adjust variables and arrive at a solution without actually solving the above equations.

9.2.4.10 The second step, correction of B, F, and C, was done by the technique called bending. Lens bending means changing the shape of a lens without affecting its focal length. Equation 6-(22)

gives the expression for the power ϕ of a lens as $(c_1 - c_2)(n-1)$. As long as $c_1 - c_2$ remains constant, c_1 may take on any value without affecting ϕ. If the lens is thin, then bending does not change the angles of the axial and oblique paraxial rays after passage through the lens. If the lens is thick, keeping $(c_1 - c_2)$ constant is not quite the same thing as keeping the focal length fixed because f' depends on t as well as $(c_1 - c_2)$. Usually in bending thick lenses, it is advisable to solve for the second curvature so that the axial ray remains at a constant angle with the optical axis. Bending of a lens has no effect on a, b and P for a thin lens and a very small effect in a thick lens. The bending affects primarily B, F, and C.

9.2.4.11 Therefore, before the widespread use of computers, designers found solutions for given values of B, F, and C by setting up three simultaneous equations. Usually many of the possible degrees of freedom were not used. Experienced lens designers seldom actually solved the equations, but they would keep adjusting the lens by a trial and error method. In the lens designers' slang, the method for finding a solution is jiggle in or poke at it. It is amazing how successfully an experienced designer could jiggle in a design. This method appears to be an art. With experience a designer apparently develops a procedure analogous to solving these equations in his head, by developing a feel for the system.

9.2.4.12 With the modern computer it is now feasible to find automatically a solution of Equations (1) through (7). In Section 10 several examples will be shown illustrating how this is done. Up to the present, the equations solved automatically by the computer have not included the terms with the glass type as a variable. Many problems have been solved using curvatures and thicknesses as variables. The automatic program does essentially the following:

(1) All the first and third order calculations are computed for an initial system. Call this system No. 1.

(2) Each system parameter (c or t) is varied one at a time, and all the first and third order aberrations are calculated for each altered system. The designer may specify which curvatures and thicknesses to change. Each parameter is changed by 0.01% of its initial value.

(3) Differential coefficients are then computed for each variable and aberration. For example,

$$(c_{new} - c_{old})_j = \Delta c_j ,$$

and

$$(\Sigma B_{new} - \Sigma B_{old})_j = \Delta \Sigma B_j .$$

Then

$$\left(\frac{\partial \Sigma B}{\partial c}\right)_j \approx \frac{\Delta \Sigma B_j}{\Delta c_j}$$

(4) When all the differential coefficients are known, the data for the seven equations (1) through (7) are known. The numbers on the left hand side of the equation are found by taking the difference between the aberrations in system No. 1 and the final target (desired) values for the aberrations. For example,

$$\Delta \Sigma B = (\Sigma B_{target} - \Sigma B_1) \text{ etc.}$$

(5) If there are seven variables in the optical system then there will be seven equations with seven unknowns. If there are more variables than equations then the set of equations cannot be uniquely solved. One technique is to impose the condition, that the sum of the squares of the changes in the parameters shall be a minimum. If there are fewer variables than equations then it is not possible to obtain an exact solution. In this case it is customary to solve for a least squares solution. This means a solution is found when the sum of the squares of the differences between the final aberrations and their target values is a minimum.

(6) If the aberrations changed linearly with parameter changes, the target values for the aberrations would be found in one step. However the changes are not usually linear, so the process has to be repeated several times. If the target values for the aberrations are far removed from the initial values, there is the real possibility that this inherently simple procedure will not converge to a solution. Knowledge of the regions of solution is an invaluable aid in helping to select the initial values for system No. 1.

9.2.5 Step 5 - Tracing a few selected meridional and skew fans.

9.2.5.1 After the third order solution is found, the next step is to trace a few selected rays to evaluate the effects of higher order aberrations. The number of rays to trace depends on the stage of the design. On the first ray trace of a new system, only a small number of rays need be traced, but as the design proceeds, additional rays may be necessary for added refinement.

9.2.5.2 One suggested plan for the ray tracing of a design is as follows:

(1) The 0° image. In D light trace three rays at $Y_1 = (Y_1)_{max.}$,

$Y_1 = 0.7\ (Y_1)_{max.}$, $Y_1 = 0.5\ (Y_1)_{max.}$,

where $(Y_1)_{max.}$ is the radius of the entrance pupil. Trace the same rays in F and C light.

(2) If the object is at infinity, trace three meridional fans of rays at angles corresponding to $L_o = (L_o)_{max.}$, $L_o = 0.7\ (L_o)_{max.}$ and $L_o = 0.5\ (L_o)_{max.}$. If the object is at a finite distance, trace the rays from three object points $\overline{Y}_o = (\overline{Y}_o)_{max.}$, $\overline{Y}_o = 0.7\ (\overline{Y}_o)_{max.}$ and $\overline{Y}_o = 0.5\ (\overline{Y}_o)_{max.}$. For each obliquity, trace at least five meridional rays to enter the entrance pupil at uniform intervals ranging from $Y_1 = (Y_1)_{max.}$ to $Y_1 = -(Y_1)_{max.}$.

(3) For each obliquity, trace three skew rays with coordinates in the entrance pupil as follows:

$(X_1)_{max.}$,	$Y_1 = 0$	$(X_1)_{max.} = (Y_1)_{max.}$
$0.7\ (X_1)_{max.}$,	$Y_1 = 0$	since the entrance pupil is assumed
$0.5\ (X_1)_{max.}$,	$Y_1 = 0$	to be a circle.

(4) Repeat steps 2 and 3 for F and C light.

9.2.5.3 The data from the ray tracing may be plotted as illustrated in Figure 8.5, and Figures 8.7 through 8.10. In practice, this data is plotted on a single diagram usually leaving out the plots shown in Figures 8.8b and 8.9 . A plot of this type is shown in Figure 9.1. In making these plots, it is advisable to use the same scale for all the plots of Y_k and X_k . At first it might appear that lenses of different focal lengths should be plotted using different scales. Actually, for most applications, the scale shown in Figure 9.1 represents the size of images used most frequently. Therefore, it simplifies plotting and helps one to assess rapidly a lens if these plots are made on this standard scale. Notice that 0.01 division on the vertical scale corresponds to 1 cm. (But this has been reduced to 0.86 cm in reproduction.) If the lens is calculated in centimeters, then 1 cm on the vertical scale of the graph corresponds to 100 microns. If the lens is calculated in inches, the 0.01 division should be replaced by 0.004, so that again 1 cm indicates a 100 micron image. If it turns out that the aberrations are so large they cannot be plotted on this scale, they are so large that they probably are not worth plotting.

9.2.6 Step 6 - Adjusting third order aberrations. Usually one attempts to make the curves in Figure 9.1 as flat as possible. In a perfect lens the curves would be horizontal straight lines. In most cases this can not be achieved, even to practical limits. The usual curves look more like the ones shown in Figure 9-1. Take for example the curves shown for the image point at 1.76. The meridional rays are focused within a strip 0.012 wide. The skew rays are confined within a strip 0.016 wide. One can say with fair assurance that the complete image is confined to an area 0.012 by 0.016. Since the meridional ray plot

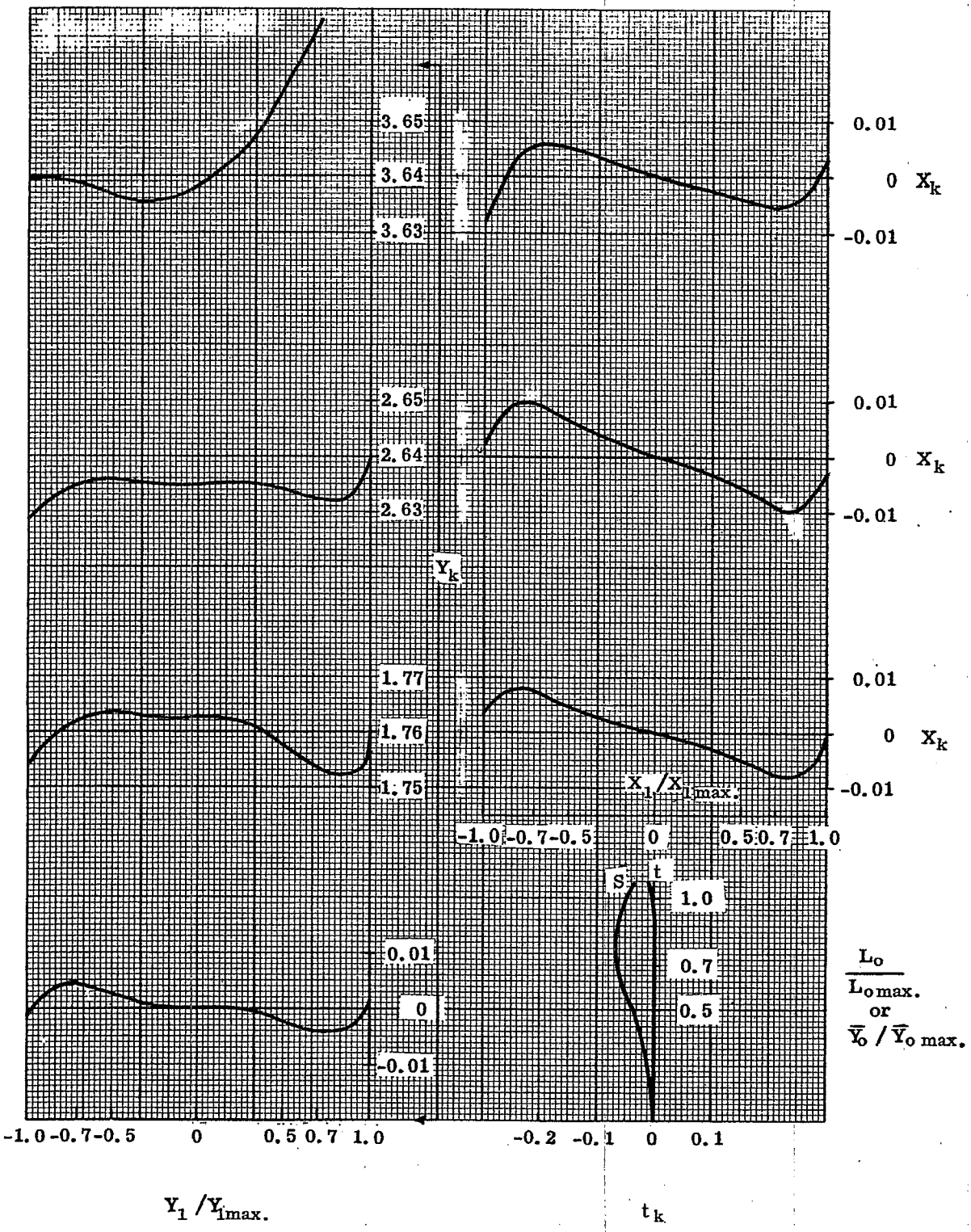

Figure 9.1- Sample plot of selected ray trace data.

shows a region where the curve is flat and horizontal, one would expect to get some concentration of energy towards the center of the spot. When one begins adjusting a design it is usually possible to tell from these curves what is needed to improve the energy concentration. For example, the basic difficulty with the design represented by Figure 9.1 is that the Petzval sum is too negative. This is the reason the skew curves are so far from the horizontal. One can also see that the image at a height of 3.64 will be poor because of the over-corrected spherical aberration in the upper meridional rays. These defects might suggest to the designer that he should try to find a solution with less negative Petzval curvature and introduce more negative third order spherical aberration. If so he would then return to Step 4 in paragraph 9.2.4 and solve for new third order aberrations, and repeat Step 5. Several alternate solutions may therefore evolve, but eventually it will be necessary to evaluate the energy concentration by proceeding to Step 7.

9.2.7 Step 7 - Calculation of spot diagrams and energy distributions. The energy distribution curves should be computed as described on page 8.1. Usually it is advisable to compute the energy distribution curves for a field point on the axis, for one half-way out in the field and for one at the edge of the field. Strictly speaking, one should also compute curves for two or three wavelengths, but this takes a great deal of computing and usually is not necessary for the average problem.

9.2.8 Step 8 - Image evaluation.

9.2.8.1 Once the designer has computed the energy distributions in several images in the field he is able to compare these with the design requirements. Seldom can one achieve the required results in the first system analyzed. The designer must then decide whether to continue with this design or to shift over to another type of lens. If he shifts over to another lens type he may then return to Step 1. If he decides to stick with the present lens type, he must decide whether to continue trying to meet the original specifications or whether to seek to modify the specifications and provide an alternative compromise solution. Usually the modern design problems end up with a give and take solution. The designer must therefore completely understand how the lens will perform, and be able to show what can be achieved by making variations in the original specifications. This means he may have to carry several designs up to the energy distribution curves in Step 7 in order to make a wise decision. It is imperative therefore that he devise ways to quickly evaluate the design.

9.2.8.2 The energy distribution curves of Step 7 may be used to check the image quality. This is a satisfactory method for many optical systems, but if the image quality is high one must consider the calculation of diffraction effects. As a general rule, one does not need to worry about diffraction effects if the wavefront departs from a perfect sphere by more than two to five wavelengths. (A method of computing this departure from ray trace data is described by H. H. Hopkins.*) There are several criteria one can apply to gauge the influence of diffraction, but this is a subject in itself. (See Sections 16, 25, 26.) However, a designer should be familiar with the wavefront tolerances suggested by Conrady.**

9.2.8.3 One must remember that it is impossible to concentrate the energy in an image into a smaller spot size than predicted by diffraction. In Figure 9.2 a plot of energy distribution is shown for a perfect lens. The abscissa Z is the following:

$$Z = \frac{\pi \, Y_e d}{\lambda \, \ell'} \quad ,$$

where

Y_e is the radius of the exit pupil

d is the diameter of the image spot

λ is the wave length of light

ℓ' is the distance from the exit pupil to the image plane which is located at the perfect focus.

The first dark ring occurs at a value of Z equal to 3.83. This has a spot diameter

$$d = \left(\frac{3.83\,\lambda}{\pi}\right)\left(\frac{\ell'}{Y_e}\right) = 1.22\,\frac{\lambda\,\ell'}{Y_e}$$

* H. H. Hopkins, Wave Theory of Aberrations (Oxford University Press, London, 1950) pp. 21-23.

**A. E. Conrady, Applied Optics and Optical Design, Part 1 (Oxford University Press, New York, 1943) pp. 126-141. See also Part I, 2nd ed. (Dover, New York, 1957) pp. 126-141, and Part II (Dover, 1960) pp. 626-639.

It is always a good idea to plot this curve on the same graph with the energy distribution curves computed for the actual lens. If the geometrical energy distribution curves lie to the left of the diffraction curve one knows that the light will not concentrate as well as the geometrical distribution curves indicate. The actual distribution curve will be inclined to follow the diffraction curve. Quite often the geometrical energy distribution curve will cross the diffraction image curve as shown in Figure 9.3 One can then estimate the energy concentration by using the formula

$$Z_{G+D} = \sqrt{Z_G^2 + Z_D^2}\ .$$

Where Z_G ~ geometrical spot diameter

Z_D ~ diffraction spot diameter of a perfect aperture

Z_{G+D} ~ estimated spot diameter.

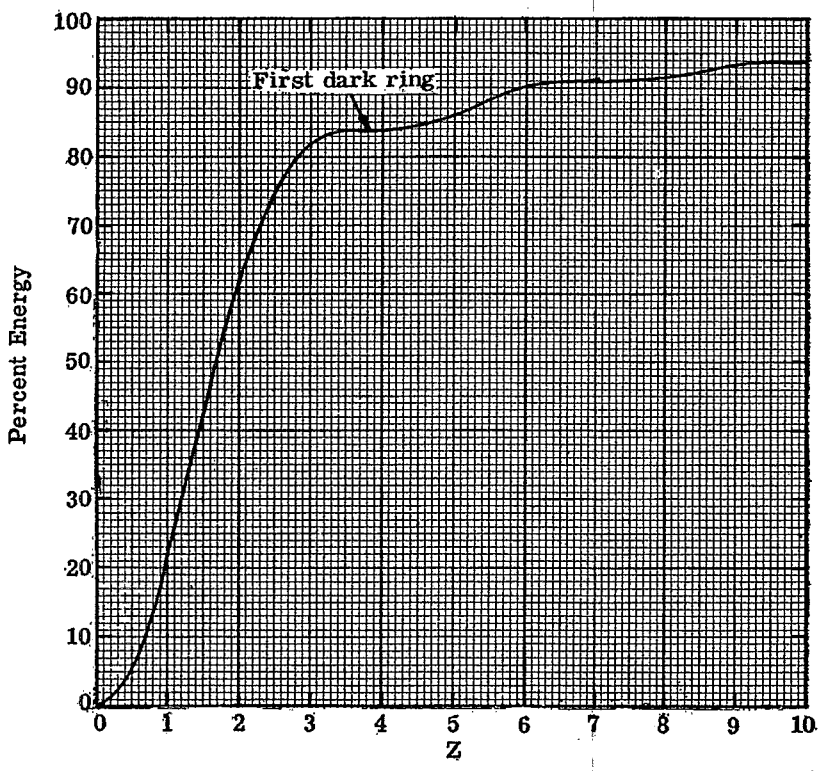

Figure 9.2 - Energy distribution for a perfect lens.

9.2.8.4 Some designers object to the energy distribution method for image evaluation because it does not take into account the orientation of the energy distribution. For example, if there is astigmatism the energy will be concentrated in a line image. The fact that the image of a point is a line might actually be favorable in some types of optical systems. For example, if the image is scanned by a slit one could certainly use this to advantage. For most optical systems however the circular energy distribution curves are adequate.

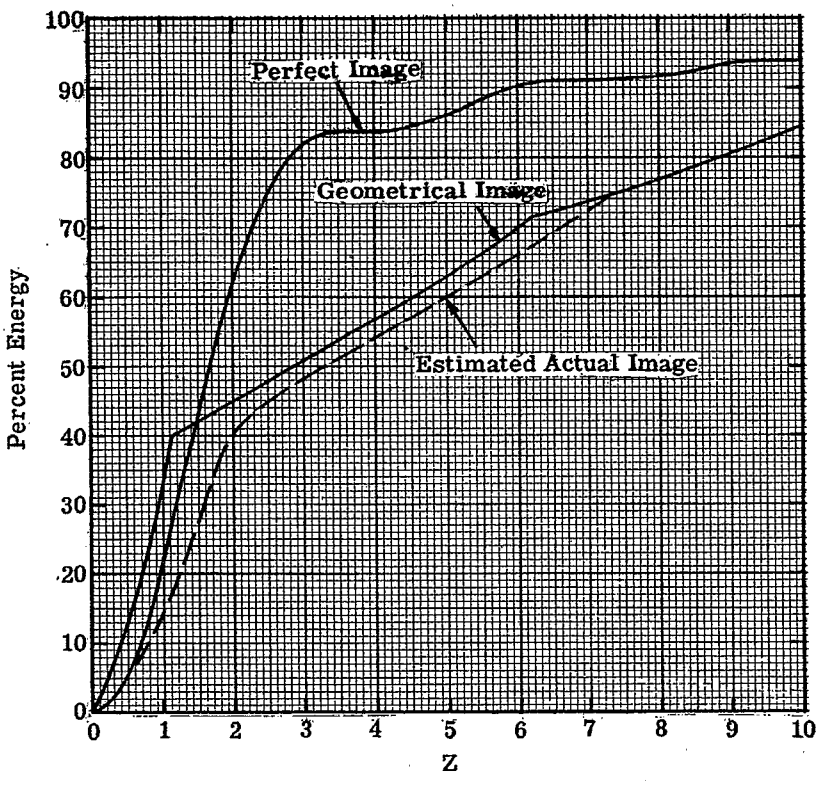

Figure 9.3 - Energy distribution curves.

9.2.8.5 The most modern method for evaluating images is to compute the optical transfer function (often called the sine wave frequency response) for the image. This can be done by performing a Fourier transform of the energy distribution in the image of a point source or a line source. Figure 9.4 shows a series of energy distribution curves. Figure 9.5 shows the corresponding modulation transfer curves. The modulation transfer function is the modulus of the complex optical transfer function. In Figure 9.4 all the curves are normalized to a maximum spot diameter of 10 mm. In Figure 9.5 the frequency is given in lines/mm. These spot diameters may of course be scaled to any other size. For example, suppose the maximum spot diameter is 100μ. Then the frequency scale should be multiplied by 100. One can multiply the modulation transfer function of a lens by the function for a detector to obtain the overall function for the entire optical system. Finally one can estimate the cutoff frequency at some particular response. A review of this approved image evaluation method may be found in Sections 26.2, 26.3 and 26.4, and in the article by Perrin ("Methods of Appraising Photographic Systems," J. Soc. Motion Picture and Television Eng., 69, 151-156, 239-249 (1960).

9.2.8.6 The problem of image evaluation is so involved that actually a designer is always forced to refer to some system which is known. Before attempting to improve a new system, a designer should try to do the following:

(1) Find out what systems have already been designed for conditions as nearly identical as possible with those specifying the new system.
(2) Evaluate the energy distribution of the nearest equivalent system.
(3) Compare the energy distribution in the new design with that of the closest equivalent to determine if improvement has been made.

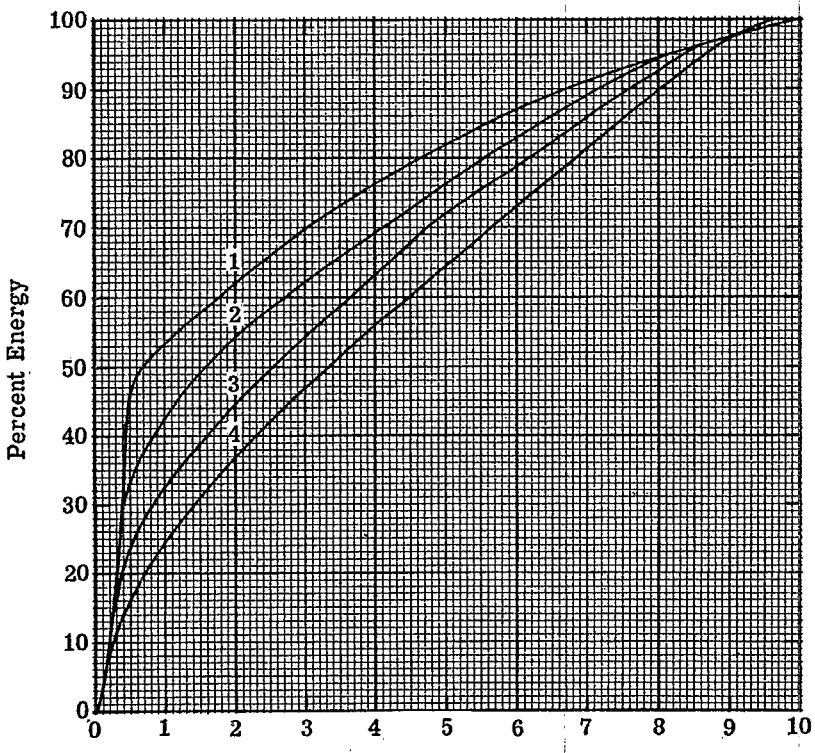

Figure 9.4 - A series of energy distribution curves.

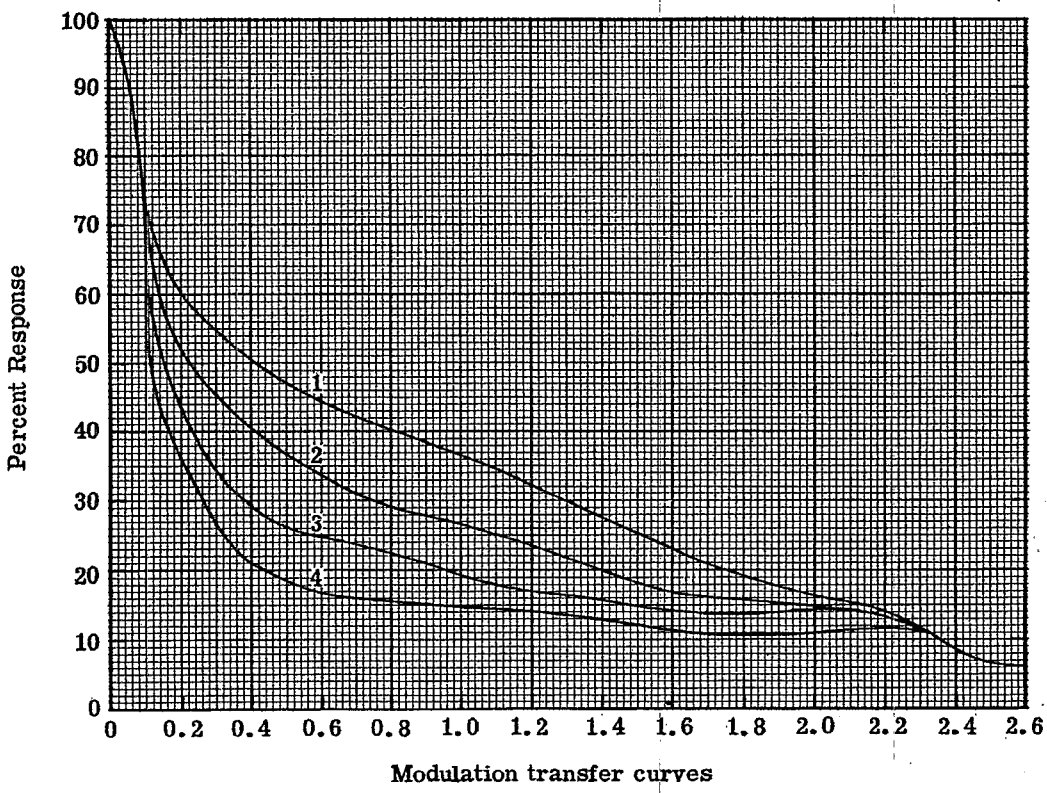

Figure 9.5 -

9.3 SUMMARY OF EQUATIONS USED IN THE CALCULATION OF THIRD ORDER ABERRATIONS

9.3.1 Paraxial ray trace equations.

$$y = y_{-1} + (t_{-1}/n_{-1})\ (n_{-1}\ u_{-1}) \qquad 5\text{-}(56)$$

$$nu = n_{-1}\ u_{-1} + y\ (n_{-1} - n)\ c \qquad 5\text{-}(57)$$

Alternate equations,

$$y = y_{-1} + t_{-1}\ u_{-1} \qquad 5\text{-}(56)$$

$$u = u_{-1} + i\left(\frac{n_{-1}}{n} - 1\right) \qquad 6\text{-}(3)$$

$$i = yc + u_{-1} \qquad 6\text{-}(4)$$

$$\Phi = \bar{y}\ (nu) - y\ (n\bar{u}) = \bar{y}\ (n_{-1}\ u_{-1}) - y\ (n_{-1}\ \bar{u}_{-1}) \qquad 6\text{-}(6)$$

9.3.2 Chromatic contribution formulae.

$$a = -yn_{-1}\ i\left(\frac{dn}{n} - \frac{dn_{-1}}{n_{-1}}\right) \qquad 6\text{-}(34)$$

$$b = -yn_{-1}\ \bar{i}\ \left(\frac{dn}{n} - \frac{dn_{-1}}{n_{-1}}\right) \qquad 6\text{-}(35)$$

9.3.3 Third order surface contributions.

$$S = yn_{-1}\left(\frac{n_{-1}}{n} - 1\right)\qquad (u + i) \qquad 8\text{-}(5)$$

$$\bar{S} = \bar{y}n_{-1}\left(\frac{n_{-1}}{n} - 1\right)\qquad (\bar{u} + \bar{i}) \qquad 8\text{-}(13)\ \text{footnote}$$

$$B = Si^2 \qquad 8\text{-}(4)$$

$$F = Si\ \bar{i} \qquad 8\text{-}(11)$$

$$C = S\bar{i}^2 \qquad 8\text{-}(12)$$

$$E = \bar{S}i\ \bar{i} + \Phi\ (\bar{u}_{-1}^2 - \bar{u}^2) \qquad 8\text{-}(13)$$

$$P = \frac{c\ (n_{-1} - n)}{n_{-1}\quad n} \qquad 8\text{-}(14)$$

For an aspheric surface with a fourth order coefficient of e,

$$B = 8\ (n_{-1} - n)\ ey^4 \qquad 8\text{-}(4a)$$

$$F = B\bar{y}/y \qquad 8\text{-}(11a)$$

$$C = B\ (\bar{y}/y)^2 \qquad 8\text{-}(12a)$$

$$E = B\ (\bar{y}/y)^3 \qquad 8\text{-}(13a)$$

9.3.4 Stop shift equations.

$$\Sigma B^* = \Sigma B \qquad 8\text{-}(18)$$

$$\Sigma F^* = Q\,\Sigma B + \Sigma F \qquad 8\text{-}(19)$$

$$\Sigma C^* = Q^2\,\Sigma B + 2Q\Sigma F + \Sigma C \qquad 8\text{-}(20)$$

$$\Sigma E^* = Q^3\,\Sigma B + 3Q^2\Sigma F + Q\Sigma(3C + P\Phi^2) + \Sigma E \qquad 8\text{-}(21)$$

$$\Sigma P^* = \Sigma P \qquad 8\text{-}(21a)$$

$$a^* = a \qquad 8\text{-}(22)$$

$$b^* = Qa + b \qquad 8\text{-}(23)$$

10 AN APPLICATION OF THE METHOD OF LENS DESIGN

10.1 STEP ONE - SELECTING THE LENS TYPE

10.1.1 The Taylor triplet. In order to illustrate the procedure described in Section 9, we shall now work through the design of a particular type of lens. The lens selected for illustration is the famous triplet, often referred to as the Taylor triplet. It is named after H. Dennis Taylor who first described how he was able to correct astigmatism and field curvature by using three air spaced lenses. His system consisted of a negative lens between two positive lenses.

10.1.2 Reasons for selection. The triplet lens system is a fundamental type, for there are enough degrees of freedom to specify the first order properties and to control all the first and third order aberrations. First order properties includes the focal length and the optical invariant. First order aberrations are axial and lateral color, and Petzval curvature. Third order aberrations are spherical aberration, coma, astigmatism, and distortion. This lens illustrates most of the problems encountered in the design of any optical system; many of the other types of lenses are merely derivatives of the basic triplet. The triplet has been used extensively in optics; there are probably more such objectives used in photographic instruments than any other type of lens. In describing this design procedure it is hoped that the logical design of an objective can be illustrated; at the same time it will be shown how exceedingly involved the design of a lens can become if it is necessary to arrive at an optimum solution.

10.1.3 Arrangement and notation. The lens arrangement for the triplet objective is shown in Figure 10.1 with the notation to be used in the following discussion. The lens is to work with an object at infinity and have a focal length of 10. It will be color corrected for F and C light. The individual lenses are shown as thick lenses but in the first stages of the design these lenses are assumed to be thin. By selecting this type of lens (the Taylor triplet), step 1 in the design procedure has been completed. The application of the method of design will therefore continue with step 2.

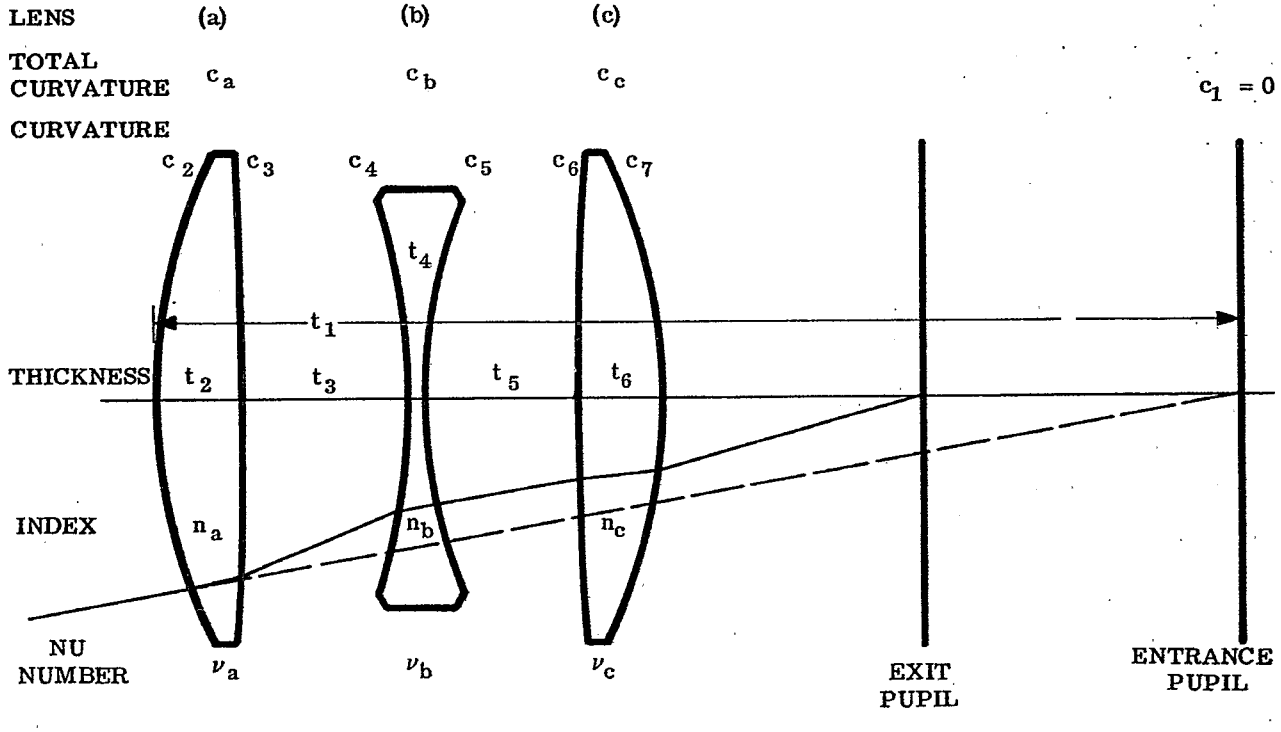

Figure 10.1- A triplet objective used to illustrate design procedure.

10.2 STEP TWO - THE FIRST ORDER THIN LENS SOLUTION

10.2.1 Power and spacing.

10.2.1.1 The first problem is to decide on the power and spacing of the elements. This is a lens system composed of three thin elements; therefore we immediately set up a thin lens table of the type shown in Table 6.14, and start to fill in the known quantities as shown in Table 10.1. At this stage nothing is known about the design, except that the object is to be at infinity ($u_o = 0$) and the focal length should be 10. Since y_1 may have any value, we choose 1 for convenience. From Equation 6-(13) if $f' = 10$ and $y_1 = 1$ then $u_{k-1} = -0.1$. The computing table appears now as shown in Table 10.2.

SURFACE NO.	Entrance Pupil 1	Lens (a) 2, 3	Lens (b) 4, 5	Lens (c) 6, 7	Focal Plane k
$-\phi$ t	0				0
y u	0				0
$\bar{y}$ $\bar{u}$	0				

Table 10.1- Computing table 1 - quantities known at start of procedure.

SURFACE NO.	Entrance Pupil 1	Lens (a) 2, 3	Lens (b) 4, 5	Lens (c) 6, 7	Focal Plane k
$-\phi$ t	0				0
y u	1 0	1 0		-0.1	0
$\bar{y}$ $\bar{u}$	0				

Table 10.2- Computing table 2 - first order assumptions added.

10.2.1.2 In order to specify the lateral color for F and C light, the conditions given in Equation 6-(41) must be fulfilled. Thus,

$$Tch_{F-C} = \frac{1}{n_{k-1}\, u_{k-1}} \left[\frac{y_a\, \bar{y}_a\, \phi_a}{\nu_a} + \frac{y_b\, \bar{y}_b\, \phi_b}{\nu_b} + \frac{y_c\, \bar{y}_c\, \phi_c}{\nu_c} \right].$$

If Tch_{F-C} is to be zero, then

$$\frac{y_a\, \bar{y}_a\, \phi_a}{\nu_a} + \frac{y_b\, \bar{y}_b\, \phi_b}{\nu_b} + \frac{y_c\, \bar{y}_c\, \phi_c}{\nu_c} = 0.$$

If we assume the condition that the chief ray shall pass through the center of lens (b) (not as shown in Figure 10.1), then $\bar{y}_b = 0$, and

$$\frac{y_a \bar{y}_a \phi_a}{\nu_a} = - \frac{y_c \bar{y}_c \phi_c}{\nu_c} .$$

Equation 6-(24) shows that in a thin lens $y\phi = (u_{-1} - u)$, which is the angular deviation that the axial ray experiences as it passes through the lens. If R is defined as

$$R = \frac{y_a \phi_a}{y_c \phi_c} ,$$

the condition for zero lateral color is then

$$\frac{\bar{y}_a}{\bar{y}_c} = - \frac{1}{R} \frac{\nu_a}{\nu_c} .$$

Since the chief ray passes through the center of the thin negative (b) lens, it is undeviated. Therefore $\bar{y}_b \phi_b = 0$, and $(\bar{u}_{-1} - \bar{u})_b = \bar{u}_4 - \bar{u}_5 = 0$. Then

$$\frac{t_3}{t_5} = - \frac{\bar{y}_a}{\bar{y}_c} = \frac{1}{R} \frac{\nu_a}{\nu_c} .$$

10.2.1.3 Up to this point, no decision has had to be made with respect to the type of glass. At this point it is necessary to decide on ν_a / ν_c. Any ratio may be used, but up until the present no one has been able to prove any advantage to a ratio other than 1. If the same glass is used for both lens (a) and lens (c), then $\nu_a / \nu_c = 1$. This choice has the practical advantage that the lens maker does not have to worry about two different glasses for the positive lenses. (Any designer who uses two elements that look alike but are of slightly different index and/or dispersion can fully expect to find the elements switched in the prototype!) With no positive evidence indicating that ν_a / ν_c needs to be other than 1, the design will proceed with glass (a) and glass (c) the same. Then it follows that

$$t_3 = \frac{1}{R} t_5 .$$

10.2.1.4 Next, it is necessary to choose a value of R. Such a value may be selected for any number of reasons. For each value of R there are many solutions (designs). In the following study an attempt will be made to show how the choice of R affects the design, but in order to proceed with the numerical example it is necessary to assume a value of R. Later (Paragraph 10.3.2.3) it will be shown that R should be near 1. This means that the (a) lens will bend the axial ray through the same angle as does the (c) lens. It follows then, that if a value can be assigned to u_3, the angle the axial ray makes with the axis after emerging from the (a) lens, then the angle u_5 is determined. (This means if u_3 is assigned, then all the angles the axial ray makes with the axis are known). For example, if u_3 is made -0.20, then it follows immediately that $u_5 = 0.10$ because $u_{k-1} = u_7 = -0.1$.

10.2.1.5 The computing table may now be filled out as shown in Table 10.3. It is still not possible to compute ϕ_a, ϕ_b, ϕ_c, and complete the table. At this point it is necessary to make another guess. Let the guess be that the space t_3 will be 1; then t_5 must also be 1. Now the system is completed and ϕ_a, ϕ_b, and ϕ_c are determined using Equations 6-(23) and 6-(24). The values are shown in Table 10.4, which is filled out completely. To trace the chief ray any angle may be assumed for it while it passes through the (b) lens. In the example, $\bar{u}_b = 0.5$ was used.

10.2.2 Glass types.

10.2.2.1 So far the only decision on glass is that (a) = (b). Now we must specify the type of glass to use for (a) and (c), and for (b). The glass types are chosen now in order to specify both axial color and Petzval curvature. When the glasses are chosen, TAch is calculated by Equation 6-(40). This calculation is illustrated in Table 6.13. The Petzval sum, ΣP, may be calculated for each lens from Equation 8-(28) and summed for the (a), (b), and (c) lenses.

10.2.2.2 The choice of glass is a critical part of the design of a triplet. It is hoped that this will be demonstrated in the following study, but in order to show this, the glasses will be picked from experience. The following glasses will be used:

	n_D	ν
Lens (a)	1.620	60.3
Lens (b)	1.617	36.6
Lens (c)	1.620	60.3

SURFACE	Entrance Pupil 1	Lens (a) 2, 3	Lens (b) 4, 5	Lens (c) 6, 7	Focal Plane k
$-\phi$	0				0
t		1	1		
y	1	1			0
u	0	0 -0.2	0.1	-0.1	
$\bar{y}$	0		0		
$\bar{u}$					

Table 10.3- Computing table 3-quantities for zero lateral color, $\nu_a/\nu_c = 1$, and R = 1 , added.

SURFACE	Entrance Pupil 1	Lens (a) 2, 3	(Lens (b) 4, 5	Lens (c) 6, 7	Focal Plane k
$-\phi$	0	-0.2	0.375	-0.222	0
t	-1.25	1	1	9	
y	1	1	0.8	0.9	0
u	0	0 -0.2	0.1	-0.1	
$\bar{y}$	0	-0.5	0	0.5	4.0
$\bar{u}$	0.4	0.5	0.5	0.389	

$f' = 10$

Table 10.4- Computing table 4 - assignment of quantities completed.

10.2.2.3 With this glass type data it is now possible to compute TAch and ΣP. The calculations for the sample are included in Table 10.5.

10.2.2.4 The values of TAch and ΣP are plotted in Figure 10.2. The dot with a surrounding square, ⊡ , indicates where the solution should be for TAch = 0 and ΣP = -0.03. At this point it will be necessary to merely accept the fact that ΣP is set at -0.03. (A negative value of ΣP indicates a negative value for the Petzval curvature. In the case of the triplet example here considered, the field is concave toward the lens and is referred to as an inward curving field.) The next step is to assume a new value of t_3 . For example, suppose we pick a value of 1.25, and repeat the process to arrive at a new value for TAch and ΣP. This point is also plotted in Figure 10.2. Next, set u_3 = 0.18 and repeat the process with t_3 = 1.0 and 1.25. The procedure for finding the values of u_3 and t_3 which will provide a solution follows obviously. With a small amount of practice one can box in a design in this manner in very short order. This is an iterative procedure which can also be programmed for automatic correction on a computer. The graphs obtained in this manner are extremely useful for visualizing how to readjust the angles in the lens after the thickness has been added (step 4).

SURFACE	Lens (a)	Lens (b)	Lens (c)	Focal Plane
$-\phi$	-0.2	0.375	-0.222	0
t				
y	1	0.8	0.9	0
u	0 -0.2	0.1	-0.1	
$\frac{\overline{y}}{\overline{u}}$				
ν	60.3	36.6	60.3	
$-\phi y^2/\nu$	-0.00332	0.00656	-0.00299	Σa= 0.00026
$-\frac{\phi}{n}$	-0.12346	0.23191	-0.13717	ΣP= -0.02872

TAch = 0.0026

Table 10.5 -Computing table 5 - calculation of TAch and ΣP.

10.2.2.5 This boxing in procedure is recommended for the preliminary set-up using thin lenses in designing a triplet. The procedure works equally well for more complicated lenses, and it provides the designer a graphical picture of how the variables affect the system. For those who prefer to manipulate algebraic equations a procedure similar to the above can be worked out to provide equations to be solved. Existing literature is adequately filled with methods of this type. A few of the well known papers are:

(1) Berek, M., Grundlagen der Praktischen Optik, Berlin, 123-130, (1930).

(2) Stephens, R. E. J. Opt. Soc. Am. 38, 1032 – 1039, (1948).

(3) Lessing, N., J. Opt. Soc. Am. 48, 558-562 (1958).

(4) Cruikshank, F. D. Rev. D'Optik 35, 292-299 , (1956).

(5) Cruikshank, F. D. Australian J. Physics 11, 41-54, (1958).

A series of solutions for triplets with different types of glass has been worked out. The significant data for these systems are included in Table 10.6, sheets 1, 2 and 3. The glasses used in this study are shown plotted in Figure 10.3 on an n_D versus ν plot, which is used extensively by lens designers. The numbers alongside each point indicate the system number. The table includes calculations for R = 1, 0.5 and 2. One solution was calculated, for each set of glasses, using a target value of ΣP = -0.03. Notice that there are examples where $(\nu_a - \nu_b)$ is constant but $(n_a - n_b)$ changes.

10.2.3 Summary of thin lens first order study contained in Table 10.6.

(1) As $\nu_a - \nu_b$ is increased, the system length, T, always increases.

(2) R = 1 systems are always shorter than systems with R = 2.0 or R = 0.5.

(3) Changing ΣP from -0.03 to -0.02 shortens the system.

(4) Changing the index of the crown and flint elements, while maintaining the ν difference, has little effect on the overall length T.

(5) As one would expect, the higher the index of the positive elements, the lower the power of all the elements.

(6) Solutions for R = 2 and R = 0.5 are essentially inverted solutions. t_3 and t_5 are almost exactly interchanged. Also, ϕ_a is changed by the ratio of 1/R.

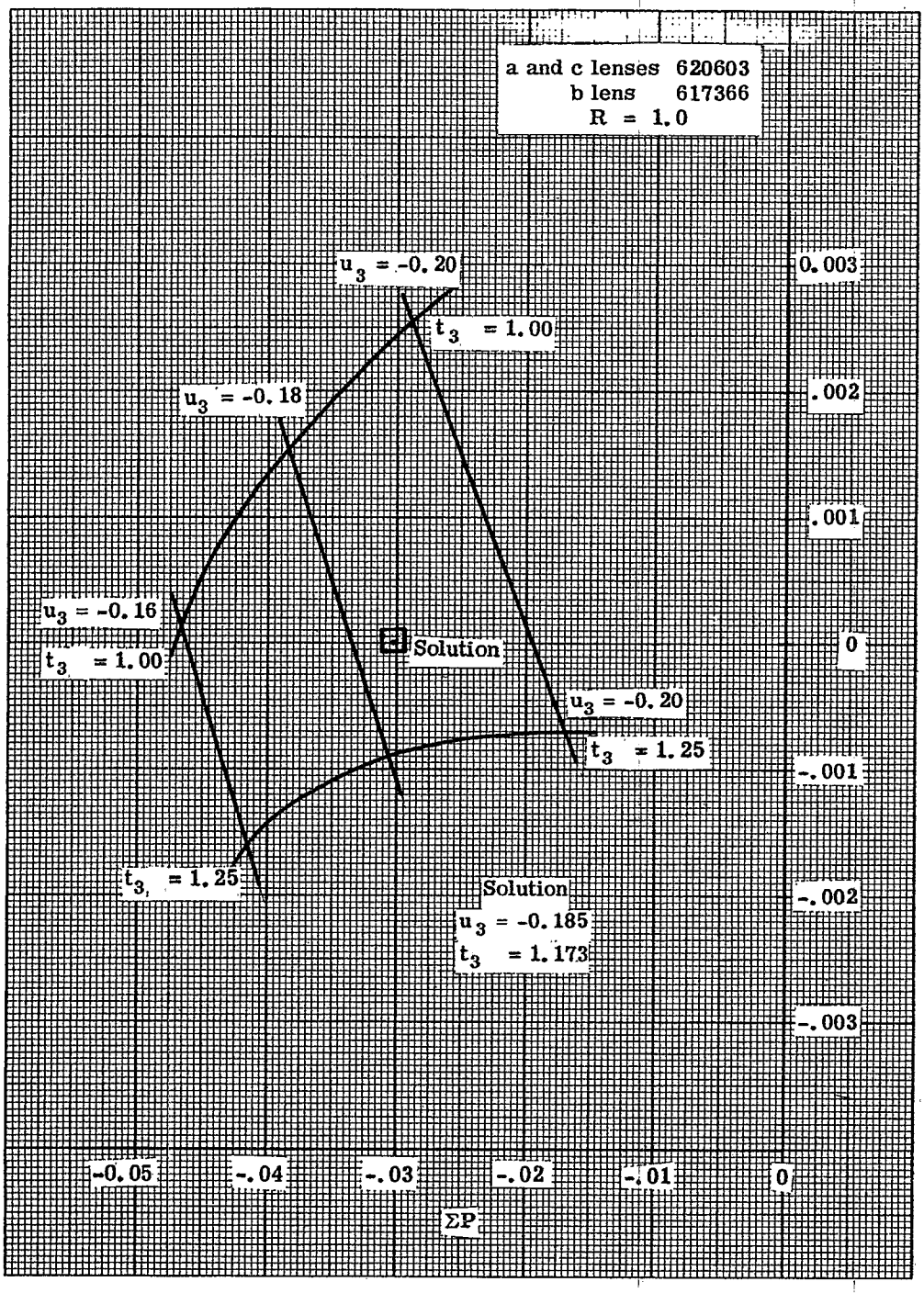

Figure 10.2- Diagram used to find a thin lens first order solution.

System No.	$R = \frac{t_5}{t_3}$	Glass (a and c) (lenses)	Glass (b lens)	$n_a - n_b$	$\nu_a - \nu_b$	ϕ_a	t_3	t_5	$T = t_3 + t_5$
1A	1	511635	596397	-.0846	23.8	0.220	1.062	1.062	2.124
1B	2	"	"	"	"	0.296	0.795	1.590	2.385
1C	0.5	"	"	"	"	0.146	1.583	0.792	2.375
2A	1	511635	617366	-.1060	26.9	0.195	1.442	1.442	2.884
2B	2	"	"	"	"	0.264	1.075	2.150	3.225
2C	0.5	"	"	"	"	0.130	2.138	1.069	3.207
3A	1	511635	649338	-.1380	29.7	0.180	1.850	1.850	3.700
3B	2	"	"	"	"	0.244	1.370	2.740	4.110
3C	0.5	"	"	"	"	0.1185	2.736	1.368	4.104
4A	1	511635	657366	-.1460	26.9	0.205	1.419	1.419	2.838
4B	2	"	"	"	"	0.275	1.066	2.132	3.198
4C	0.5	"	"	"	"	0.135	2.128	1.064	3.192
5A	1	541599	596397	-.0546	20.2	0.236	0.817	0.817	1.634
5B	2	"	"	"	"	0.317	0.615	1.230	1.845
5C	0.5	"	"	"	"	0.158	1.229	0.615	1.844
6A	1	541599	617366	-.0760	23.3	0.207	1.161	1.161	2.322
6B	2	"	"	"	"	0.278	0.874	1.748	2.622
6C	0.5	"	"	"	"	0.138	1.750	0.875	2.625
*6AA	1	541599	617366	-.0760	23.3	0.222	1.157	1.157	2.314
*6BB	2	"	"	"	"	0.298	0.867	1.734	2.601
*6CC	0.5	"	"	"	"	0.148	1.732	0.866	2.598
7A	1	541599	649338	-.1080	26.1	0.189	1.545	1.545	3.090
7B	2	"	"	"	"	0.255	1.155	2.310	3.465
7C	0.5	"	"	"	"	0.1245	2.300	1.150	3.450
8A	1	541599	657366	-.1160	23.3	0.218	1.154	1.154	2.308
8B	2	"	"	"	"	0.293	0.868	1.736	2.604
8C	0.5	"	"	"	"	0.147	1.736	0.868	2.604
9A	1	541599	689309	-.1480	29.0	0.172	2.005	2.005	4.010
9B	2	"	"	"	"	0.236	1.500	3.000	4.500
9C	0.5	"	"	"	"	0.113	3.000	1.500	4.500
10A	1	588612	596397	-.0076	21.5	0.211	0.880	0.880	1.760
10B	2	"	"	"	"	0.284	0.660	1.320	1.980
10C	0.5	"	"	"	"	0.141	1.330	0.665	1.995

Table 10.6- Thin lens triplet (first order solution), Sheet 1 of 5

System No.	$R = \frac{t_3}{t_5}$	Glass (a and c) (lenses)	Glass (b lens)	$n_a - n_b$	$\nu_a - \nu_b$	ϕ_a	t_3	t_5	$T = t_3 + t_5$
11A	1	588612	617366	-.0290	24.6	0.188	1.259	1.259	2.518
11B	2	"	"	"	"	0.253	0.947	1.894	2.841
11C	0.5	"	"	"	"	0.127	1.894	0.947	2.841
12A	1	588612	649338	-.0610	27.4	0.173	1.658	1.658	3.316
12B	2	"	"	"	"	0.235	1.246	2.492	3.738
12C	0.5	"	"	"	"	0.118	2.492	1.246	3.738
13A	1	588612	657366	-.0690	24.6	0.195	1.264	1.264	2.528
13B	2	"	"	"	"	0.264	0.950	1.900	2.850
13C	0.5	"	"	"	"	0.132	1.900	0.950	2.850
14A	1	611588	617366	-.0060	22.2	0.195	1.080	1.080	2.160
14B	2	"	"	"	"	0.261	0.790	1.580	2.370
14C	0.5	"	"	"	"	0.129	1.570	0.785	2.355
15A	1	620603	596397	.0244	20.6	0.207	0.810	0.810	1.620
15B	2	"	"	"	"	0.280	0.614	1.228	1.842
15C	0.5	"	"	"	"	0.140	1.228	0.614	1.842
16A	1	620603	617366	.0030	23.7	0.185	1.173	1.173	2.346
16B	2	"	"	"	"	0.248	0.882	1.764	2.646
16C	0.5	"	"	"	"	0.124	1.764	0.882	2.646
17A	1	620603	621362	-.0010	24.1	0.184	1.240	1.240	2.480
17B	2	"	"	"	"	0.246	0.930	1.860	2.790
17C	0.5	"	"	"	"	0.121	1.830	0.915	2.745
18A	1	620603	649338	-.0290	26.5	0.170	1.600	1.600	3.200
18B	2	"	"	"	"	0.231	1.180	2.360	3.540
18C	0.5	"	"	"	"	0.113	2.353	1.177	3.530
19A	1	620603	657366	-.0370	23.7	0.193	1.188	1.188	2.376
19B	2	"	"	"	"	0.259	0.895	1.790	2.685
19C	0.5	"	"	"	"	0.130	1.790	0.895	2.685
20A	1	620603	668323	-.0480	28.0	0.163	1.830	1.830	3.660
20B	2	"	"	"	"	0.222	1.372	2.744	4.116
20C	0.5	"	"	"	"	0.111	2.744	1.372	4.116

Table 10.6-Thin lens triplet (first order solution). Sheet 2 of 5

System No.	$R = \frac{t_3}{t_5}$	Glass (a and c) (lenses)	Glass (b lens)	$n_a - n_b$	$\nu_a - \nu_b$	ϕ_a	t_3	t_5	$T = t_3 + t_5$
21A	1	657572	617366	.0400	20.6	0.193	0.911	0.911	1.822
21B	2	"	"	"	"	0.258	0.686	1.372	2.058
21C	0.5	"	"	"	"	0.129	1.372	0.686	2.058
22A	1	657572	649338	.0080	23.4	0.176	1.289	1.289	2.578
22B	2	"	"	"	"	0.238	0.978	1.956	2.934
22C	0.5	"	"	"	"	0.119	1.956	0.978	2.934
23A	1	657572	668323	-.0110	24.9	0.168	1.540	1.540	3.080
23B	2	"	"	"	"	0.228	1.158	2.316	3.474
23C	0.5	"	"	"	"	0.114	2.316	1.158	3.474
24A	1	657572	689309	-.0320	26.3	0.162	1.773	1.773	3.546
24B	2	"	"	"	"	0.221	1.337	2.674	4.011
24C	0.5	"	"	"	"	0.108	2.625	1.313	3.938
25A	1	691548	649338	.0420	21.0	0.180	1.063	1.063	2.126
25B	2	"	"	"	"	0.242	0.805	1.610	2.415
25C	0.5	"	"	"	"	0.121	1.610	0.805	2.415
26A	1	691548	689309	.0020	23.9	0.166	1.530	1.530	3.060
26B	2	"	"	"	"	0.224	1.161	2.322	3.483
26C	0.5	"	"	"	"	0.112	2.322	1.161	3.483
27A	1	691548	720293	-.0290	25.5	0.159	1.836	1.836	3.672
27B	2	"	"	"	"	0.216	1.376	2.752	4.128
27C	0.5	"	"	"	"	0.108	2.752	1.376	4.128
28A	1	720475	689309	.0310	16.6	0.199	0.842	0.842	1.684
28B	2	"	"	"	"	0.266	0.632	1.264	1.896
28C	0.5	"	"	"	"	0.133	1.264	0.632	1.896
29A	1	720475	720293	.0000	18.2	0.188	1.082	1.082	2.164
29B	2	"	"	"	"	0.248	0.820	1.640	2.460
29C	0.5	"	"	"	"	0.125	1.620	0.810	2.430
29D	1.5	"	"	"	"	0.228	0.890	1.335	2.225

Table 10.6-Thin lens triplet (first order solution). Sheet 3 of 5

System No.	Vertex of Parabola $_3Y_k$	FD for c_2 at Vertex	Slope of FD Curve	c_2 at Vertex $_3Y_k$	c_4 at Vertex $_3Y_k$	c_6 at Vertex $_3Y_k$	c_a	c_b	c_c
1A	.029	-.008	-.19	.4320	-.2954	.1272	.4305	-.7449	.4817
1B	-.023	.004	-.30	.5150	-.2759	-.0504	.5792	-.7553	.3444
1C	-.030	-.021	-.18	.3750	-.3120	.1960	.2857	-.7381	.6205
5A	.094	-.005	-.11	.4500	-.3126	.1154	.4362	-.7738	.4750
5B	.029	.005	-.16	.5100	-.3015	.0082	.5860	-.7831	.3341
5C	.025	-.014	-.11	.4000	-.3435	.1947	.2921	-.7793	.6223
6A	.014	-.010	-.20	.4000	-.2518	.1209	.3826	-.6699	.4329
6B	-.030	.007	-.27	.4600	-.2466	.0299	.5139	-.6787	.3114
6C	-.032	-.022	-.19	.3400	-.2843	.1698	.2551	-.6709	.5591
*6AA	.033	-.010	-.25	.4200	-.2928	.1322	.4104	-.7502	.4640
*6BB	-.016	.002	-.38	.5050	-.2770	.0534	.5508	-.7583	.3332
*6CC	-.019	-.025	-.20	.3600	-.3128	.1789	.2736	-.7497	.5990
7A	-.021	-.015	-.38	.3650	-.2188	.1115	.3494	-.6050	.4132
7B	-.046	.010	-.50	.4120	-.1650	.0667	.4713	-.6170	.3065
7C	-.050	-.031	-.33	.3000	-.2347	.1521	.2301	-.5905	.5201
8A	-.003	-.010	-.35	.4150	-.2450	.1179	.4030	.6833	.4555
8B	-.054	.002	-.40	.5000	-.2194	.0603	.5416	-.6930	.3277
8C	-.053	-.025	-.24	.3600	-.2710	.1816	.2717	-.6969	.5951
10A	.057	-.005	-.11	.4000	-.2534	.0964	.3588	-.6639	.3935
10B	.016	.003	-.14	.4520	-.2319	.0082	.4830	-.6736	.2782
10C	.010	-.013	-.10	.3450	-.3087	.1490	.2398	-.6675	.5138
11A	.009	-.009	-.22	.3480	-.2170	.0993	.3197	-.5860	.3658
11B	-.020	.006	-.31	.4000	-.2013	.0262	.4303	-.5957	.2654
11C	-.022	-.023	-.19	.3050	-.2558	.1474	.2160	-.5997	.4772
13A	.004	-.010	-.25	.3580	-.2153	.1014	.3316	-.5858	.3796
13B	-.029	.003	-.35	.4250	-.1922	.0386	.4490	-.6014	.2771
13C	-.029	-.024	-.22	.3130	-.2523	.1504	.2245	-.6014	.4961
14A	.027	-.006	-.16	.3500	-.2319	.0828	.3191	-.5954	.3578
14B	-.007	.001	-.18	.4180	-.1769	.0340	.4272	-.5952	.2537
14C	-.012	-.014	-.14	.3130	-.2651	.1346	.2111	-.5833	.4582

Table 10.6- Thin lens triplet (third order solution). Sheet 4 of 5

System No.	Vertex of Parabola $_3Y_k$	FD for c_2 at Vertex	Slope of FD Curve	c_2 at Vertex $_3Y_k$	c_4 at Vertex $_3Y_k$	c_6 at Vertex $_3Y_k$	c_a	c_b	c_c
15A	.059	-.003	-.09	.3800	-.2544	.0655	.3339	-.6334	.3633
15B	.025	.003	-.13	.4350	-.2117	-.0043	.4516	-.6488	.2574
15C	.021	-.010	-.08	.3350	-.3162	.1252	.2258	-.6488	.4812
16A	.016	-.008	-.15	.3380	-.2057	.0780	.2984	-.5589	.3380
16B	-.013	-.002	-.20	.4000	-.1578	.0463	.4000	-.5643	.2428
16C	-.014	-.017	-.13	.2900	-.2563	.1271	.2000	-.5643	.4387
17A	.013	-.009	-.20	.3360	-.2028	.0911	.2968	-.5591	.3388
17B	-.015	.004	-.24	.3960	-.1571	.0548	.3968	-.5617	.2437
17C	-.020	-.018	-.19	.2880	-.2430	.1278	.1952	-.5440	.4296
19A	.014	-.007	-.20	.3400	-.2157	.0832	.3113	-.5648	.3533
19B	-.016	.001	-.28	.4100	-.1674	.0423	.4177	-.5716	.2544
19C	-.019	-.020	-.17	.3050	-.2480	.1390	.2097	-.5753	.4606
21A	.034	-.004	-.10	.3480	-.2170	.0601	.2938	-.5624	.3232
21B	.004	.001	-.18	.4050	-.1541	.0122	.3927	-.5652	.2276
21C	.000	-.010	-.09	.3000	-.2816	.1024	.1963	-.5652	.4216
22A	.005	-.010	-.18	.3200	-.1693	.0873	.2679	-.5022	.3075
22B	-.015	.003	-.27	.3620	-.1468	.0270	.3623	-.5161	.2252
22C	-.017	-.020	-.16	.2750	-.2273	.1192	.1811	-.5161	.4015
25A	.014	-.006	-.13	.3200	-.1792	.0612	.2605	-.4954	.2915
25B	-.007	.001	-.17	.3680	-.1278	.0300	.3502	-.5033	.2087
25C	-.011	-.014	-.13	.2800	-.2410	.0992	.1751	-.5033	.3807
29A	.015	-.006	-.13	.3200	-.1710	.0607	.2611	-.4812	.2928
29B	-.012	.002	-.20	.3650	-.1136	.0130	.3444	-.4742	.2060
29C	-.010	-.016	-.11	.2950	-.2118	.1084	.1736	-.4789	.3778
29D	.008	-.002	-.18	.3520	-.1417	.0261	.3167	-.4879	.2436

Table 10.6-Thin lens triplet (third order solution). Sheet 5 of 5

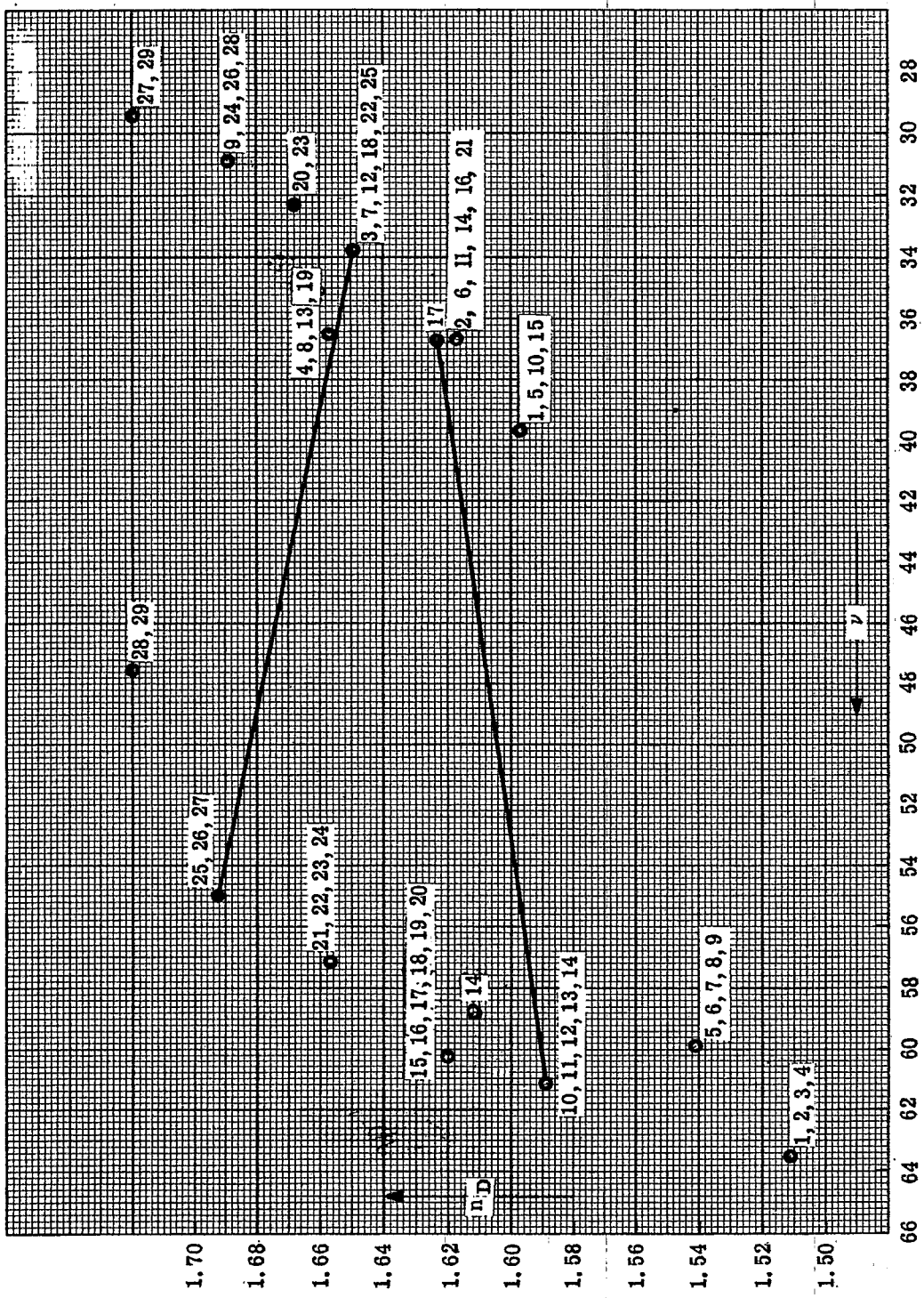

Figure 10.3 - Plot of n_D versus ν for glasses used in triplet study.

10.3 STEP THREE - THE THIRD ORDER THIN LENS SOLUTION

10.3.1 Evaluation of third order coefficients.

10.3.1.1 With the thin lens first order equations worked out so that ϕ_a , ϕ_b , ϕ_c , t_3 and t_5 are known, it is now possible to evaluate the coefficients in Equations 8-(36) through 8-(39) for each lens. In order to simplify the equations, the chief ray is again chosen to pass through the center of the (b) lens. Then the problem is to solve the following equations:

$$B_a^* + B_b + B_c^* = \Sigma B = 0 \quad (1)$$

$$F_a^* + F_b + F_c^* = \Sigma F = 0 \quad (2)$$

$$C_a^* + C_b + C_c^* = \Sigma C = -\frac{1}{3} \Sigma P \Phi^2 \quad (3)$$

$$E_a^* + 0 + E_b^* = \Sigma E = 0 \quad (4)$$

10.3.1.2 The value of ΣC was not set equal to zero because ΣP is not zero. Instead the value of ΣC is chosen to make $t_{kT} = 0$, as it is defined in Equation 8-(9). For these equations,

$$B_a^* = \alpha_1^* + \alpha_2^* c_2 + \alpha_3^* c_2^2 \quad (5)$$

$$B_b = \alpha_1 + \alpha_2 c_4 + \alpha_3 c_4^2 \quad \text{Note: The } \alpha\text{'s are} \quad (6)$$

$$B_c^* = \alpha_1^* + \alpha_2^* c_6 + \alpha_3^* c_6^2 \quad \text{different for each lens.} \quad (7)$$

$$F_a^* = \beta_1^* + \beta_2^* c_2 + \beta_3^* c_2^2 \quad (8)$$

$$F_b = \beta_1 + \beta_2 c_4 \quad \text{The } \beta\text{'s are different} \quad (9)$$

$$F_c^* = \beta_1^* + \beta_2^* c_6 + \beta_3^* c_6^2 \quad \text{for each lens.} \quad (10)$$

$$C_a^* = \gamma_1^* + \gamma_2^* c_2 + \gamma_3^* c_2^2 \quad (11)$$

$$C_b = -\phi_b \Phi^2 \quad \text{The } \gamma\text{'s are different} \quad (12)$$

$$C_c^* = \gamma_1^* + \gamma_2^* c_6 + \gamma_3^* c_6^2 \quad \text{for each lens.} \quad (13)$$

$$E_a^* = \delta_1^* + \delta_2^* c_2 + \delta_3^* c_2^2 \quad (14)$$

$$E_b = 0 \quad \text{The } \delta\text{'s are different} \quad (15)$$

$$E_c^* = \delta_1^* + \delta_2^* c_6 + \delta_3^* c_6^2 \quad \text{for each lens.} \quad (16)$$

This appears like a rather formidable array of equations to solve. But the problem can be tackled by a combination of algebraic and graphical solutions, and enough common sense to realize that there really is little point in trying to find an exact solution for thin lenses anyway. Any solution for thin lenses will be changed as soon as thicknesses are added.

10.3.1.3 The problem is approached by noting that the astigmatism of the (b) lens, C_b , is constant and does not depend on the bending of the lens. This means that Equation (3) in this section can be written in two variables, c_2 and c_6 . By using c_2 as a free variable, and choosing a numerical value of c_2 , c_6 may be found by solving a quadratic equation. If there are two real solutions one must choose between the positive or negative sign before the square root. In all the work to follow, the positive sign has been taken for the solution. The solutions provided by the negative root are not promising optical systems, because the lens surfaces have too high a curvature.

10.3.1.4 With c_2 and c_6 determined, Equation (2) becomes a linear equation which can be solved for a single value of c_4 . Now c_2 , c_4 , c_6 are determined, so Equations (1) and (4) determine ΣB and ΣE. This procedure may then be repeated for several values of c_2 . The values of ΣB and ΣE should then be plotted on a graph with c_2 as the abscissa. A plot of this type is illustrated in Figure 10.4. The ordinates of this graph are $\Sigma B/2\,(n_{k-1}\, u_{k-1}) = {}_3Y_k$ and $\Sigma E/2\Phi$ = F.D., which are the actual transverse third order spherical aberration and the fractional distortion. The thin lens coefficients were computed using $y_1 = 1$ and $\bar{u}_1 = 0.3$. Therefore, the graph in Figure 10.4 shows the spherical aberration and fractional distortion for an $f/5$ system with an image height of 3.0. The graphs in Figure 10.4 show that there are two solutions where the spherical aberration is zero, while the fractional

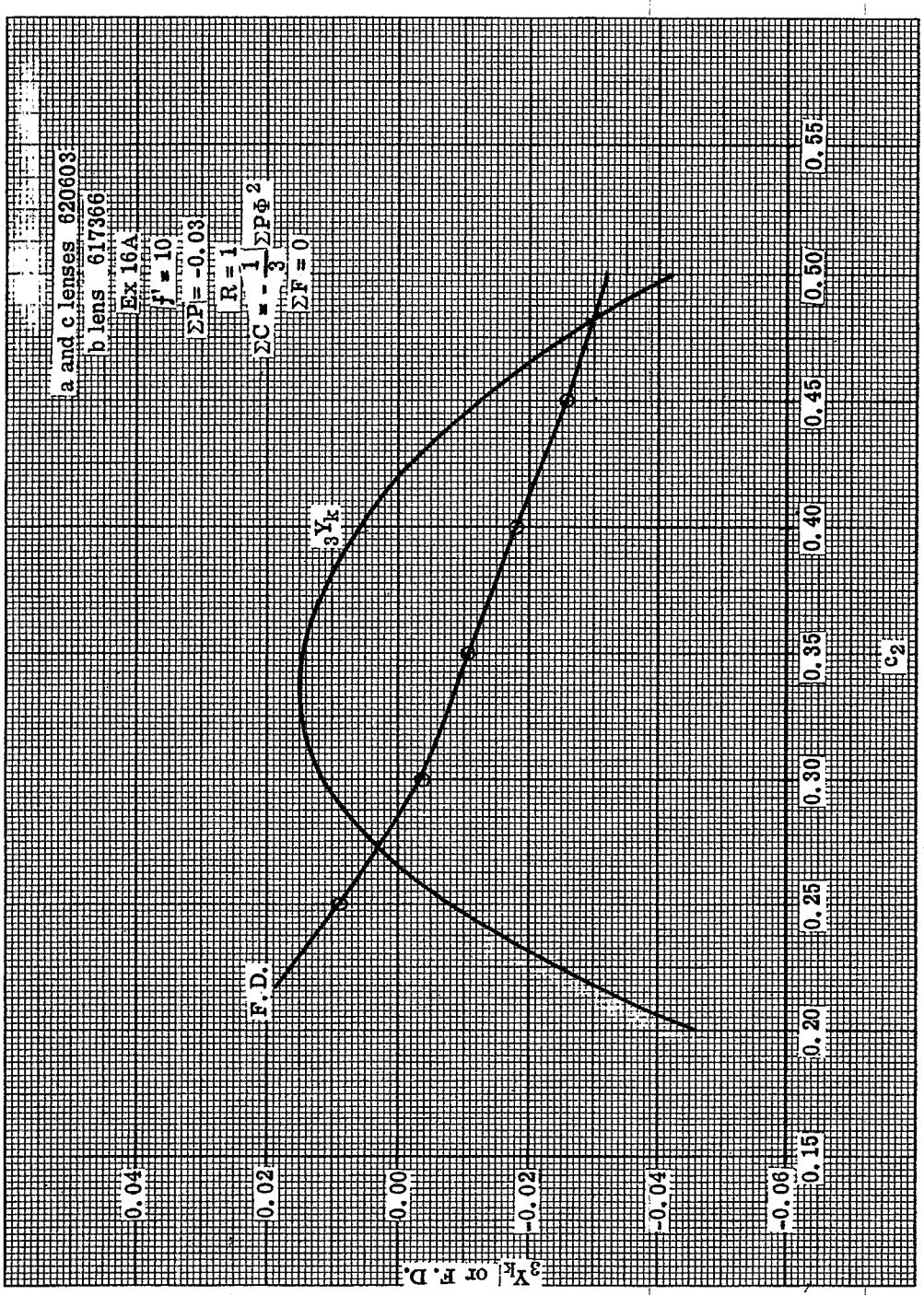

Figure 10.4 - Variation of distortion and spherical aberration with curvature c_2.

distortion is positive for one and negative at the other. The solution with the smaller value of c_2 has the least amount of distortion.

10.3.1.5 Curves of the type shown in Figure 10.4 have been worked out for all the systems included in sheets 1, 2, and 3 of Table 10.6. An attempt to summarize the data is included in Table 10.6, sheets 4 and 5. In nearly every case, the curve for spherical aberration can be represented by a parabola, while the distortion curve can be approximated by a straight line. The data in Table 10.6, sheets 4 and 5, give the information defining the constants of the parabola and the slope of the straight line. For practical purposes, all the parabolas and straight lines can be fitted to the same constants. Therefore,

$$ {}_3Y_k = -2.0\,(c_i - c_{i\ \text{vertex}})^2 + {}_3Y_{k\ \text{vertex}}. $$

In the tables, c_2, c_4, and c_6 are given for the vertex of the parabola. Therefore one can calculate c_2, c_4, and c_6 for any desired ${}_3Y_k$ from the above equation. Using example 16A in Table 10.6, sheet 5, the values for c_2, c_4, and c_6 for ${}_3Y_k = 0$ are given by

$$ 0 = -2.0\,(c_2 - 0.3380)^2 + 0.016, \quad c_2 = 0.249 \text{ and } .427 $$

$$ 0 = -2.0\,(c_4 + 0.2057)^2 + 0.016, \quad c_4 = -0.295 \text{ and } -.116 $$

$$ 0 = -2.0\,(c_6 - 0.0780)^2 + 0.016, \quad c_6 = -0.011 \text{ and } .167 $$

10.3.2 Analysis of the data.

10.3.2.1 Notice that the c_2 values for ${}_3Y_k = 0$, calculated above, do not agree with the data in Figure 10.4, where $c_2 = 0.262$ and 0.416. This is because the equation of the parabola has been simplified to meet all the cases. The slight discrepancy is of little concern at this step of the design, for introducing the thicknesses will change conditions anyway. These figures, therefore, give adequate starting data for the next step of the design. However, before proceeding, the following features of the data in Table 10.6, sheets 4 and 5, should be observed.

(1) Changing the value of R from 1 to 2.0, or from 1 to 0.5, has the effect of moving the parabola downward, with a horizontal vertex shift towards increased c_2 values for $R = 2.0$, and toward decreased c_2 values for $R = 0.5$.

(2) Changing R from 1.0 to 2.0, or from 1 to 0.5, has the effect of moving the F.D. versus c_2 curves upward for $R = 2.0$, and downward for $R = 0.5$ with no appreciable change in slope.

(3) Decreasing ΣP from -0.03 to -0.02 has the effect of moving the parabolas upward, with little effect on the F.D. curves.

10.3.2.2 The ${}_3Y_k$ and F.D. curves for the same solution for values of $R = 2$ and 0.5, are shown in Figure 10.5. At some value of R (about $R = 0.80$), the distortion curve and the spherical aberration parabola will intersect each other at 0.0 for a c_2 value around 0.27. For an R about 1.5, the curves cross again at 0.0 for a value of $c_2 = 0.35$. This means that if R is variable, there are two solutions corrected for both spherical aberration and distortion. Since ΣP, ΣC, and ΣF are specified for all the curves, these two solutions are then completely corrected to the desired third order aberrations. The solution with the smaller value of c_2 will be referred to as the left hand triplet solution, while the other solution will be called the right hand solution.

10.3.2.3 If glasses with larger $\Delta\nu$ are used, the parabolas are lowered and the two solutions approach each other on the c_2 plot, the final single solutions tend towards a value of R slightly greater than 1.0. The indices of the elements seem to have only a secondary effect on the design while the $\Delta\nu$ difference has a very significant effect.

10.3.3 Ray trace analysis. The designer cannot be sure from the thin lens data how to choose from all the possible choices of glass. There are a very large number of triplets for which the third order distortion and spherical aberration are zero; and the number, of course, is unlimited if distortion residuals are allowed. The only way to really check on the advantage of one design over another is to ray trace the various possibilities. One instinctively feels, however, that if the left hand and right hand solutions can be made to come together that this design will be a good solution. Under this condition the spherical aberration para-

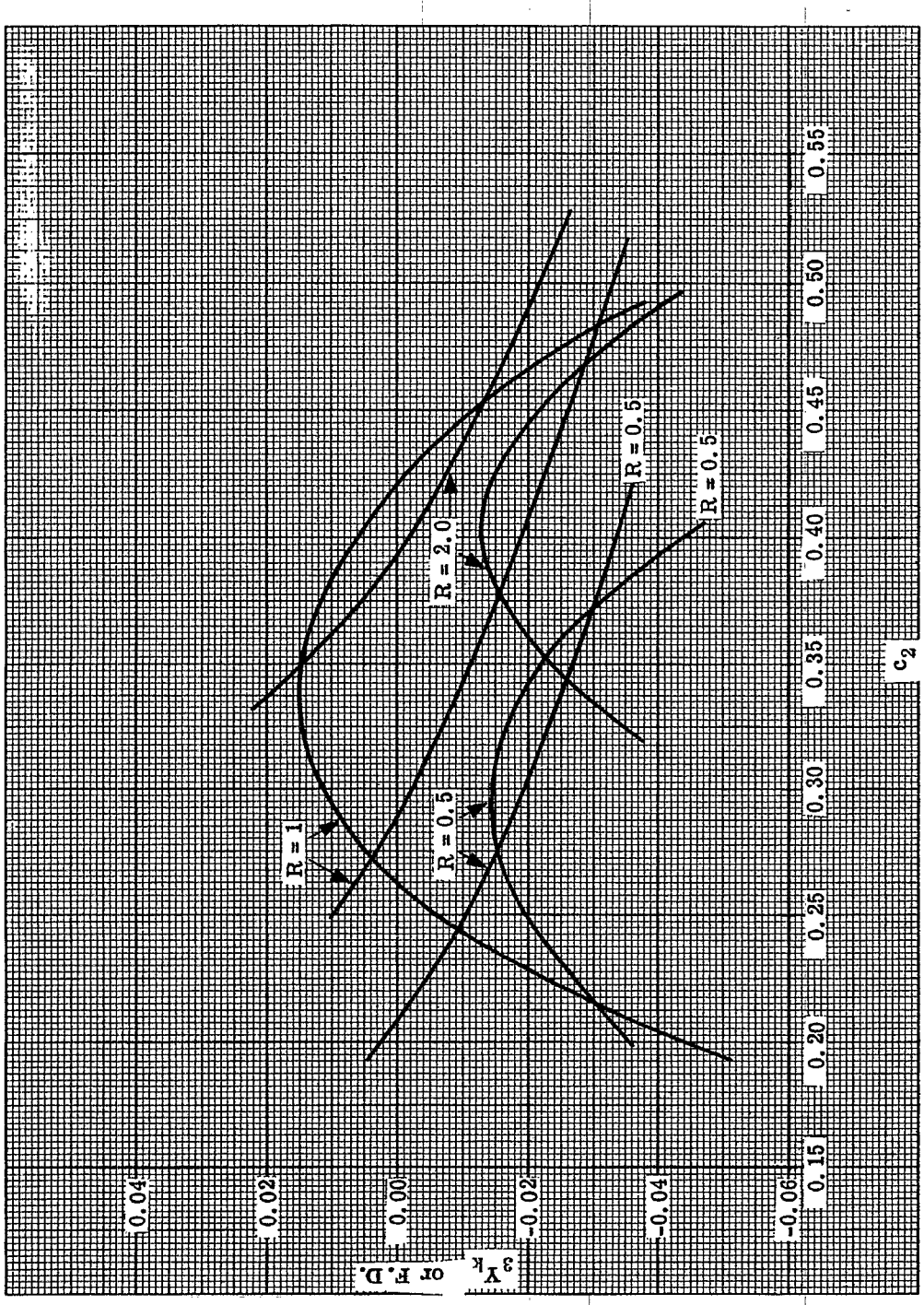

Figure 10.5 - Same plot as in Figure 10.4 with different values of R,

bola and the distortion curve intersect at the maximum of the parabola. Therefore the solution will be somewhat insensitive to changes in curvature, and consequently should be less sensitive to errors in manufacture. Later work on ray trace results will also substantiate that these solutions are preferred to others.

10.3.4 Summary of thin lens design for a triplet objective.

(1) There are two main solutions for $B = F = E = 0$ and $C = -\frac{1}{3} P\Phi^2$. One solution is called the left hand solution, $(R < 1)$. The other is the right hand solution, $(R > 1)$.

(2) These solutions are brought together to form a single solution, by increasing the $\Delta\nu$ between the positive elements and the negative element. The R values also converge to a value slightly greater than 1. It is believed that this provides a near optimum solution.

(3) If the $\Delta\nu$ is made too large, there is no solution.

(4) If the value of ΣP is made more positive, the two solutions (if they exist) separate, and in order to bring them together again, the $\Delta\nu$ must be made greater.

10.4 STEP FOUR - THE THICK LENS FIRST ORDER AND THIRD ORDER ABERRATIONS

10.4.1 Lens thickness.

10.4.1.1 Introducing the proper thicknesses in a lens system is also a problem. One has to be sure the positive lenses are of large enough aperture to pass the necessary rays, and the negative lenses have to be made thick enough to resist warping during manufacture. The thickness of the negative lenses can be usually assigned quite easily by adopting the rule that a negative lens should not be thinner than 1/10 its diameter. This usually provides a lens with sufficient strength. In special cases thinner lenses can be made if there is a real need for it; hence this rule is merely a guide.

10.4.1.2 The positive lens thickness is more difficult to ascertain because it depends on the system. It is necessary that the system be almost completely designed before deciding on the diameters of the positive lenses. The designer usually vignettes the oblique beams by cutting the clear aperture of some of the positive lenses. He seldom makes the positive elements with clear apertures large enough to pass the complete oblique beams. Drawings of the lens with pictures of the rays passing through it are very useful in visualizing the thickness required. After the clear apertures of a lens are determined it is still necessary for the diameter to be somewhat larger in order to take care of the edge thickness and mounting rims. When the maximum diameter is known, the thickness is calculated using the thin lens curvatures.

10.4.1.3 Rules for the increased diameter needed to mount the lens vary from shop to shop; thus the problem of lens mounting is a subject in itself and will not be treated here. A designer will have to learn these things through experience, although a shop practice manual may help. The designer must remember, however, that shop people have a natural tendency to resist doing things differently. A designer can miss some good designs if he lets shop people talk him out of a very thin lens, or a glass that is difficult to handle. Formerly designers also had a tendency to resist change, insisting on sticking with their design simply because it was so difficult to recalculate. Today, with modern computing machines, there is no excuse for this. It is now very inexpensive to redesign a system completely just to provide a bit more thickness if it is required by the shop people. There are, however, times when the designer needs a thin element for the reduction of weight or to fit into a tight spot, or an expensive hard-to-handle glass may be required to optimize the design. The designer today can back up his design with proof, so he should be able to violate some shop rules.

10.4.1.4 In order to proceed with the thick lens system, the problem of assignment of thickness will not be discussed further. For the present example thicknesses will be inserted without further explanation.

10.4.1.5 The thin lens first order study of the triplet was started using the glasses 620603 for the crowns, and 617366 for the flint, System No. 16. The thin lens third order study shows that the spherical aberration parabola for these glasses extends far above the zero axis. The two solutions are therefore widely separated. For this reason, it appears that the parabola should probably be lowered. This can be done by choosing a flint with a lower ν value. The thick lens set-up is, therefore, System No. 17 in Table 10.6, sheet 2, with 621362 glass for the negative lens. Using the data from Table 10.6, sheet 5, and the parabolic equation, it is possible to compute the first curvatures for the two solutions with $R = 1$ for zero spherical aberra-

tion. These thin lens solutions are as follows:

Left Hand Solution		Right Hand Solution	
c_2	= 0.26	c_2	= 0.41
c_4	= -0.28	c_4	= -0.13
c_6	= 0.016	c_6	= 0.22
t_3	= 1.28	t_3	= 1.28
t_5	= 1.28	t_5	= 1.28

10.4.1.6 The angle the axial ray makes with the optical axis may be computed from the data in Table 10.6, sheet 2, by setting up a table as in Table 10.4. The values of ϕ_a and t_3 are known; therefore the table is completely determined.

10.4.1.7 As soon as it is necessary to assign thicknesses, the designer has to decide on the f-number and the focal length of the lens. For the following study, it will therefore be assumed that the diameter of the entrance pupil will be 3 and the focal length 10. It is also important to assign a maximum field of obliquity for the lens. Let this (object field) be 20° half angle.

10.4.1.8 The axial paraxial ray should therefore be traced through the system as follows:

$$y_1 = 1.5$$

$$u_o = 0$$

The thin lens axial ray trace for this example then appears as in Table 10.7.

SURFACE	1	2,3	4,5	6,7
$-\phi$	0	-0.184	0.347	-0.210
t		1.24	1.24	
y	1.5	1.5	1.158	1.314
u	0	-0.276	0.126	-0.15

Table 10.7 - Thin lens solution for example 17A in Table 10.6.

10.4.2 Computing the thick lens solution.

10.4.2.1 The thick lens is then set up using the values c_2, c_4, c_6, t_3 and t_5 for either the right hand or the left hand solution with the thicknesses of the lenses inserted. For this example the positive lenses are assigned thicknesses of 0.6 and the negative lens a thickness of 0.25.

10.4.2.2 The second curvatures of the lenses are then computed to maintain the paraxial angles, shown in Table 10.7, between the lenses. The spaces between the lenses may at this time be set at about 1.0.

10.4.2.3 With this initial system, the first order and third order contributions are calculated as shown in Table 8.2.

10.4.3 Iterative analysis and adjustment.

10.4.3.1 As the formalized step-by-step procedure of Section 9 is followed through the remaining steps, it is necessary to examine results and repeat, with changes, earlier steps in order to balance the higher order

aberrations. This iterative appraisal and recomputation is the means by which the design can be refined and developed to the desired degree. The mechanics of computation are well described in the foregoing sections and will not be repeated in detail.

10.4.3.2 This discussion, then, will be devoted only to the examination and interpretation of results and to the analytical processes which dictate the iterative changes as design refinement proceeds. With this orientation in mind, and also remembering that by properly programming an automatic computer, the results of one run will produce much of the data necessary for analysis, the discussion will proceed.

10.4.3.3 Next comes the problem of ray tracing, analyzing, and readjusting the lens to the desired third order aberrations. The recommended procedure for doing this is to make small changes in the system and solve Equations 9-(1) through 9-(7). A procedure of this type has been programmed for the I.B.M. 650 computer, and with this program the foregoing triplet system has been studied extensively. A brief account of this study is presented below.

10.4.3.4 First it was decided that the quantities c_2, t_3, c_4, t_5, c_6 would be used as variables. This provided only five variables so it was necessary to provide another variable in order to correct the six quantities B, F, C, P, a, and b. c_5 was used as the extra variable, meaning that the solution departed from $R = 1$. It was possible with three iterations to find the left and right hand solutions, but neither of these solutions were ray traced because it was not possible to tell what value of R the final solution would have. Therefore, it was decided to let c_3 also vary. This provided an extra degree of freedom so the distortion was corrected. In other words, R was allowed to be a variable for the purposes of correcting distortion. In other words, with the seven variables c_2, c_3, t_3, c_4, t_5, c_6, and R, the seven aberration coefficients, B, F, C, P, E, a, and b could be specified. As one would predict from the graphs in Figure 10.5, two solutions were found. This same technique was used in the further study of this lens; hence all the solutions are corrected to exactly zero third order distortion. It was thus possible to compare several designs by varying single parameters, and the third order aberrations could be brought to precisely the required values.

10.5 STEP FIVE - TRACING A FEW SELECTED RAYS

10.5.1 Analysis of the ray tracing results. One finds immediately upon ray tracing that the first and third order aberrations should not be set to zero. The reason for this is that high order aberrations are always present and the third order aberrations have to be set to compensate for them. For example, if the triplet is corrected with $\Sigma B = 0$, the rays traced at $Y = 1.5$ will strike the paraxial image plane at large positive values indicating that the high order aberrations have over-corrected the lens. This is also the reason why ΣP was made equal to -0.03 instead of zero. The same is true with respect to color aberrations. In the triplet it turns out that ΣF, ΣE, and Σb can be set at zero, but the remaining ones, ΣB, ΣC, ΣP, and a have to be set at negative values.

10.5.2 Target values and solutions.

10.5.2.1 Early in the study of this system it was found that the value for ΣP had to be changed from -0.03 to $= -0.035$ and the spherical aberration had to be under-corrected to $\Sigma B = -0.006$. The first solutions showing interest were computed with the following target values for the third order coefficients:

$$\Sigma B = -0.006$$

$$\Sigma F = 0$$

$$\Sigma C = -\frac{1}{3} P \Phi^2$$

$$\Sigma E = 0$$

$$\Sigma P = -0.035$$

$$\Sigma a = -0.0004$$

$$\Sigma b = 0$$

The chromatic aberrations were left small and unchanged throughout, since the study was done primarily to show how the monochromatic aberrations are corrected.

10.5.2.2 With these target values, two solutions were found. The lens data are included in Table 10.8. The data include the overall thickness T of the lens. Aberration plots similar to Figure 9.1 are shown

in Figures 10.6 and 10.7 for the two solutions.

Left Hand Solution		Right Hand Solution	
c	t	c	t
0.2209		0.3116	
	0.600		0.600
-0.0124		-0.0282	
	1.3949		0.8572
-0.2407		-0.1734	
	0.2500		0.2500
0.2606		0.3319	
	0.9631		1.628
0.0777		0.0683	
	0.600		0.600
-0.2822		-0.1891	
	8.453		7.599
R = 0.7685		R = 1.82	
T = 3.808		T = 3.935	

Table 10.8 - Left and right hand solutions for a triplet with $\Sigma P = -0.035$.

10.6 STEP SIX - READJUSTING THE THIRD ORDER ABERRATIONS

10.6.1 Analysis of the aberration curves.

10.6.1.1 The aberration curves show that the meridional rays depart from third order drastically at 20°. In the lens designer's language, the tangential field has pulled in rapidly. On the other hand, the sagittal field has moved back relative to the third order field by a much smaller amount. These lenses cannot perform well beyond a 15° half angle. The sagittal rays tend to follow the third order curve much more closely than the meridional rays. Notice also how the skew fan appears similar to the axial fan, but over-corrects in spherical aberration as the field angle increases. The left hand solution appears to be somewhat better than the right hand solution at 20°, but there is little to choose between them at the smaller field angles.

10.6.1.2 It can be seen from Table 10.8 that the left and right hand solutions are widely separated on the c_2 scale. This means the spherical aberration parabola should be lowered. Now this can be done by many methods. One way is to increase $\Delta\nu$ by changing the glass in the flint element. The 649338 glass could be used. However, as the thin lens data indicate (System No. 18), this would lengthen the system and the result would be that the tangential field pulls in even faster. An additional disadvantage is that the 649338 glass lowers the parabola so far that there is no solution with the present glass thicknesses. A second method of lowering the parabola is to make the Petzval sum more negative. One might think at first that this would make the system longer, which is likely to make the tangential field pull in even more, but if the parabola is lowered, the R values will be closer to 1, and the thin lens study showed that for this value of R, the systems are the shortest. Therefore, making $\Sigma P = -0.040$ probably will not make the system much longer.

10.6.2 Readjustment procedure.

10.6.2.1 The value of ΣP was therefore changed to -0.040, and solutions were found with all the other aberrations identically the same. The two solutions and the aberration plots are shown in Table 10.9, and Figures 10.8 and 10.9.

10.6.2.2 The aberration curves now show real improvement. The skew ray fans for the two solutions are quite similar. However the left hand solution appears more symmetrical than the right hand solution, and at 20° it is definitely superior. The R values are now closer together and the barrel length, T, is actually shortened. Notice that the left hand solution is shorter than the right. This may be the reason why the tangential field pulls in further with the right hand solution. Notice also that the left hand solution has a value of R closer to 1.0 than the right. If the parabola were lowered still further, the two solutions would converge to a single solution with $R > 1$ as predicted from the thin lens system.

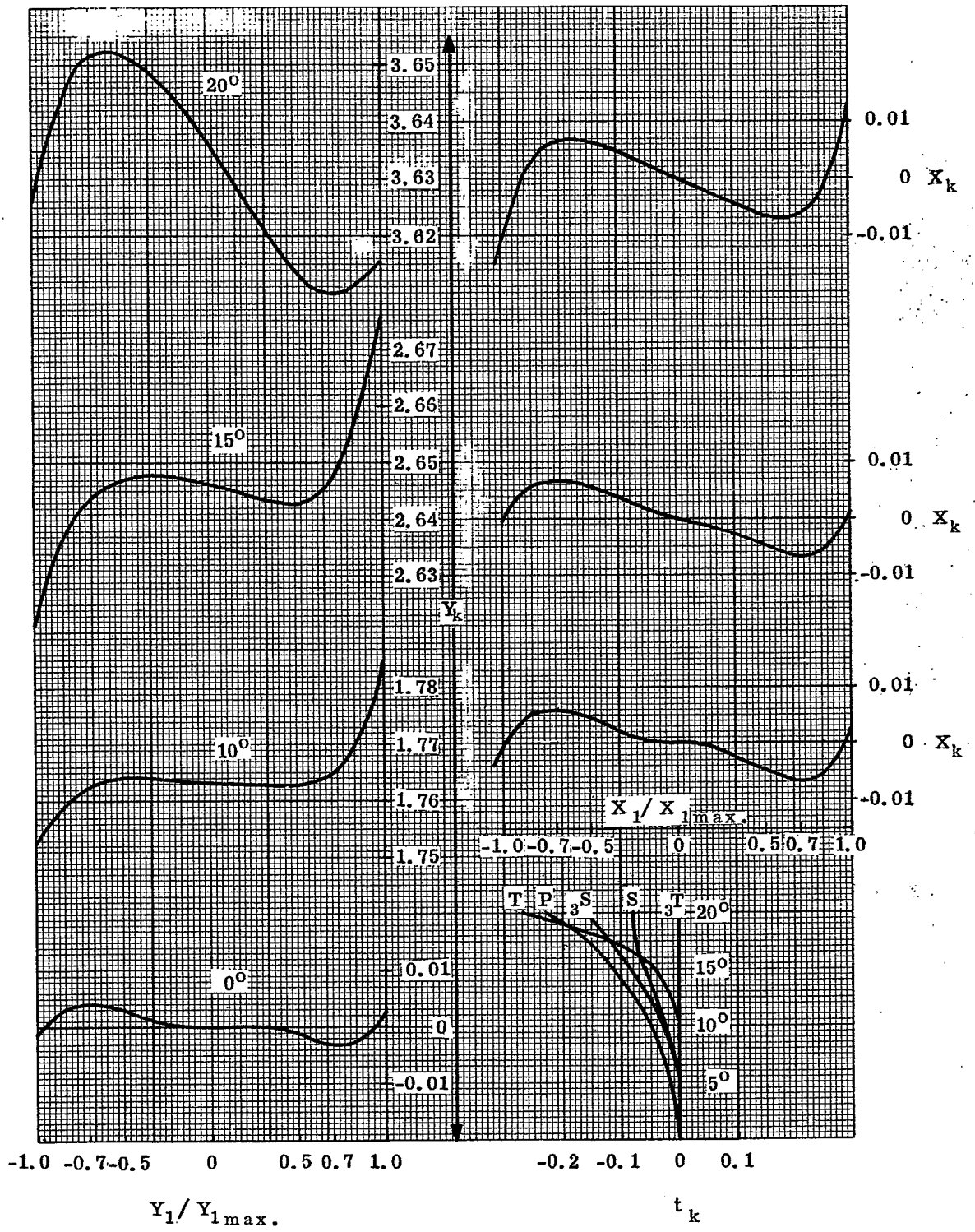

Figure 10.6 - Aberration plots for left hand solution of lenses in Table 10.8.

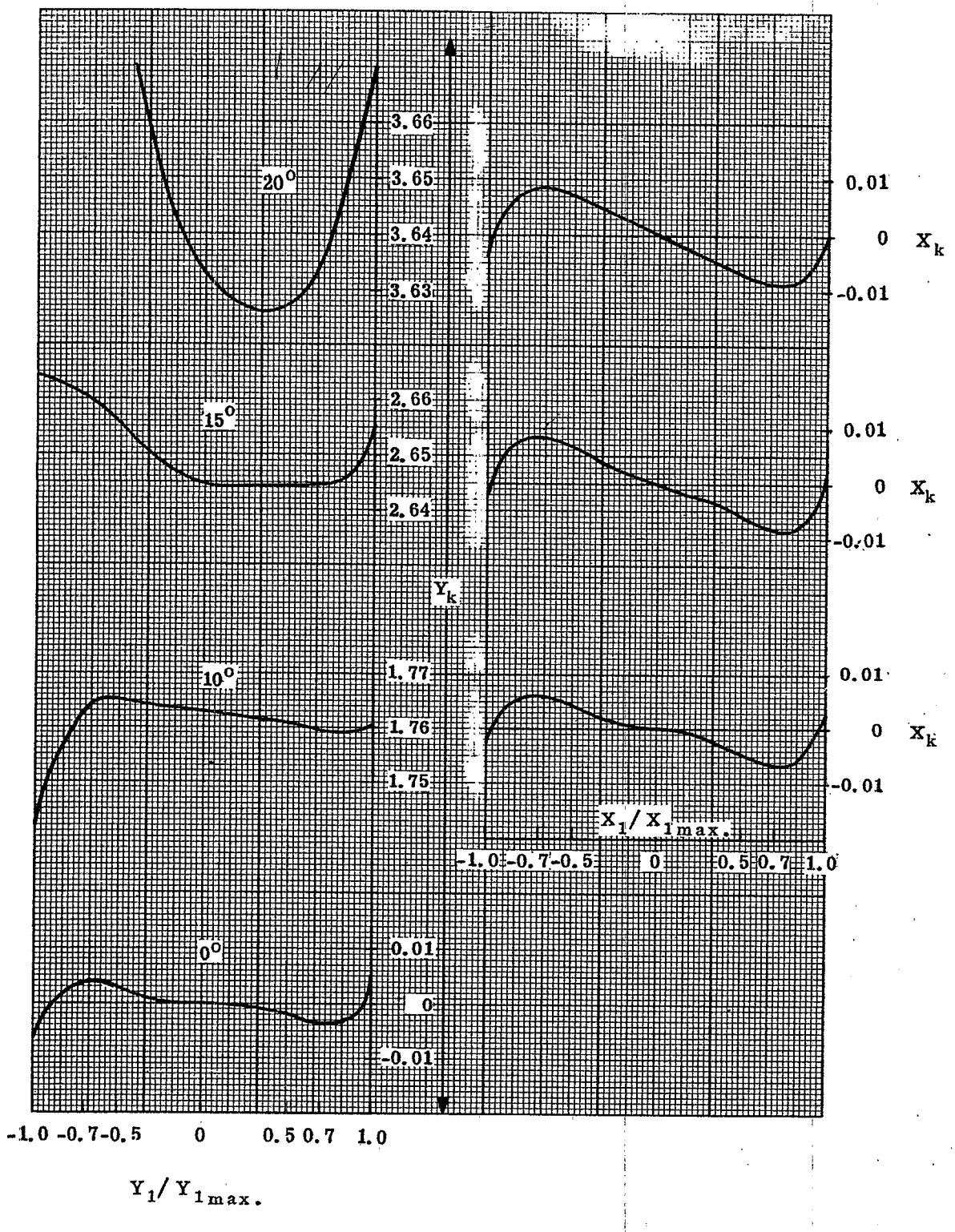

Figure 10.7- Aberration plots for right hand solution of lenses in Table 10.8.

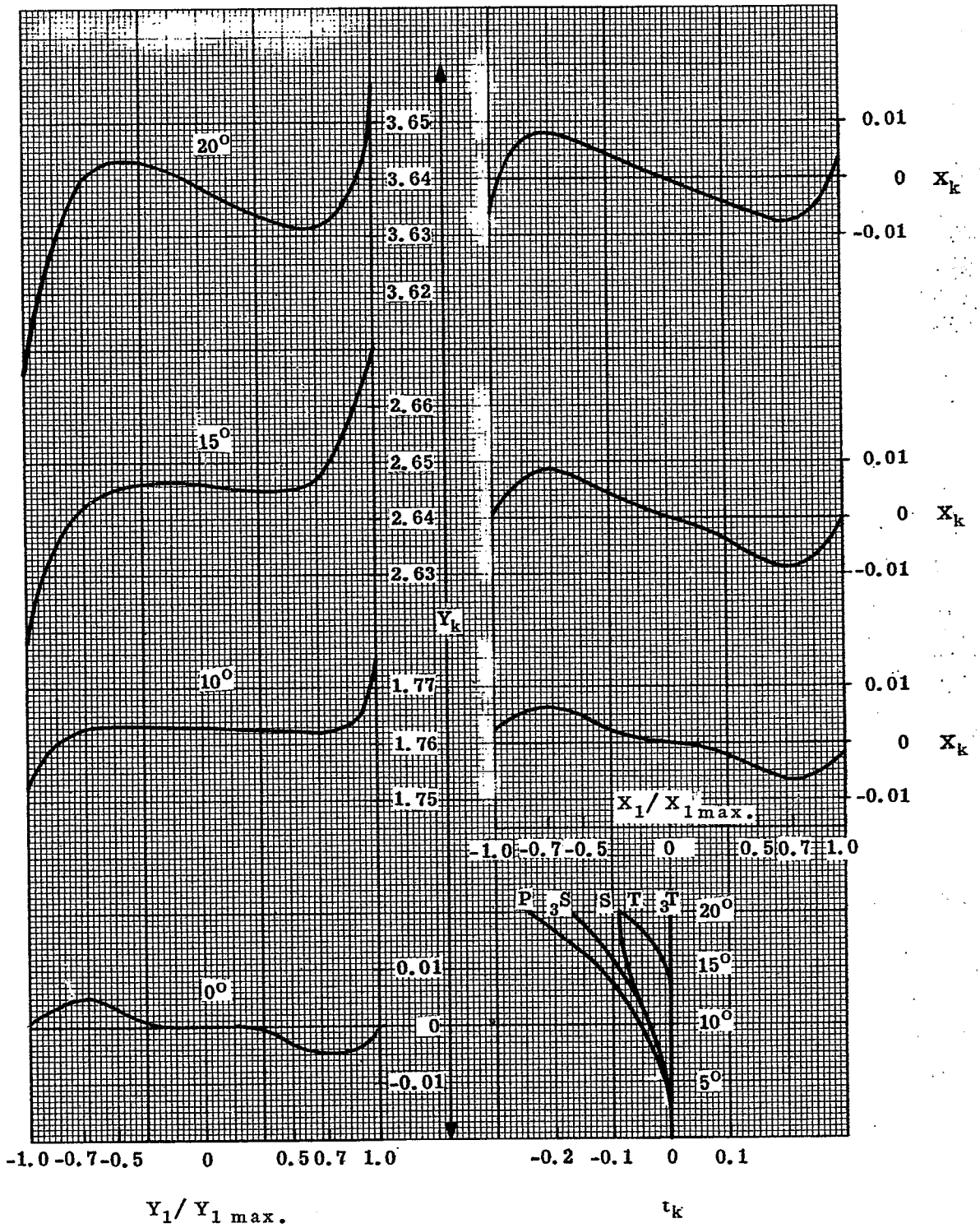

Figure 10.8- Aberration plots for left hand solution of lenses in Table 10.9.

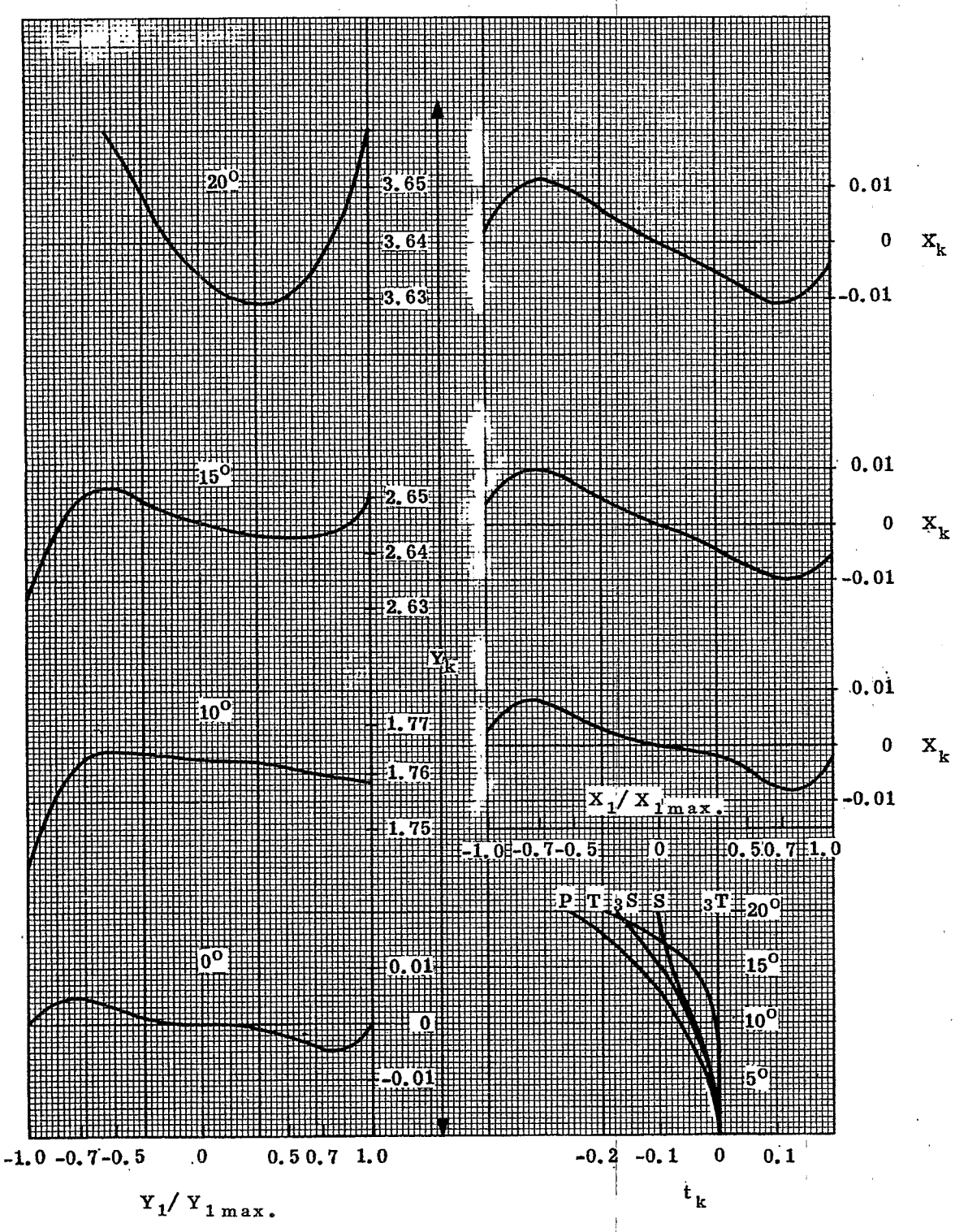

Figure 10.9- Aberration plots for right hand solution of lenses in Table 10.9.

Left Hand Solution c	t	Right Hand Solution c	t
0.2339		0.2882	
	0.60		0.60
-0.0098		-0.0193	
	1.211		0.8900
-0.2107		-0.1641	
	0.25		0.25
0.2516		0.2998	
	1.016		1.426
0.06799		0.0650	
	0.60		0.60
-0.2556		-0.1963	
	8.363		7.847
R = 0.9003		R = 1.493	
T = 3.677		T = 3.766	

Table 10.9 - Left and right hand solutions for $\Sigma P = -0.040$.

10.6.2.3 At this point, it was noticed that the system still was not as good as that described in Table 8.2. It was finally apparent that the thickness of the negative lens was 0.15, instead of 0.25. This indicated that the aberration parabola was lowered in this solution because of the decreased thickness of the negative lens. Then a new solution was found and the only change was to make $t_b = 0.15$. The result is that left and right hand solutions have R values 0.987 and 1.363. They are drawing closer together and the tangential field does not pull in as rapidly. The surface data for these solutions are included in Table 10.10 (step seven). Figures 10.10 and 10.11 show spot diagrams for these two solutions. In these diagrams only half of the symmetrical image is shown. The diagrams include the appearance of the images as the focal plane is shifted, clearly showing how a shift towards the lens provides a better concentration of light than in the paraxial focus. These diagrams show that there are only slight differences between the imagery in the left and right solutions, out to a half field angle of 15°. However, beyond 15° the left hand solution definitely is superior to that of the right hand. Notice how it shows better concentration and is more symmetrical.

Left Hand Solution c	t	Right Hand Solution c	t
0.2469		0.283	
	0.60		0.60
-0.00775		-0.01227	
	1.128		0.9289
-0.2024		-0.1692	
	0.15		0.15
0.2568		0.2911	
	1.0738		1.3209
0.0608		0.05869	
	0.60		0.60
-0.2487		-0.2113	
	8.346		8.033
R = 0.987		R = 1.363	
T = 3.552		T = 3.5998	

Table 10.10 - Left and right hand solution for $\Sigma P = -0.040$.

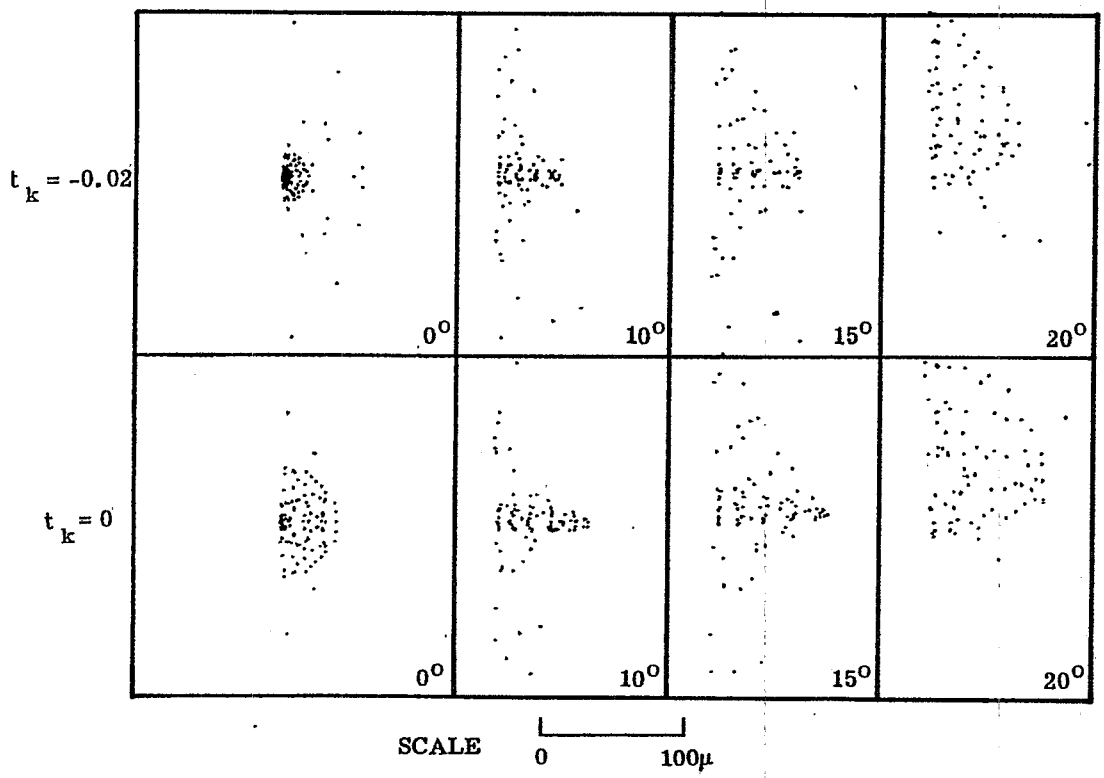

Figure 10.10- Spot diagrams for left hand solution in Table 10.10.

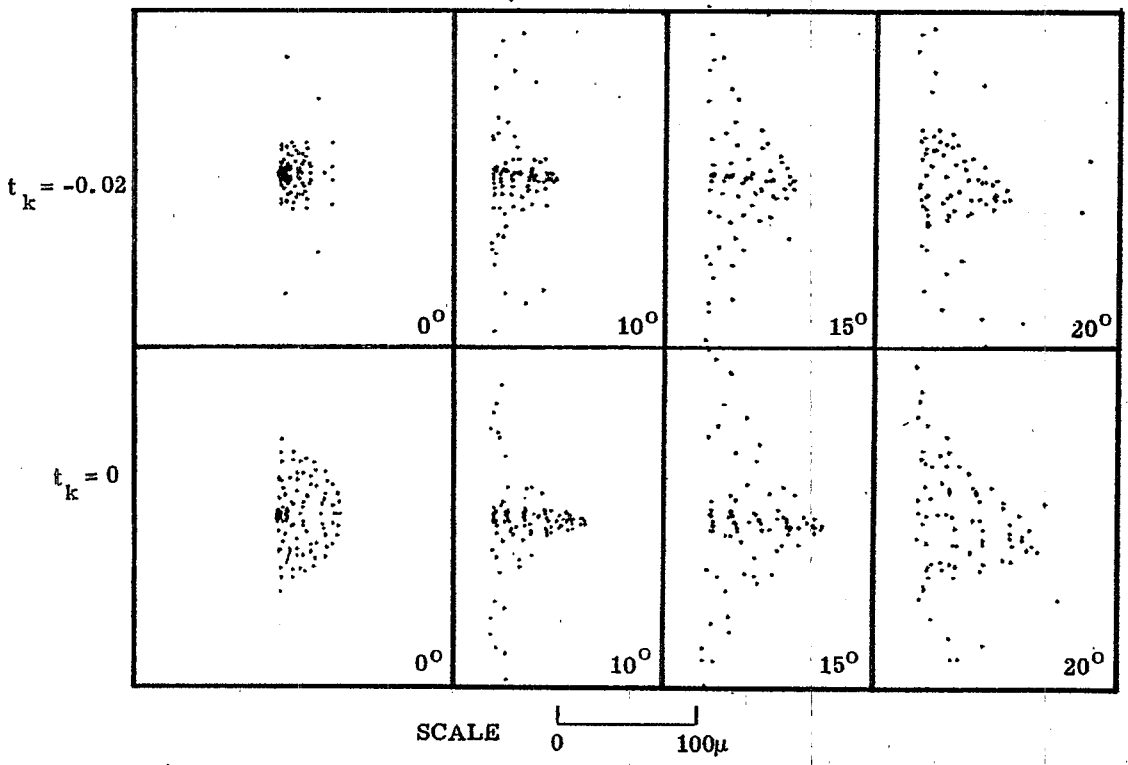

Figure 10.11 - Spot diagrams for right hand solution in Table 10.10.

10.6.3 Analysis of the readjustment procedure.

10.6.3.1 This study showed that reducing the thickness of the negative lens lowers the spherical aberration parabola. This effect then suggested investigating the effect of varying the thicknesses of the positive lenses. The effect is the same, namely lowering the parabola, but not as marked as in the case of the negative lens. This technique of changing the thicknesses of the lenses can be a useful way to compensate for the fact that the parabola is not quite where it should be. The parabola could be lowered still further by reducing the thicknesses, for the case of $\Sigma P = -0.040$, but this is not practical.

10.6.3.2 It is interesting to notice, that in these solutions for the triplet, c_2 is close in value to c_5, and c_4 is close to c_7. For the left hand solution these four surfaces have approximately equal curvatures. It would be very interesting if a solution could be found where all these four curves are identical.

10.7 EVALUATION OF OVER-ALL PERFORMANCE

The design of the optimum triplet is still far from complete, for one must investigate these images carefully by calculating the spot diagrams and energy distributions to be sure the best values for ΣP, ΣC, ΣF and ΣB have been chosen. To do this in detail is an enormous task which realistically can only be done on a very large computer. However with patience and judgment it is possible for designers to arrive at very good solutions.

10.8 SUMMARY

10.8.1 Guide lines. This study has indicated a few guide lines to follow in designing a triplet.

(1) One should always try to design as short a lens as possible to cover a given field.

(2) The spherical aberration parabola can be raised or lowered by the choice of ΣP, thicknesses of lenses, or glass.

(3) It appears that near optimum solutions occur with an R value slightly greater than 1.

10.8.2 Unsolved problems. The study made on this lens merely initiates the reader to the possibilities which need further clarification. A few of the problems are:

(1) What happens as the index of the crown element is increased?

(2) What kinds of solutions can be obtained by first lowering the parabola by glass choice so that there is no solution and then raising the parabola by thickness choice?

(3) What effect has raising the index of the negative lens if $\Delta\nu$ is maintained constant?

(4) When the parabola is too high, is it beneficial to lower it by using aspheric surfaces?

(5) What happens if the number of elements is increased beyond three, and at the same time two or more are cemented together? What happens if the negative element is cemented to either or both positive elements?

(6) If the lens is to cover a wider field, how does one choose the glass?

(7) At finite conjugate will the effect of glass choice and lens thicknesses be the same as at infinite conjugate?

11 TELESCOPE OBJECTIVES

11.1 INTRODUCTION

11.1.1 Scope. Sections 11 through 15 will be devoted to the demonstration of design principles using the simple telescope as a working example. Section 11 will discuss the detailed design of objectives; Section 12, lens erecting systems; Section 13, mirror and prism systems; Section 14, eyepieces; Section 15, complete telescope. It is assumed at this point that the reader has studied all the foregoing material and now has considerable knowledge of optical design. The inexperienced reader should not be concerned if he does not fully grasp the following material on first reading. As he gains experience it will become more and more useful.

11.1.2 The complete telescope. In describing the telescope, it will be assumed that the object is at infinity and that the eyepiece will be focused to place the virtual image at infinity. This means that the distant object will be brought to focus or imaged at the second focal point of the objective and that the first focal point of the eyepiece will coincide with this image. The telescope is then said to be in afocal adjustment.

11.1.3 The Petzval curvature of the system.

11.1.3.1 To start the design of an optical system, one of the first calculations to be made is an estimate of the amount of field curvature in the system, i.e., an estimate of ΣP. This is done by calculating P for each surface using Equation 8-(14), and summing. From Equations 8-(15) and 8-(16), if ΣB, ΣF, and ΣC are all zero, then

$$\alpha_y = \left(\frac{L_{k-1}}{M_{k-1}} - \frac{\bar{L}_{k-1}}{\bar{M}_{k-1}} \right) = \frac{\Sigma P \Phi^2}{2 n_{k-1} \; y_{k-1}} \left(\frac{Y_1}{y_1} \right) \left(\frac{\bar{Y}_o}{\bar{y}_o} \right)^2 \quad (1)$$

$$\alpha_x = \frac{K_{k-1}}{M_{k-1}} = \frac{\Sigma P \Phi^2}{2 n_{k-1} \; y_{k-1}} \left(\frac{X_1}{y_1} \right) \left(\frac{\bar{Y}_o}{\bar{y}_o} \right)^2 . \quad (2)$$

*

These equations show that P introduces angular aberrations, α_y and α_x, which are linearly proportional to Y_1 / y_1 and to X_1 / y_1. This means that for oblique object points the fan of rays entering the objective from a distant object point, do not emerge from the eyepiece as a parallel bundle. Instead the rays come to a finite focus. When $\bar{Y}_o$ is zero, Equations 8-(15) and 8-(16) indicate that the rays from the object point do emerge parallel to the axis because the telescope is in afocal adjustment and $\Sigma B = 0$. For the case described by Equations (1) and (2), the amount of the angular aberration varies as the square of the object height, $\bar{Y}_o$.

11.1.3.2 If the telescope objective is assumed to be thin, then from Equation 8-(28), $P = -\phi/n$. It is possible to change the value of P by using a photographic type of objective, but a simple doublet objective is by far the most common type of lens used in telescopes. In order to derive a general formula for the aberration, it is possible to write $P_o = -\phi_o / \gamma_o$, where γ_o is a constant ranging in value from 1.5 to ∞. For a doublet γ_o is approximately 1.5.

11.1.3.3 The value of P for the eyepiece also depends on how it is designed, but here again it is possible to write $P_e = -\phi_e / \gamma_e$, where ϕ_e is the power of the eyepiece and γ_e is a constant depending on the type of eyepiece. γ_e will range in value from 2.6 to 0.7 for most eyepieces.

11.1.3.4 Using these values of P for the objective and the eyepiece, it is possible to compute, from Equation (1), the angular aberration,

$$\alpha_y = - \frac{n_o^2 \quad u_o^2}{2 \, n_{k-1} \quad y_{k-1}} \left(\bar{Y}_o^2 \right) \left(\frac{Y_1}{y_1} \right) \left(\frac{\phi_o}{\gamma_o} + \frac{\phi_e}{\gamma_e} \right) .$$

Since a telescope is usually used in air, n_o and n_{k-1} are 1. Then,

$$\alpha_y = - \frac{1}{2} \left(\frac{\bar{Y}_o}{t_o} \right)^2 \left(\frac{Y_1}{y_1} \right) MP^2 \quad y_{k-1} \quad \phi_e \left(\frac{-1}{\gamma_o \, MP} + \frac{1}{\gamma_e} \right) . \quad (3)$$

*For a telescope with an object point at infinity one should strictly speaking use $(\tan U_o)/u_o$ instead of $\bar{Y}_o / \bar{y}_o$ but it is satisfactory to use the above equations and assume that the object distance is very large but finite.

This equation shows that the angular aberration due to Petzval curvature only varies

(1) as the square of the object height,

(2) approximately as the square of the MP,

(3) linearly with y_{k-1} .

11.1.3.5 For a given $(\bar{Y}_o / t_o)$ MP, the angular aberration in a telescope can be made small by making ϕ_e or y_{k-1} small. It is customary to specify the angular aberration of telescopes in diopters using the definition $d = 100\alpha / y_{k-1}$, where d is in diopters when y_{k-1} is given in centimeters and α is expressed in radians.

11.1.3.6 As a numerical example consider Table 11.1 which shows the values of α in minutes of arc and in diopters for telescopes of three different magnifications. To make these calculations the following assumptions were made:

$$y_{k-1} = -0.35 \text{ cm}$$
$$f_e = 2.00 \text{ cm}$$
$$(\bar{Y}_o / t_o)\,MP = -0.6$$
$$Y_1 / y_1 = 1.0$$
$$\gamma_o = \gamma_e = 1.5$$

The angular aberrations in Table 11.1 are all positive which means that the oblique bundles are focused behind the observer's eye making it impossible for him to focus on the image. It also means that the eyepiece must be focused towards the objective in order to remove the angular aberration for the off-axis object point. If it is moved towards the objective then the telescope will have angular aberration of the opposite sign for the central image. This indicates that the observer can accommodate and completely focus-out the angular error. The large angular aberration due to field curvature in telescopes is therefore not as serious as it may appear for it is possible for the eye to change focus as the observer views different parts of the field.

$\frac{\bar{Y}_o}{t_o}$. MP \ MP	-2	-5	-10	
-0.6	-9.0	-7.2	-6.6	Diopters
-0.6	107'	87'	79'	Minutes

Table 11.1- Angular aberration for telescopes of three magnifying powers.

11.1.3.7 In military telescopes it is often necessary to insert a reticle in the focal plane of the objective. Since a reticle is used to measure distances in the object space, it is important to design the objective with a flat field on the reticle, which usually means that the lens has to be more complex than the usual telescope doublet objective. Because the Petzval curvature of the eyepiece cannot be made zero, the eyepiece cannot focus the entire reticle with a single setting. Hence the reticle may not appear perfectly sharp, but if the objective is well corrected there is no parallax between the object and the reticle.

11.1.3.8 If a reticle is not needed in the design there is usually very little need to attempt to reduce the Petzval curvature of the objective by using a compound photographic lens type of objective. Equation (3) shows that the objective contribution, γ_o , is multiplied by the magnifying power of the telescope. For high power telescopes therefore, the objective adds a negligible amount of field curvature. This is why the majority of telescopes use simple doublets for the objective. If the power of the telescope is low then one must consider using some type of lens other than a doublet objective.

11.2 DESIGN PROCEDURE FOR A THIN LENS TELESCOPE OBJECTIVE

11.2.1 First order, thin lens.

11.2.1.1 The doublet, of course, consists of two lenses, and one can immediately start to fill out a table as was done with the triplet objective in Section 10.2. This has been done in Table 11.2.

	Lens a	Lens b	Image Plane
$-\phi$	$-\phi_a$	$-\phi_b$	0
t	0	$\frac{1}{\phi_a + \phi_b}$	
y	1	1	0
u	0	$-\phi_a$	$-\phi_a-\phi_b$
$\bar{y}$	0	0	$\frac{1}{\phi_a + \phi_b}$
$\bar{u}$	1	1	1
ν	ν_a	ν_b	0
$-\phi y^2/\nu$	$-(\phi/\nu)_a$	$-(\phi/\nu)_b$	$\Sigma a = -\frac{\phi_a}{\nu_a} - \frac{\phi_b}{\nu_b}$
$\frac{-\phi y \bar{y}}{\nu}$	0	0	$\Sigma b = 0$
$-\phi/n$	$-\phi_a/n_a$	$-\phi_b/n_b$	$\Sigma P = -\frac{\phi_a}{n_a} - \frac{\phi_b}{n_b}$

Table 11.2 - Computing table for the thin lens telescope doublet.

11.2.1.2 In order to solve for ϕ and have the axial color zero, assuming the two elements are close together, the following two equations must be satisfied:

$$\phi_a + \phi_b = \phi \quad , \tag{4}$$

and

$$\frac{\phi_a}{\nu_a} + \frac{\phi_b}{\nu_b} = 0 \quad . \tag{5}$$

The solution of these equations is

$$\phi_a = \phi \frac{\nu_a}{\nu_a - \nu_b} \quad , \tag{6}$$

and

$$\phi_b = \phi \frac{\nu_b}{\nu_b - \nu_a} \quad . \tag{7}$$

By using these equations, the value of ΣP from Equation 8-(28) is

$$\Sigma P = -\phi \left(\frac{\nu_a / n_a - \nu_b / n_b}{\nu_a - \nu_b} \right) \quad . \qquad (8)$$

11.2.1.3 These equations show that any two glasses with a difference in ν may be used to design a doublet. As will be seen later however, $\Delta \nu$ should be large in order to reduce the monochromatic aberrations. In principle the ΣP may be made equal to zero by the proper choice of glass. Actually, the ratio

$$\frac{\nu_a / n_a - \nu_b / n_b}{\nu_a - \nu_b}$$

is nearly constant for any glasses chosen with a reasonable value of $(\nu_a - \nu_b)$. It is therefore not practical to attempt to reduce P in a doublet by choosing the proper glasses. Once the two glasses for the doublet are chosen the following is known about the lens:

(1) The focal lengths of the (a) and (b) lenses, using Equations (6) and (7).

(2) The axial color, which was set equal to zero using Equation 6-(42).

(3) The transverse color, which is zero, using Equation 6-(41), because the objective is the entrance pupil.

(4) The Petzval curvature, using Equation (8).

(5) The third order astigmatism, using Equation 8-(26).

(6) The third order distortion, using 8-(27).

Only two aberrations of the third order, B and F, remain uncorrected.

11.2.2 Third order, thin lens.

11.2.2.1 As explained in Section 8.10.1, it is possible to compute the coefficients (α and β) for the following thin lens equations:

$$B_a = \alpha_{1a} + \alpha_{2a} c_1 + \alpha_{3a} c_1^2 \qquad (9)$$

$$B_b = \alpha_{1b} + \alpha_{2b} c_3 + \alpha_{3b} c_3^2 \qquad (10)$$

$$F_a = \beta_{1a} + \beta_{2a} c_1 \qquad (11)$$

$$F_b = \beta_{1b} + \beta_{2b} c_3 \qquad (12)$$

11.2.2.2 By setting $B_a + B_b = 0$ and $F_a + F_b = 0$, the above equations may be reduced to a second degree equation in c_1. There are then two real solutions called the left and right hand solutions. Examples of the two solutions are shown in Figure 11.1. The doublet used in the example was computed for the following glasses:

Lens (a) $n_D = 1.511$ $\nu = 63.5$

(b) $n_D = 1.649$ $\nu = 30.6$

11.2.2.3 The doublets shown in Figure 11.1 have the low dispersion glass in the front element facing the infinite conjugate side of the lens. Doublet solutions can equally well be found with the high dispersion glass in the front. Figure 11.2 shows the left hand solution for the same glasses with the positions reversed. The left hand solutions with the positive lens in front have the most favorable shape for the passage of the axial rays. Therefore most telescope objectives are solutions of this type, and they are referred to as Fraunhofer objectives.

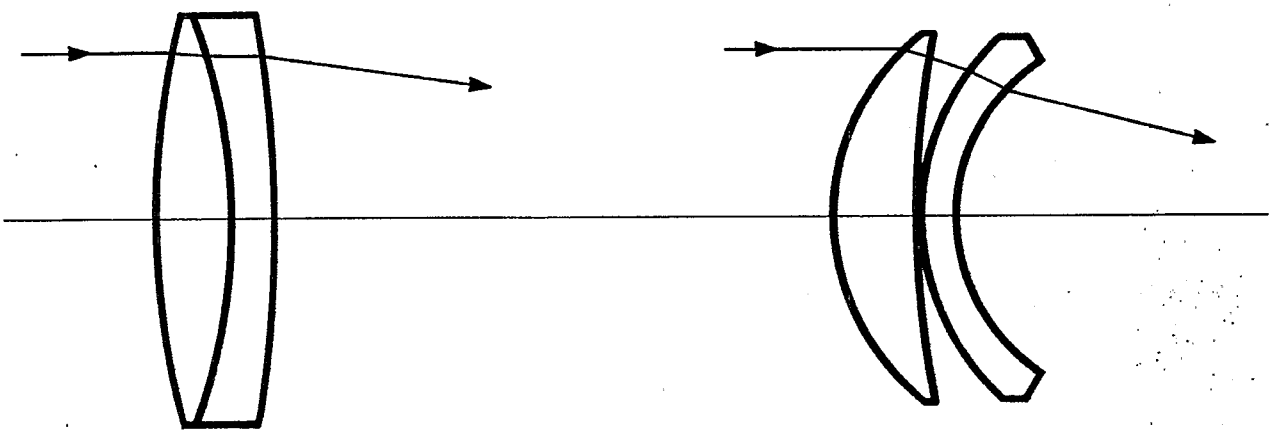

Left hand solution

Right hand solution

Figure 11.1 - Two types of doublets. For both types, the positive lens is in front and is of low dispersion glass.

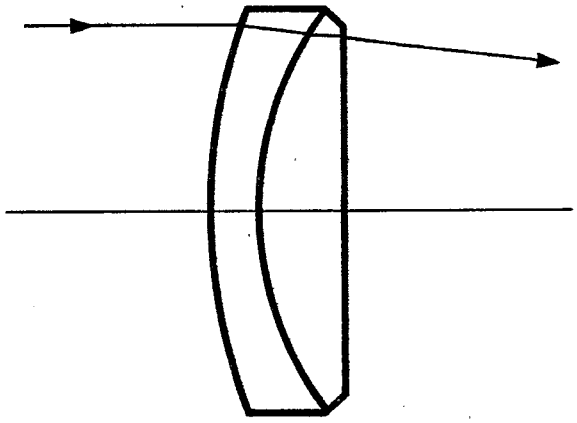

Figure 11.2 - Doublet with negative lens in front. The glasses are the same as the left hand solution in Figure 11.1 with the positions reversed.

11.2.3 Thin lens solutions.

11.2.3.1 Table 11.3 contains a selection of left hand solutions for 38 thin lens systems of the Fraunhofer type. Table 11.4 includes a list of the left hand solution for lenses with the negative lens in front. Systems with the negative lens in front appear to offer no advantages over the Fraunhofer type and so will not be discussed further.

11.2.3.2 There are of course numerous other combinations of glass one can pick, but those shown in Table 11.3 provide a sufficient variety of choices to build up an understanding of the solutions. The following points should be noted about the solutions:

(1) The series of solutions 1 to 8 have the same glass for the positive lens. The negative lenses however are all selected from the ordinary glass line shown in Figure 6.18. Notice that the first curvature for each solution is approximately 0.165 and the last curvature is about -0.08. The outside appearance of these lenses is therefore very similar. The difference between the lenses is in the curvatures of the internal surfaces.

(2) When combinations of glasses with small ν differences are selected, the curvature of the second surface is stronger than that of the third surface. This means that the surfaces do not edge contact and a spacer is needed. As the ν difference is increased, the difference in curvature of these two surfaces decreases, and at large ν differences the third surface becomes stronger than the second. The lenses then contact at the edge.

11.3 DESIGN PROCEDURE FOR A THICK LENS TELESCOPE OBJECTIVE

11.3.1 The thick lens doublet.

11.3.1.1 Very little choice can be made, from the thin lens data alone, between the numerous telescope objectives. In order to make a selection from the possible glass choices, it is necessary to trace rays through the designs.

11.3.1.2 As was pointed out in Section 10.4.1.7, when a lens is studied by ray tracing it is necessary to decide on a definite f - number. Changing the f - number requirement changes completely the conclusions one draws from the ray tracing. In order to illustrate the design procedure, a study will be made for a particular lens of f - number 3.57 with a focal length of 10.

11.3.2 Automatic correction of the third order aberrations.

11.3.2.1 After thicknesses are added to the thin lens solutions, it is necessary to readjust the curvatures to correct the spherical aberration, coma, and axial color to the required residuals. One cannot set the third order aberrations to zero if the total aberrations are to be zero, for the actual ray tracing will reveal the presence of higher order aberration.

11.3.2.2 In order to compare various glass choices in doublets it is necessary to hold constant many variables. In the study to be described the following parameters were held constant.

(a) The focal length of each lens was 10.0.

(b) The marginal ray entered the lens at $Y_1 = 1.4$.

(c) The third order spherical aberration was adjusted until the marginal ray at $Y_1 = 1.4$ in D light focused at the paraxial D focus.

(d) The axial first order color was adjusted until the rays traced at a value of $Y_1 = 1.0$ for F and C light united in the paraxial focal plane.

(e) The thickness of the positive and negative element was made 0.5 and 0.3, respectively

(f) The space between the lenses was maintained automatically. There were two alternatives. Where $r_2 > r_3$, the elements were spaced by 0.01 at the aperture height of $y \geq 1.4$; where $r_2 < r_3$, a space of 0.01 was set at the vertex.

(g) The third order coma was corrected to zero in all cases.

Glass values Element n_{Da} ν_a a	n_{Db} ν_b b	Total curvatures c_a	c_b	Individual surface curvatures c_1	c_2	c_3	c_4	Case No.
1.511 63.5	1.5795 41.0	0.5523	−0.3145	0.1652	−0.3871	−0.3802	−0.0658	1
1.511 63.5	1.621 36.2	0.4552	−0.2135	0.1658	−0.2893	−0.2848	−0.0713	2
1.511 63.5	1.649 33.8	0.4184	−0.1754	0.1660	−0.2525	−0.2499	−0.0746	3
1.511 63.5	1.689 30.9	0.3812	−0.1376	0.1659	−0.2152	−0.2163	−0.0787	4
1.511 63.5	1.720 29.3	0.3634	−0.1190	0.1659	−0.1975	−0.2009	−0.0819	5
1.511 63.5	1.8052 25.5	0.3270	−0.0833	0.1656	−0.1614	−0.1730	−0.0896	6
1.511 63.5	1.5704 48.1	0.8070	−0.5476	0.1563	−0.6507	−0.6351	−0.0875	7
1.511 63.5	1.5838 46.0	0.7101	−0.4503	0.1595	−0.5506	−0.5354	−0.0851	8
1.511 63.5	1.605 43.6	0.6245	−0.3622	0.1620	−0.4625	−0.4476	−0.0854	9
1.511 63.5	1.617 36.6	0.4798	−0.2353	0.1657	−0.3141	−0.3077	−0.0723	10
1.511 63.5	1.717 48.2	0.8123	−0.4394	0.1411	−0.6711	−0.6259	−0.1865	11
1.511 63.5	1.720 50.3	0.9415	−0.5293	0.1228	−0.8186	−0.7630	−0.2337	12
1.511 63.5	1.8037 41.8	0.5727	−0.2397	0.1631	−0.4095	−0.3779	−0.1382	13
1.517 64.5	1.689 30.9	0.3713	−0.1335	0.1648	−0.2065	−0.2091	−0.0756	14
1.611 58.8	1.5795 41.0	0.5516	−0.4090	0.1594	−0.3922	−0.4009	0.0080	15
1.611 58.8	1.617 36.6	0.4397	−0.2734	0.1538	−0.2859	−0.2903	−0.0170	16
1.611 58.8	1.621 36.2	0.4318	−0.2638	0.1535	−0.2782	−0.2824	−0.0186	17
1.611 58.8	1.649 33.8	0.3895	−0.2126	0.1525	−0.2369	−0.2403	−0.0277	18
1.611 58.8	1.689 30.9	0.3482	−0.1637	0.1519	−0.1963	−0.2002	−0.0366	19
1.611 58.8	1.720 29.3	0.3290	−0.1403	0.1518	−0.1773	−0.1819	−0.0416	20
1.611 58.8	1.689 30.9	0.3448	−0.1607	0.1519	−0.1930	−0.1973	−0.0366	21
1.620 60.3	1.617 36.6	0.3910	−0.2308	0.1521	−0.2389	−0.2459	−0.0151	22
1.620 60.3	1.649 33.8	0.3526	−0.1827	0.1510	−0.2016	−0.2080	−0.0253	23
1.620 60.3	1.7506 27.8	0.2904	−0.1067	0.1500	−0.1404	−0.1503	−0.0437	24
1.620 60.3	1.8052 25.5	0.2731	−0.0861	0.1498	−0.1232	−0.1362	−0.0502	25
1.620 60.3	1.8037 41.8	0.4902	−0.2537	0.1490	−0.3412	−0.3253	−0.0716	26
1.638 55.5	1.617 36.6	0.4603	−0.3139	0.1527	−0.3075	−0.3144	−0.0005	27
1.638 55.5	1.649 33.8	0.4009	−0.2400	0.1503	−0.2506	−0.2551	−0.0151	28
1.638 55.5	1.689 30.9	0.3536	−0.1823	0.1493	−0.2044	−0.2083	−0.0260	29
1.638 55.5	1.720 29.3	0.3308	−0.1542	0.1490	−0.1818	−0.1861	−0.0319	30
1.5286 51.6	1.5497 45.8	1.6831	−1.437	0.1206	−1.563	−1.548	−0.1113	31
1.5286 51.6	1.5795 41.0	0.9209	−0.6675	0.1481	−0.7729	−0.7568	−0.0893	32
1.5286 51.6	1.621 36.2	0.6339	−0.3785	0.1584	−0.4755	−0.4604	−0.0819	33
1.5286 51.6	1.649 33.8	0.5484	−0.2926	0.1610	−0.3874	−0.3736	−0.0810	34
1.5286 51.6	1.689 30.9	0.4716	−0.2167	0.1629	−0.3087	−0.2975	−0.0808	35
1.5286 51.6	1.72 29.3	0.4378	−0.1825	0.1635	−0.2742	−0.2646	−0.0822	36
1.5286 51.6	1.72 42.0	0.4981	−0.2268	0.1623	−0.3357	−0.3193	−0.0926	37
1.5286 51.6	1.76 29.3	0.4378	−0.1729	0.1639	−0.2738	−0.2620	−0.08913	38

Table 11.3 - Thin lens aplanatic doublets of focal length 10.

Glass values Element n_{Da} ν_a	n_{Db} ν_b	Total curvatures c_a	c_b	Individual surfaces curvatures c_1	c_2	c_3	c_4	Case No.
1.5795 41.	1.511 63.5	-0.3145	0.5523	0.2270	0.5415	0.5473	-0.0050	1
1.621 36.2	1.511 63.5	-0.2135	0.4552	0.2332	0.4467	0.4496	-0.0056	2
1.649 33.8	1.511 63.5	-0.1754	0.4184	0.2369	0.4123	0.4127	-0.0057	3
1.689 30.9	1.511 63.5	-0.1376	0.3812	0.2417	0.3793	0.3755	-0.0057	4
1.720 29.3	1.511 63.5	-0.1190	0.3634	0.2453	0.3643	0.3577	-0.0057	5
1.8052 25.5	1.511 63.5	-0.0833	0.3270	0.2543	0.3376	0.3217	-0.0053	6
1.5704 48.1	1.511 63.5	-0.5476	0.8070	0.2487	0.7962	0.8109	0.0039	7
1.5838 46.0	1.511 63.5	-0.4503	0.7101	0.2465	0.6968	0.7108	0.0007	8
1.605 43.6	1.511 63.5	-0.3622	0.6245	0.2471	0.6092	0.6227	-0.0018	9
1.617 36.6	1.511 63.5	-0.2353	0.4798	0.2342	0.4695	0.4744	-0.0055	10
1.717 48.2	1.511 63.5	-0.4394	0.8123	0.3500	0.7895	0.8315	0.0193	11
1.720 50.3	1.511 63.5	-0.5293	0.9415	0.3974	0.9267	0.9791	0.0376	12
1.8037 41.8	1.511 63.5	-0.2397	0.5727	0.3029	0.5426	0.5699	-0.0027	13
1.689 30.9	1.517 64.5	-0.1335	0.3713	0.2385	0.3718	0.3666	-0.0045	14
1.5795 41.0	1.611 58.8	-0.4090	0.5516	0.1532	0.5622	0.5540	0.0023	15
1.617 36.6	1.611 58.8	-0.2734	0.4397	0.1788	0.4521	0.4476	0.0079	16
1.621 36.2	1.611 58.8	-0.2638	0.4318	0.1805	0.4443	0.4399	0.0082	17
1.649 33.8	1.611 58.8	-0.2126	0.3895	0.1900	0.4026	0.3986	0.0092	18
1.689 30.9	1.611 58.8	-0.1637	0.3482	0.1994	0.3631	0.3580	0.0098	19
1.720 29.3	1.611 58.8	-0.1403	0.3290	0.2049	0.3452	0.3390	0.0100	20
1.689 30.9	1.611 58.8	-0.1607	0.3448	0.1995	0.3602	0.3548	0.0098	21
1.617 36.6	1.620 60.3	-0.2308	0.3910	0.1769	0.4077	0.4007	0.0097	22
1.649 33.8	1.620 60.3	-0.1827	0.3526	0.1876	0.3703	0.3634	0.0108	23
1.7506 27.8	1.620 60.3	-0.1067	0.2904	0.2074	0.3141	0.3023	0.0118	24
1.8502 25.5	1.620 60.3	-0.0861	0.2731	0.2147	0.3007	0.2851	0.0121	25
1.8037 41.8	1.620 60.3	-0.2537	0.4902	0.2361	0.4898	0.5031	0.0130	26
1.617 36.6	1.638 55.5	-0.3139	0.4603	0.1623	0.4762	0.4696	0.0094	27
1.649 33.8	1.638 55.5	-0.2400	0.4009	0.1774	0.4174	0.4127	0.0118	28
1.689 30.9	1.638 55.5	-0.1823	0.3536	0.1889	0.3712	0.3665	0.0128	29
1.720 29.3	1.638 55.5	-0.1542	0.3308	0.1951	0.3494	0.3439	0.0131	30
1.5497 45.8	1.5286 51.6	-1.437	1.6831	0.2721	1.7087	1.7231	0.0399	31
1.5795 41.0	1.5286 51.6	-0.6675	0.9209	0.2505	0.9180	0.9333	0.0124	32
1.621 36.2	1.5286 51.6	-0.3785	0.6339	0.2438	0.6223	0.6360	0.0021	33
1.649 33.8	1.5286 51.6	-0.2926	0.5484	0.2433	0.5359	0.54795	-0.00047	34
1.689 30.9	1.5286 51.6	-0.2167	0.4716	0.2438	0.4604	0.4692	-0.0024	35
1.72 29.3	1.5286 51.6	-0.1825	0.4378	0.2456	0.4281	0.4347	-0.0030	36
1.72 42.0	1.5286 51.6	-0.2268	0.4981	0.2560	0.4827	0.4962	-0.0018	37
1.76 29.3	1.5286 51.6	-0.1729	0.4378	0.2531	0.4260	0.4344	-0.0034	38

Table 11.4 - Telescope objectives with flint in front.

11.3.2.3 In designing a doublet of a particular glass choice, it is necessary to estimate the values at which to set the third order spherical aberration, B, and axial color, a. Then surfaces 1, 2, and 3 are varied to provide derivatives for B, F, and a. The following three equations are then solved for the required values of B, F, and a.

$$\Delta\Sigma B = \frac{\partial\Sigma B}{\partial c_1}\Delta c_1 + \frac{\partial\Sigma B}{c_2}\Delta c_2 + \frac{\partial\Sigma B}{\partial c_3}\Delta c_3 ,$$

$$\Delta\Sigma F = \frac{\partial\Sigma F}{\partial c_1}\Delta c_1 + \frac{\partial\Sigma F}{\partial c_2}\Delta c_2 + \frac{\partial\Sigma B}{\partial c_3}\Delta c_3 ,$$

$$\Delta\Sigma a = \frac{\partial\Sigma a}{\partial c_1}\Delta c_1 + \frac{\partial\Sigma a}{\partial c_2}\Delta c_2 + \frac{\partial\Sigma a}{\partial c_3}\Delta c_3 .$$

This is the method described in Section 9.2.4.12. Since the changes are not linear, it is necessary to repeat the procedure for several iterations. When the desired third order values are found, the solution is then ray traced in D, F, and C light at 0° with values of $Y_1 = 1.4$, 1.2, 1.0, and 0.8. From this ray tracing data it is possible to determine if condition c and d are fulfilled. If they are not it is necessary to assign a new value to B and a and repeat the process.

11.3.2.4 Tables 11.5, 11.6, and 11.7 show the data for three doublets designed in this manner. The design shown in Table 11.7 illustrates a careful balance of high order aberrations for D light. In order to arrive at this design it was necessary to choose just the right ν number for the negative lens. If a flint with a larger ν number had been chosen, the rays at an aperture of $Y_1 = 1.4$ would have crossed the paraxial focal plane at a larger negative value and this would have been impossible to correct without introducing a large positive zonal aberration. Notice how the F light starts out to be under-corrected (negative Y_k), but as Y_1 is increased it becomes over-corrected (positive Y_k). The C light starts out positive and then turns toward the negative side. This is evidence of chromatic variation of spherical aberration. Note also how the aberration for the lenses in Tables 11.5 and 11.6 are larger than in Table 11.7 even though all the curvatures are smaller. If a different f - number is needed one would choose a different flint element for optimum correction.

11.3.2.5 The aberration curves in Figure 11.3 are for the ray data given in Table 11.6. The D light curve is typical for a telescope objective. The third order spherical aberration is undercorrected. The curve, for small values of Y_1, starts out below the reference axis following the third order aberration, but it then starts to depart and swings towards the positive side. This is due to higher order aberrations which, in this case, are positive. By evaluating the constants in Equation 8-(1) for this aberration curve we find that

$$b_o = 0,\ b_3 = -0.0014,\ \text{and}\ b_5 = 0.000619$$

Lens specifications				
c	t	n	ν	
0.1672	0.5	1.511	63.5	$f' = 9.995478$
-0.1594	0.0218	1.0		$l' = 9.624807$
-0.1709	0.3	1.80489	25.4	
-0.0886				
Ray-trace data				
Y_1	Y_D	Y_F	Y_C	
1.4	0.000279	0.002047	0.000618	Y is the height of the ray in the D light paraxial focal plane.
1.2	-0.000689	0.000362	-0.000233	
1.0	-0.000777	-0.000202	-0.000291	
0.8	-0.000542	-0.000267	-0.000089	

Table 11.5 - Lens specification and ray trace data for an achromatic doublet with large ν difference.

Lens specifications				
c	t	n	ν	
0.167876		1		
	0.5	1.511	63.5	f'= 10.000000
-0.244936				
	0.01	1.0		l'= 9.597161
-0.243789				
	0.3	1.649	33.8	
-0.073862				

Ray-trace data				
Y_1	Y_D	Y_F	Y_C	
1.4	0.000201	0.002359	0.000334	
1.2	-0.000423	0.000786	-0.000079	
1.0	-0.000526	0.000060	-0.000089	
0.8	-0.000387	-0.000176	0.000055	

Table 11.6 - Lens specification and ray trace data for an achromatic doublet with moderate ν difference.

Lens specifications				
c	t	n	ν	
0.168413				
	0.5	1.511	63.5	f'= 10.0000
-0.290972				
	0.01	1.0		l'= 9.578138
-0.289068				
	0.3	1.605	38.0	
-0.067287				

Ray-trace data				
Y_1	Y_D	Y_F	Y_C	
1.4	-0.000366	0.001065	0.000038	
1.2	+0.000083	0.000618	0.000673	
1.0	-0.000034	-0.000064	0.000628	
0.8	-0.000092	-0.000411	0.000542	

Table 11.7 - Lens specification and ray trace data for an achromatic doublet with small ν difference.

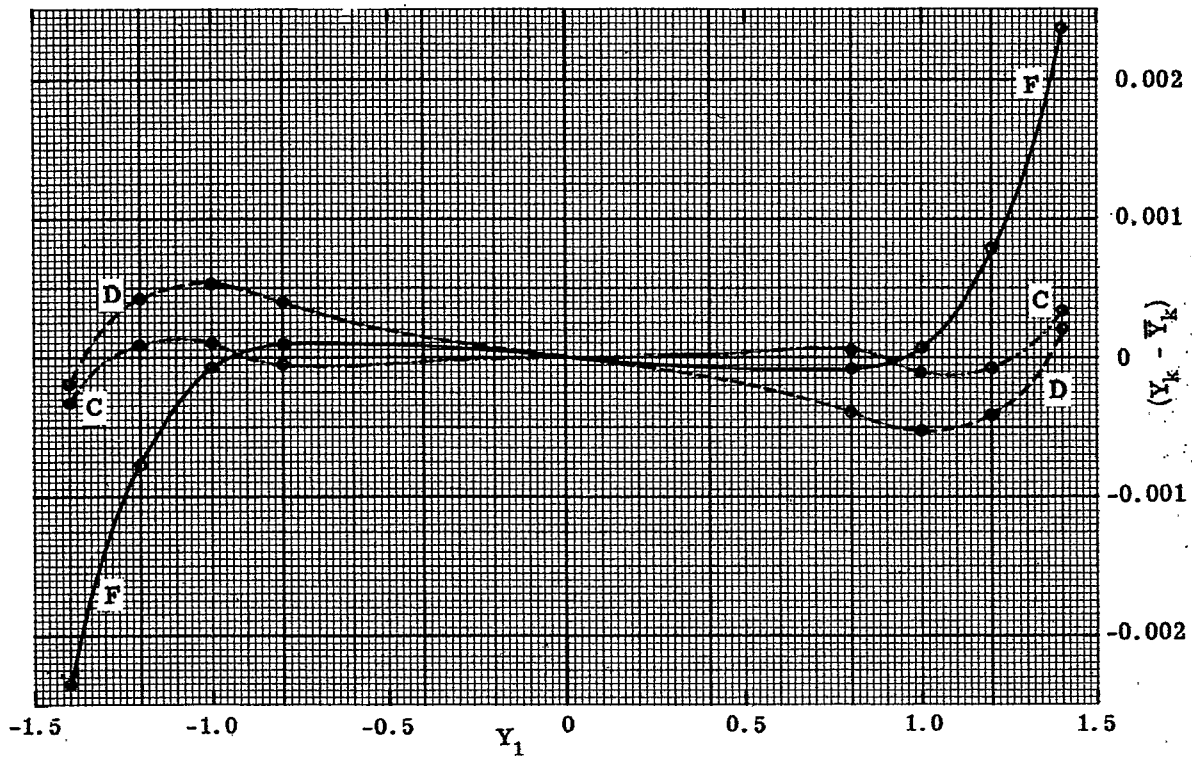

Figure 11.3 - Meridional ray plot at 0^{o} for a doublet lens.

11.3.2.6 The third order calculations for this lens are included in Table 11.8. Inspection of these data gives a clue to why b_5 is positive. Surfaces 1, 2 and 4 have negative values of B. The only source of positive B is the 3rd surface. A surface always adds higher order aberration of the same sign as the third order. Since the 3rd surface introduces such a large positive third order contribution it over-balances the negative higher order contributions from the other surfaces. The result is a positive fifth order term. In designing the doublet it is considered advisable to adjust the third order aberration so that the higher order correction brings the curve back to $Y_k = 0$ for the rays at $Y_1 = Y_{1\,max.}$ This leaves a residual aberration called zonal aberration. In figure 11.3 the zonal aberration for D light amounts to -0.000526.

c	0.16788	-0.24494	-0.24379	-0.07386	
t	0.50	0.01	0.30		
n	1.511	1.0	1.649		
y	1	0.97161	0.96954	0.95972	
u	-0.05677	-0.20739	-0.03274	-0.1	
B	-0.00106	-0.03273	0.03580	-0.00225	$\Sigma B = -0.00023$ $_3Y_k = -0.00115$

Table 11.8 - Third order spherical contribution on each surface of the doublet shown in Table 11.6

11.3.3 Tolerance on zonal aberration.

11.3.3.1 The question of the tolerance on the zonal aberration cannot be explained fully here, but a few guide lines can be given.

(1) If the axial image must be corrected to be physically perfect it is necessary to reduce the zonal aberration to the following tolerance.

$$(Y_k)_{zone} = \frac{4.6\lambda}{L_{k-1}}$$

L_{k-1} = optical direction cosine of the emerging ray.

This tolerance assumes that the ray traced at a height of $Y_{1\,max.}$ is adjusted so that $Y_k = 0$. Tolerance is calculated as a positive number.

(2) If the objective is used in a telescope, one can compute the angular aberration presented to the eye, and set the tolerance by using the principle that the angular resolution of the eye is limited to one part in 3000. However, there is no need to attempt to reduce the zonal aberration below the value given above for the diffraction image case (1). In this region the size of the image is actually determined by the physical nature of the light and not by the geometrical aberrations.

11.3.3.2 The $Y_{1\,max.}$ for the lens shown in Table 11.6 is 1.4. The focal length is 10. Therefore, L_{k-1} is approximately -0.14 The zonal tolerance $(Y_k)_{zone}$ is then calculated as follows.

$$(Y_k)_{zone} = \frac{4.6 \times 0.5893 \text{ microns}}{0.14}$$

$$= 19.4 \text{ microns} = 0.0194 \text{ mm.}$$

The zonal aberration for the lens in Table 11.6 is -0.000526. This means that the lens could have a focal length 10 x 0.0194/0.000526 = 369mm and remain corrected within the tolerance. This assumes, of course, that the light is monochromatic. One can see that F and C light are not corrected as well as this. More will be said about this in a later section (Section 11.4) on secondary spectrum.

11.3.4 Methods for reducing the zonal aberration.

11.3.4.1 If the zonal aberration is too large in a lens it may be reduced by four methods. These methods will now be described for they illustrate a powerful technique of design. The methods are:

(1) Choosing the proper glasses.

(2) Using an air space.

(3) Introducing an aspheric surface.

(4) Adding an extra positive lens.

11.3.4.2 Tables 11.5, 11.6, and 11.7 illustrate the influence of glass choice.

11.3.4.3 If the air space is made larger the marginal rays have a chance to drop more before they strike the negative lens. The higher order negative aberration on the positive lens then causes the rays to actually strike the over-correcting surface at a lower aperture than predicted from first and third order theory. This cuts down on the higher order over-correcting tendency of this surface. Therefore as the space is increased the positive fifth order term is reduced. The third order value can then be made less negative, resulting in a reduced zone. Figures 11.4, 11.5, and 11.6 show some of the aberration curves for doublets where the air space has been adjusted to minimize the spherical aberration in D light. These lenses were also corrected so that the $Y_{1\,max.}$ was 1.4. The zonal aberration has been reduced to a remarkable degree. Table 11.9 contains the curvatures and thicknesses for many optimum solutions of this type. The last two columns are headed OSC', which stands for offense against the sine condition. This quantity, OSC', is proportional to coma, for a given image height, Y_k. These last two columns, therefore, are a measure of third order coma, and total coma for the marginal ray, respectively.

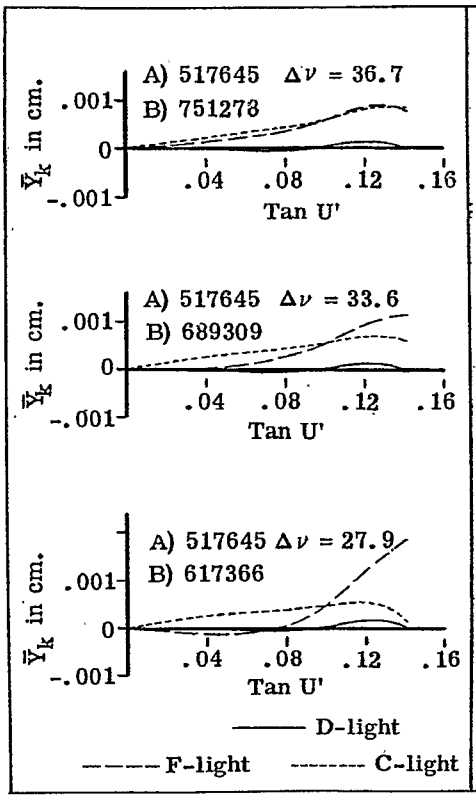

Figure 11.4- Effects of ν difference on spherochromatism (glass A used in positive lens, glass B used in negative lens).

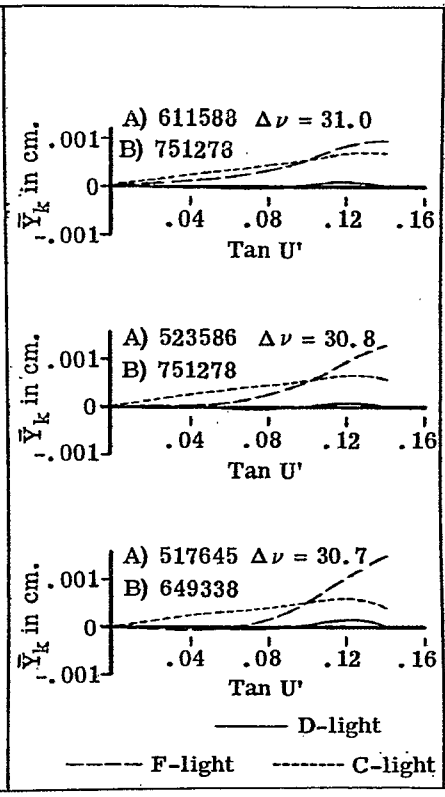

Figure 11.5- Effects of index of positive (A) lens on spherochromatism.

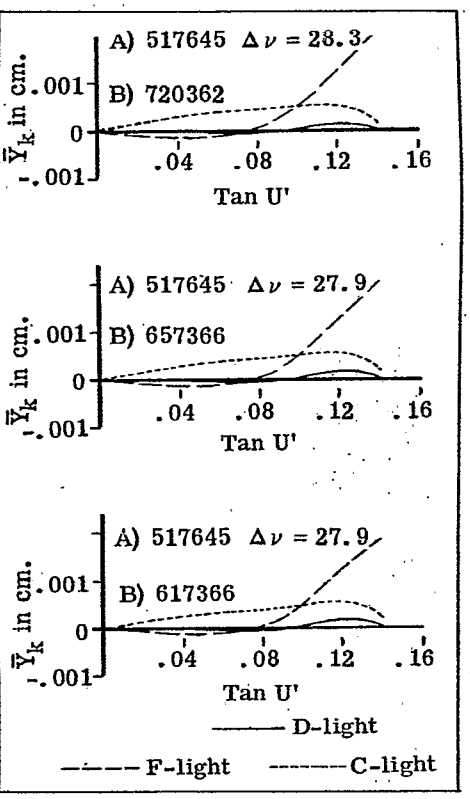

Figure 11.6- Effects of index of negative lens (B) on spherochromatism.

Glasses + lens	Glasses - lens	Δν	c_1	c_2	c_3	c_4	t_2	OSC' Third order	OSC' Marginal
517 645	751 278	36.7	+0.2582	−0.1450	−0.2222	−0.0489	+0.7364	−0.0030	−0.0017
517 645	720 293	35.2	+0.2379	−0.1630	−0.2159	−0.0470	+0.5353	−0.0026	−0.0014
517 645	689 309	33.6	+0.2205	−0.1825	−0.2173	−0.0468	+0.3596	−0.0022	−0.0012
517 645	649 338	30.7	+0.1955	−0.2215	−0.2348	−0.0516	+0.1412	−0.0015	−0.0009
517 645	617 366	27.9	+0.1780	−0.2638	−0.2663	−0.0575	+0.0400	−0.0007	−0.0006
517 645	657 366	27.9	+0.1634	−0.2716	−0.2671	−0.0783	+0.0022	+0.0003	−0.0000
517 645	720 362	28.3	+0.1526	−0.2733	−0.2632	−0.0986	−0.0261	+0.0010	+0.0004
523 586	751 278	30.8	+0.2091	−0.1801	−0.2067	−0.0593	+0.3141	−0.0016	−0.0009
523 586	720 293	29.3	+0.1955	−0.2016	−0.2161	−0.0612	+0.1826	−0.0013	−0.0008
523 586	689 309	27.7	+0.1829	−0.2260	−0.2317	−0.0641	+0.0883	−0.0008	−0.0006
523 586	649 338	24.8	+0.1611	−0.2776	−0.2730	−0.0751	−0.0014	+0.0004	+0.0000
523 586	617 366	22.0	+0.1373	−0.3417	−0.3334	−0.0926	−0.0221	+0.0028	+0.0015
523 586	657 366	22.0	+0.1149	−0.3787	−0.3653	−0.1282	−0.0311	+0.0048	+0.0026
523 586	720 362	22.4	+0.1009	−0.3636	−0.3478	−0.1523	−0.0444	+0.0064	+0.0039
611 588	751 278	31.0	+0.2149	−0.1381	−0.1858	−0.0111	+0.4904	−0.0020	−0.0011
611 588	720 293	29.5	+0.2052	−0.1551	−0.1913	−0.0086	+0.3540	−0.0019	−0.0011
611 588	689 309	27.9	+0.2006	−0.1731	−0.2027	−0.0030	+0.2606	−0.0020	−0.0011
611 588	649 338	25.0	+0.1971	−0.2091	−0.2308	+0.0079	+0.1481	−0.0025	−0.0015
611 588	617 366	22.2	+0.2161	−0.2426	−0.2662	+0.0389	+0.1128	−0.0050	−0.0032
611 588	657 366	22.2	+0.1713	−0.2598	−0.2652	−0.0142	+0.0347	−0.0013	−0.0009
611 588	720 362	22.6	+0.1439	−0.2676	−0.2623	−0.0538	−0.0128	+0.0008	+0.0003

Table 11.9- Final solution lens data resulting from least-squares correction program. For all lenses, $f' =$ 10.0 cm, t_1 = 0.5 cm, t_3 = 0.3 cm.

11.3.4.4 Probably the simplest (from a theoretical point of view) method to reduce the zonal aberration is to introduce an aspheric surface on the last surface. Thus one can introduce high order terms of deformation and geometrically correct any amount of zonal aberration in the lens. The method used to compute the necessary coefficients is usually quite straight forward; briefly, it is as follows:

(1) Add a fourth order deformation term to reduce the third order aberration to zero. See Equation 8-(4a).

(2) Make an arbitrary guess at a sixth order coefficient (f). See Section 5.5.2.

(3) Trace through a ray at a finite aperture and determine how much of a deflection ΔY_k this aspheric term causes.

(4) It may then be assumed that this deflection

$$\Delta Y_k = \lambda \left[6fS^5 + 8gS^7 + 10hS^9 + \ldots\ldots \right] .$$

(5) It is then possible to write a set of equations to bring as many rays to the axis as there are aspheric constants. It is possible to write as many equations as rays traced through the system, but if there are more equations than terms in the aspheric, one has to resort to a method of least squares rather than expect an exact solution.

(6) Since the equation in step 4 is not exact, it may be necessary to repeat the process a few times.

This method is usually satisfactory, but if either the aperture of the lens or the zonal aberration is large, it may not be possible to fit a power series deformation which will reduce the aberration for all rays. This is because not enough terms are used in the expansion. In practice if one cannot fit a curve with a 10th degree polynomial then it helps very little to add a few more terms in the series; it takes a large number of terms to reduce the aberration for many rays. Sometimes it becomes necessary to abandon the use of the polynomial expression. The aspheric must then be expressed as a series of Y and Z coordinates. This is computed by actually calculating the optical path along the ray, and adding glass thickness to produce a spherical wavefront. This procedure is almost never necessary, but if it is, then one seriously questions whether it would be possible to make an aspheric of this type.

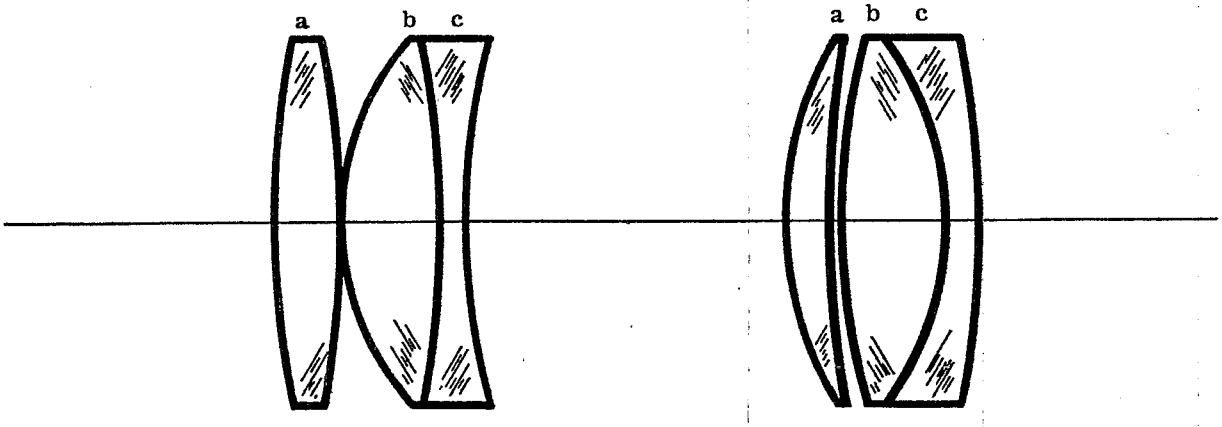

Solution No 1 Solution No 2

Figure 11.7 - Two types of triplet solution.

11.3.4.5 The zonal spherical aberration can be reduced by splitting off some of the power in the positive lens in the doublet. This would make a triplet similar to the types illustrated in Figure 11.7. By so doing, two extra degrees of freedom are created, namely the power ϕ of the extra positive lens, and its first curvature, c_1. One degree of freedom will be eliminated by cementing the last two elements. The problem then becomes, what is ϕ_a ? In other words, how should ϕ_a and ϕ_b be distributed? The manner one uses to find an answer to this problem is typical of one of the techniques used by a lens designer. The reasoning goes as follows:

(1) If the lens is assumed to be thin, the power $\phi_a + \phi_b$ will equal the same power as for the positive lens in a doublet. Therefore one may start by using the powers for the lenses as given in Table 11.3.

(2) By cementing the b and c lenses, there are only two degrees of freedom left. The first curvatures, c_1 and c_3, are the variables. If ϕ_a is decided upon, then the thin lens formulae, described in Section 8.9, enable one to compute the coefficients of the equations

$$B_a = \alpha_{1a} + \alpha_{2a} c_1 + \alpha_{3a} c_1^2 ,$$

$$B_{b+c} = \alpha_{1(b+c)} + \alpha_{2(b+c)} c_3 + \alpha_{3(b+c)} c_3^2 ,$$

$$F_a = \beta_{1a} + \beta_{2a} c_1 ,$$

$$F_b = \beta_{1b} + \beta_{2b} c_3 .$$

In exactly the same way as for the doublet, two types of solutions may be found. They are illustrated in Figure 11.7.

(3) Next plot B_c for these two solutions on a plot as shown in Figure 11.8. B_c is the total spherical aberration due to the negative lens. By finding the two solutions for several values of ϕ_a it is possible to plot the curves shown in Figure 11.8. These curves show that if $\phi_a = 0$ we then have a simple doublet and the two solutions require different amounts of positive spherical aberration. For the doublet, of course, the (b) and (c) lenses must be considered to be separated. As more and more power is put into lens (a), less and less positive B is required of lens (c). Now we know that the higher order aberrations will be minimized when the lens is corrected with B_c having a minimum positive value because the higher order spherical aberration has the same sign as the third order. From this reasoning one would predict that the type 1 solution with a value of $\phi_a = 0.066$ would provide an optimum solution. Solution 1, shown in Figure 11.7, is a lens of this type. The type 2 lens was also chosen with a value of $\phi_a = 0.066$.* Table 11.10 shows the results of ray tracing these solutions after adjustments were made to the residual third order aberration so that the marginal ray comes to focus at $Y_k = 0$. Table 11.11 contains the data for these two solutions.

(4) It is interesting to see that the type 1 lens is remarkably well corrected. The zonal aberration is 10 times less than the type 2. The type 2 lens may be thought of as a derivative of a separated doublet of the left hand branch. With the choice of glass used, the doublet would be an air spaced lens. By cementing it, it would be under-corrected for spherical aberration. Now by splitting off a small part of the positive lens and by bending slightly the lens can be re-corrected for spherical aberration, thus leading to the lens type 2. The type 1 lens is actually a derivative from the right hand branch of the doublet. Note that the better solution comes from the poorer doublet type. This is mentioned because, in designing this type lens, if one started by trying to modify a left hand doublet lens he might easily converge on a type 2 solution and find no advantage in using the split positive lens. Notice that the zonal aberration in the type 2 lens is

* It is true that the type 2 solution would probably be better at $\phi_a = 0.082$ or at $\phi_a = 0.138$, but the value of $\phi_a = 0.066$ was selected to illustrate that for a given value of ϕ_a there are two solutions quite close together.

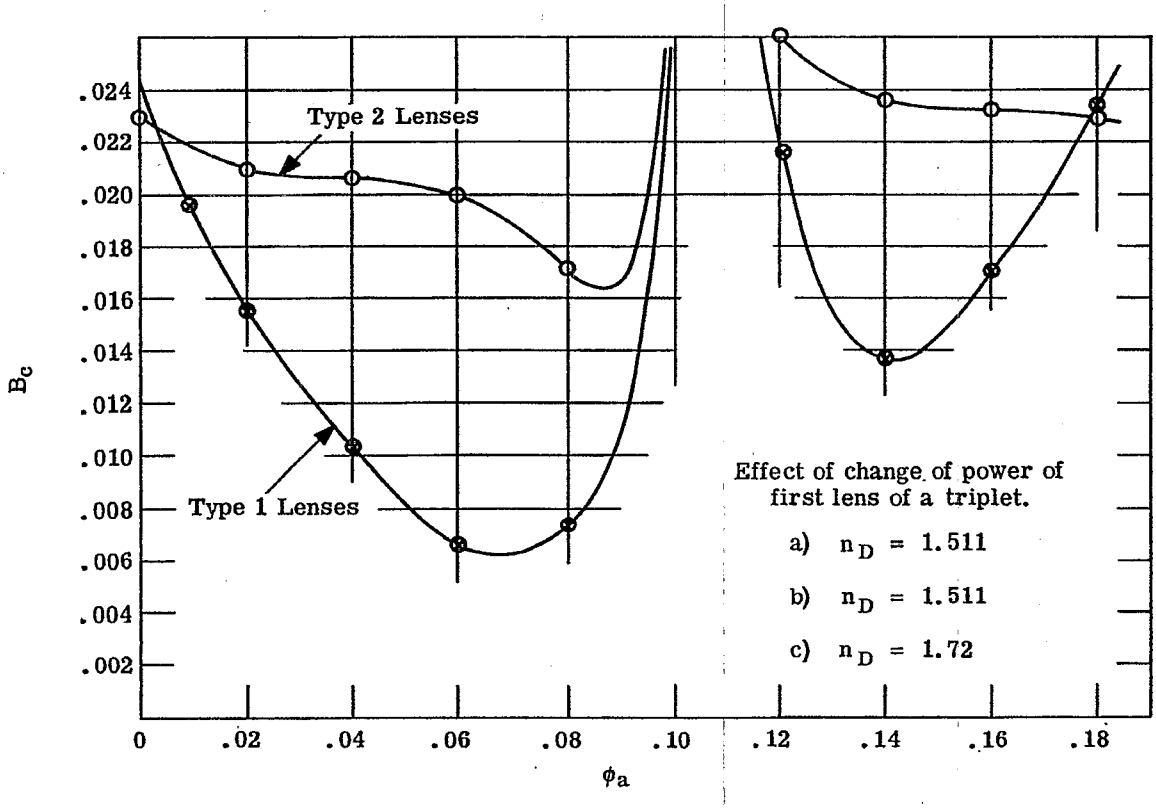

Figure 11.8 - A plot of B_c the total spherical aberration of the negative lens as a function of ϕ_a .

Y_1	TYPE 1 Y_k	TYPE 2 Y_k
1.4	0.000210	-0.000101
1.2	0.000070	-0.000706
1.0	0.000010	-0.000696
0.8	-0.000007	-0.0004681

Table 11.10 - Ray trace data in D light showing a comparison between type 1 and type 2 solutions in triplet telescope objectives

Type 1				Type 2	
c	t	n_D	ν	c	t
0.07121	0	1.511	63.5	0.1641	0
-0.05525	0			0.0349	0
0.20132	0	1.511	63.5	0.0472	0
-0.03572	0	1.72	29.3	-0.1871	0
0.08337				-0.0680	
		$f' = 10$			

Table 11.11 - Lens data on type 1 and type 2 lenses

almost identical with the doublets shown in Table 11.6. If we had happened to choose a glass combination which would have resulted in a cemented doublet, then a type 2 solution would offer no advantage. One would have to go to type 1. The curves shown in Figure 11.8 change as the glass is varied. In Figure 11.9 the type 1 branch is shown for another pair of glasses. One can see that it is quite different, for most of the positive power should be placed in the (a) lens.

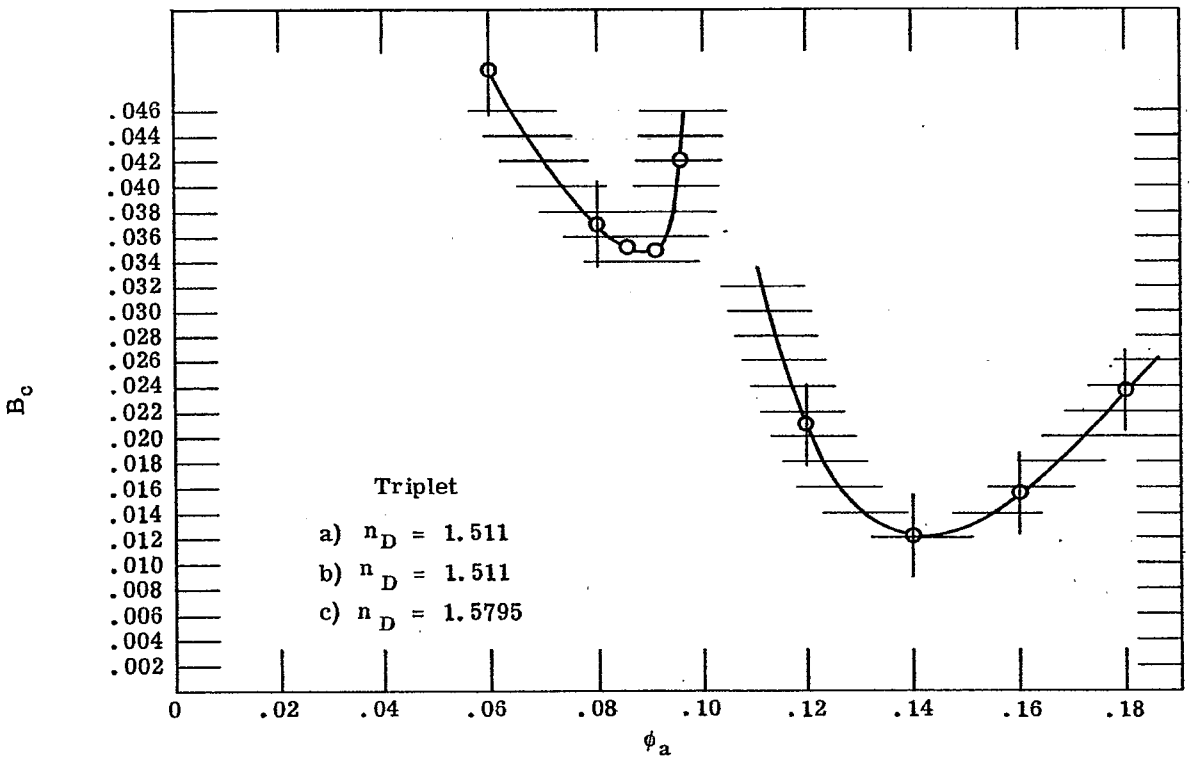

Figure 11.9 - A plot of B_c as a function of ϕ_a for a triplet.

11.3.5 Discussion of zonal correction methods.

11.3.5.1 This study illustrates that there are many possible solutions, and the designer must investigate them all in order to be sure he has exhausted the possibilities. This study also illustrates that there are regions where no solutions exist even though there appear to be a sufficient number of degrees of freedom.

11.3.5.2 If possible, a doublet design should be used. However if the zonal spherical aberration exceeds the tolerance, there are the four methods for reducing the zonal aberration described in the above section. Of these methods the fourth method of adding the extra element is strongly recommended, for this method does not involve the balance of large aberrations. The other three methods depend upon the balancing of large aberrations. The extra element method provides a solution with no large surface contributions. One will find in practice that it also will provide a lens much easier to manufacture, for it will be much less sensitive to decentering or spacing errors.

11.3.6 Coma correction. So far practically nothing has been said about coma correction. All the doublet solutions were corrected to have the third order coma exactly zero. This provides optimum correction for most of the designs. However, if the zonal spherical aberration is corrected by a large air space, one will encounter high order coma aberration, and it may be necessary to introduce residual coma in the third order. This however is very unsatisfactory, so everything possible should be done to find a solution with minimized high order coma. For this reason also, the split doublet lens offers a far better way to reduce the zonal aberrations than does the unsplit doublet, as the former has excellent coma correction.

11.4 SECONDARY SPECTRUM OF TELESCOPE OBJECTIVES

11.4.1 The difference in focus for F, C, and D light.

11.4.1.1 In the preceding paragraphs, it was shown (11.3.4.3) how the zonal spherical aberration could be reduced by a large factor. However, the aberration curves of Figures 11.4 through 11.6 clearly show that since the lens must be designed to image F and C light, as well as D light, the high degree of zonal correction in D light is of small practical significance. The F and C light focus does not coincide with the D focus. This defect in focus for F, C, and D light is a paraxial ray defect and was briefly discussed in Section 6.10.8, where the transverse aberration, $TAch_{F-D}$, was defined as the secondary spectrum.

11.4.1.2 It was also stated (6.10.8.4) that the three principal methods for reduction of this aberration are:

(1) Use special materials with equal partial dispersions.

(2) Use more than two types of glass.

(3) Use proper combination of lenses.

Paragraphs 11.4.2 and 11.4.3 will describe methods (1) and (2) respectively.

11.4.2 Reduction of secondary spectrum in a doublet. ($\tilde{P}_a - \tilde{P}_b = 0$ Method).

11.4.2.1 Equation 6-(49) tells us that when the partial dispersion ratios of both lenses of a doublet are equal for F and D light, then $\tilde{P}_a - \tilde{P}_b = 0$ and the F, C, and D light will unite in a common focus. Now, depending on the shapes of the dispersion curves of the glasses used in the doublet, there is still the question of where other wavelengths will focus.

11.4.2.2 Equation 6-(49) can also be used to calculate the $TAch_{\lambda-D}$ for any other wavelength. If the partial dispersion ratios for other wavelengths are not equal, i.e., $\tilde{P}_a - \tilde{P}_b \neq 0$, then there is still residual chromatic aberration. In choosing glass types, then, a designer must consider the following compromises:

(1) Should he settle for a small $(\nu_a - \nu_b)$ by setting $(\tilde{P}_a - \tilde{P}_b)$ exactly equal to zero, or should a larger $(\nu_a - \nu_b)$ be chosen and some secondary color be allowed? The decision, of course, will depend on the focal length and the numerical aperture required of the objective.

(2) Does the need for correction for a large range of wavelengths require that $(\tilde{P}_a - \tilde{P}_b)$ be set at a value other than zero?

11.4.2.3 It is clear that these considerations, combined with the task of correcting the spherical aberration, and the variation of spherical aberration with wavelength, pose a formidable array of problems.

11.4.2.4 The designer's difficulties are further increased by the need for extremely accurate measurements of the index of refraction. One can, by differentiating Equation 6-(49), determine that the following relation holds for an achromatic doublet.

$$dn_\lambda = \frac{d\left(TAch_{\lambda-D}\right)}{TAch_{\lambda-D}} \left(\frac{n_D - 1}{2200}\right) \qquad (13)$$

Therefore, if it is desired that the secondary spectrum of a doublet be held to 1/10 of its normal value, then it should be sufficient to know the index of refraction at each wavelength with an accuracy of 2 in the fifth decimal place. With an index error of this magnitude in each of the wavelengths used to calculate $\tilde{P}$, and ν, it is possible for the errors to combine so as to cause a doubling of the total error. Thus, it is necessary that the index be accurate to at least half of this value, or 1.0 in the fifth decimal place.

11.4.2.5 It is not only difficult to make measurements of the index of refraction with this accuracy; it is even more difficult to manufacture glass to specification with this degree of precision. The reputable optical glass manufacturers claim the required accuracy of their measurements but do not claim to be able to furnish samples to catalog values with this exactness. If, in the manufacture of precision lenses, it is necessary to have glass whose index of refraction is accurate to this degree, then it is necessary to have measurements of index made on a sample of the actual glass to be used in the lens.

11.4.3 Correction of secondary spectrum in a triplet lens. (Multiple glass-type method).

11.4.3.1 By using three glass types in the telescope objective it is possible in principle to bring at least three wavelengths to a common focus. If it is assumed the lenses are all thin and closely spaced then it is possible to write the following equations.

$$\phi_a + \phi_b + \phi_c = \phi \qquad \text{(Focal length)} \qquad (14)$$

$$\frac{\phi_a}{\nu_a} + \frac{\phi_b}{\nu_b} + \frac{\phi_c}{\nu_c} = 0 \qquad \text{(F and C light brought to same axial focus)} \qquad (15)$$

$$\frac{\phi_a P^*_a}{\nu_a} + \frac{\phi_b P^*_b}{\nu_b} + \frac{\phi_c P^*_c}{\nu_c} = 0 \qquad \text{(D light brought to the F-C axial focus)} \qquad (16)$$

11.4.3.2 By defining $\tilde{P}^* = \dfrac{n_F - n_D}{n_F - n_C}$, the third equation must be fulfilled if D light is to be focused at the F and C focus. The above equations may be solved to give the following values of ϕ_a, ϕ_b, and ϕ_c.

$$\phi_a = \phi \frac{\nu_a \left[\tilde{P}^*_c - \tilde{P}^*_b\right]}{\Delta}, \qquad (17)$$

$$\phi_b = \phi \frac{\nu_b \left[\tilde{P}^*_a - \tilde{P}^*_c\right]}{\Delta}, \qquad (18)$$

$$\phi_c = \phi \frac{\nu_c \left[\tilde{P}^*_b - \tilde{P}^*_a\right]}{\Delta}, \qquad (19)$$

where

$$\Delta = \begin{vmatrix} \tilde{P}^*_a & \nu_a & 1 \\ \tilde{P}^*_b & \nu_b & 1 \\ \tilde{P}^*_c & \nu_c & 1 \end{vmatrix}. \qquad (20)$$

One can recognize that Δ is a determinant, the value of which is the area of a triangle connecting points plotted with $\tilde{P}^*$ as the ordinate and ν as the abscissa.

11.4.3.3 Figure 11.10 is such a plot for several glasses. From the above equations one can see that points for three glasses must be found so as to form a triangle of finite area on the $\tilde{P}^*$ versus ν plot. It is important to pick glasses that will have the smallest possible values of ϕ_a, ϕ_b, and ϕ_c. If three glasses are picked, as shown in Figure 11.10 marked as a, b, c, then the (b) lens becomes negative, for $(\tilde{P}^*_a - \tilde{P}^*_c)$ is negative and Δ is positive. In order to minimize ϕ_b, the ratio of $(\tilde{P}^*_a - \tilde{P}^*_c)/\Delta$ must be made a minimum. If one draws a line from a to b it is clear that any glasses located on this line will have the same ratio of $(\tilde{P}^*_a - \tilde{P}^*_c)/\Delta$. If $\tilde{P}^*_a - \tilde{P}^*_c$ is made smaller, the area Δ of the triangle is made smaller by the same ratio. This can be seen to be true by remembering that ac is the base of the triangle and a perpendicular from b to this base line is the altitude of the triangle. Therefore,

$$\frac{(\tilde{P}^*_a - \tilde{P}^*_c)}{\cos\theta} \, h = \Delta,$$

and

$$\left[\frac{\tilde{P}^*_a - \tilde{P}^*_c}{\Delta}\right] = \frac{\cos\theta}{h}.$$

$\cos\theta$ is the angle between the line connecting a and c and the vertical axis. As long as $\cos\theta$ and h remain constant then $(\tilde{P}^*_a - \tilde{P}^*_c)/\Delta$ is constant. The procedure to pick glasses, then, is to try to find a triangle with as large an h as possible. It is also logical to suggest that the two positive lenses [the (a) and the (c) lenses] should have approximately the same power.

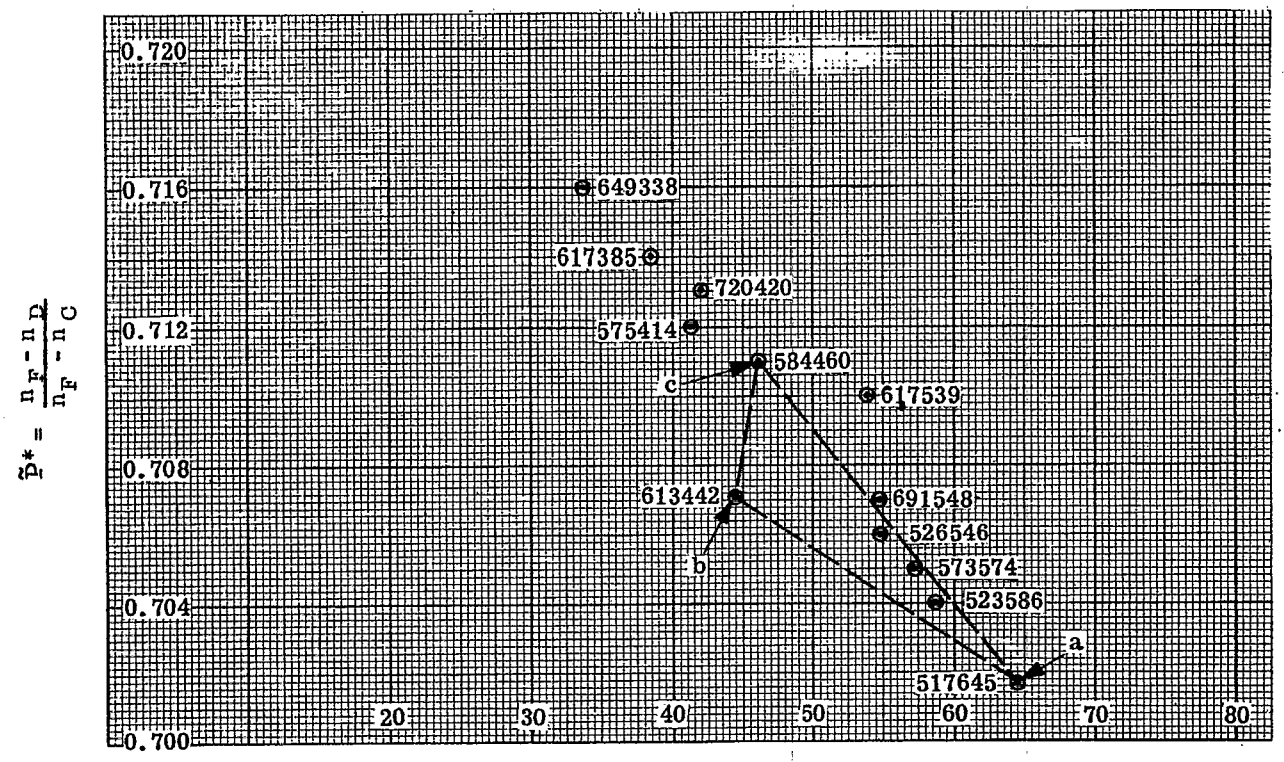

Figure 11.10 - A plot of $\tilde{P}^*$ vs ν for different glasses.

11.4.3.4 Dividing equation (17) and (19) provides the ratio ϕ_a / ϕ_c .

$$\frac{\phi_a}{\phi_c} = \frac{\nu_a}{\nu_c} \left(\frac{\tilde{P}^*_c - \tilde{P}^*_b}{\tilde{P}^*_b - \tilde{P}^*_a} \right)$$

Since ν_a / ν_c is greater than 1, it then follows that $(\tilde{P}^*_c - \tilde{P}^*_a)$ should be less than $(\tilde{P}^*_b - \tilde{P}^*_a)$. A glass combination selected with these considerations is shown in Figure 11.10. There are, however, other factors one must consider in selecting the glasses for the reduction of secondary color, namely, tertiary color as described below.

11.4.3.5* By satisfying the conditions in Equations (14), (15) and (16), the three wavelengths F, D, and C focus at a common axial point. One may now calculate the residual transverse aberration for any other wavelength λ , from the equation

$$\left(\frac{\phi \tilde{P}_{\lambda - D}}{\nu} \right)_a + \left(\frac{\phi \tilde{P}_{\lambda - D}}{\nu} \right)_b + \left(\frac{\phi \tilde{P}_{\lambda - D}}{\nu} \right)_c = \text{TAch}_{F-\lambda} \left(\frac{n_{k-1}\, u_{k-1}}{y^2} \right) \qquad (21)$$

$\tilde{P}_{\lambda - D}$ will be hereafter referred to as $\tilde{P}^{**}$. By inserting the expressions for (ϕ / ν) given in Equations (17), (18), (19), and (20), Equation (21) becomes

$$\frac{\tilde{P}^{**}_a (\tilde{P}^*_c - \tilde{P}^*_b) + \tilde{P}^{**}_b (\tilde{P}^*_a - \tilde{P}^*_c) + \tilde{P}^{**}_c (\tilde{P}^*_b - \tilde{P}^*_a)}{\Delta} = \text{TAch}_{F-\lambda} \frac{n_{k-1}\, u_{k-1}}{y^2\, \phi} \qquad (22)$$

* The notation P* and P** and the ideas suggested in this section have been described by Herzberger, Optica Acta, 6, 197 (1959).

The left hand side of the equations is equal to

$$\frac{\begin{vmatrix} \tilde{P}^*_a & \tilde{P}^{**}_a & 1 \\ \tilde{P}^*_b & \tilde{P}^{**}_b & 1 \\ \tilde{P}^*_c & \tilde{P}^{**}_c & 1 \end{vmatrix}}{\Delta}$$

The value of the determinant in the numerator is again the area of a triangle in a coordinate system with P* plotted as abscissa and P** plotted as ordinate. This tells us then, that if we wish to have small residual aberration for other wavelengths it is necessary to pick three glasses that lie on a straight line when plotted on the P* versus P** diagram. Plots of this type are shown in Figure 11.11. There are three sets of wavelength data plotted on this graph. The values of P** are $P_{A'-D}$, P_{e-D}, and P_{g-D}. The glasses used in a sample calculation are shown connected by dotted lines. These plots show that A', g and e light will have residual aberration because the three glasses do not lie on a straight line. As the data is plotted the triangles show that A' will have a positive TAch. The e light will be slightly negative, and g will be slightly positive. An actual curve for these three glasses is shown in Figure 11.12. It is plotted on the same coordinates as the data in Figure 6.20. The corresponding curve for a doublet is shown in the same figure. The powers of the lenses in the triplet are shown compared with a doublet in Table 11.12. The strong curves in the triplet indicate clearly the reason why lenses corrected for secondary color must have small relative apertures.

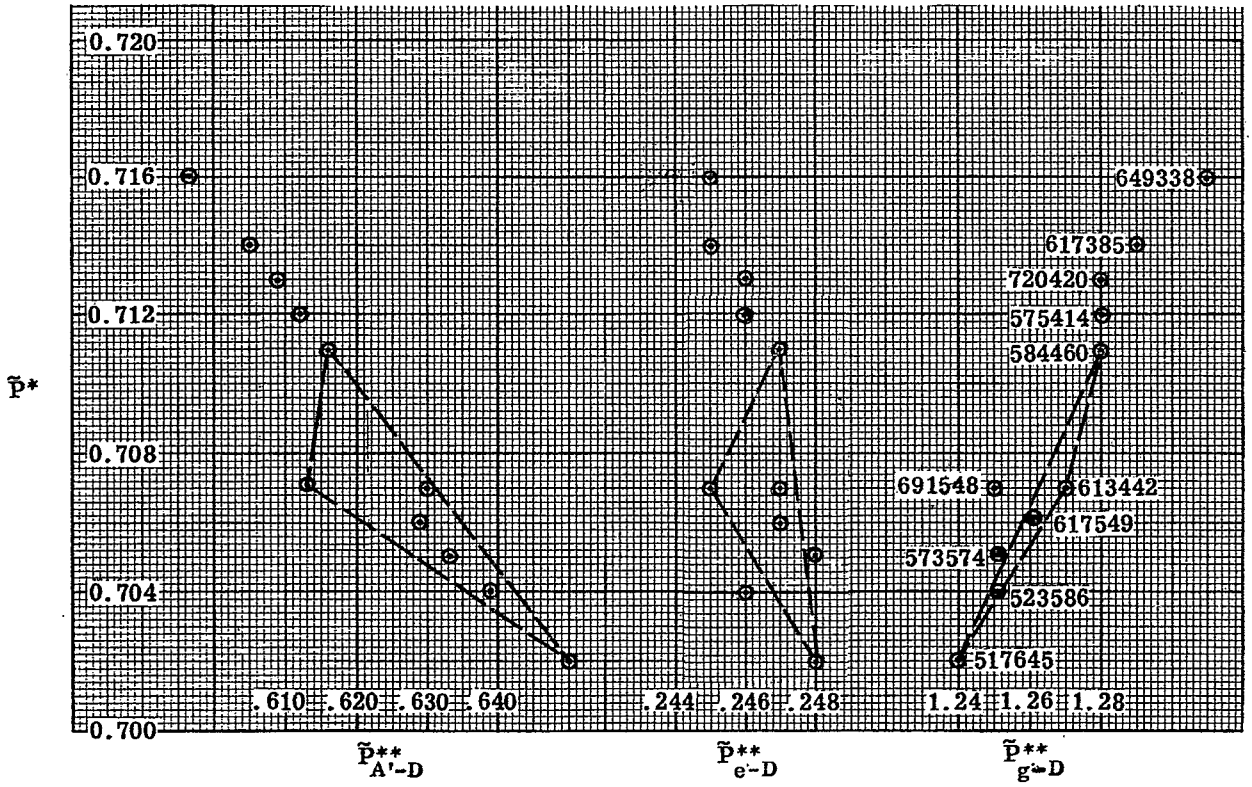

Figure 11.11 - A plot showing tertiary spectrum.

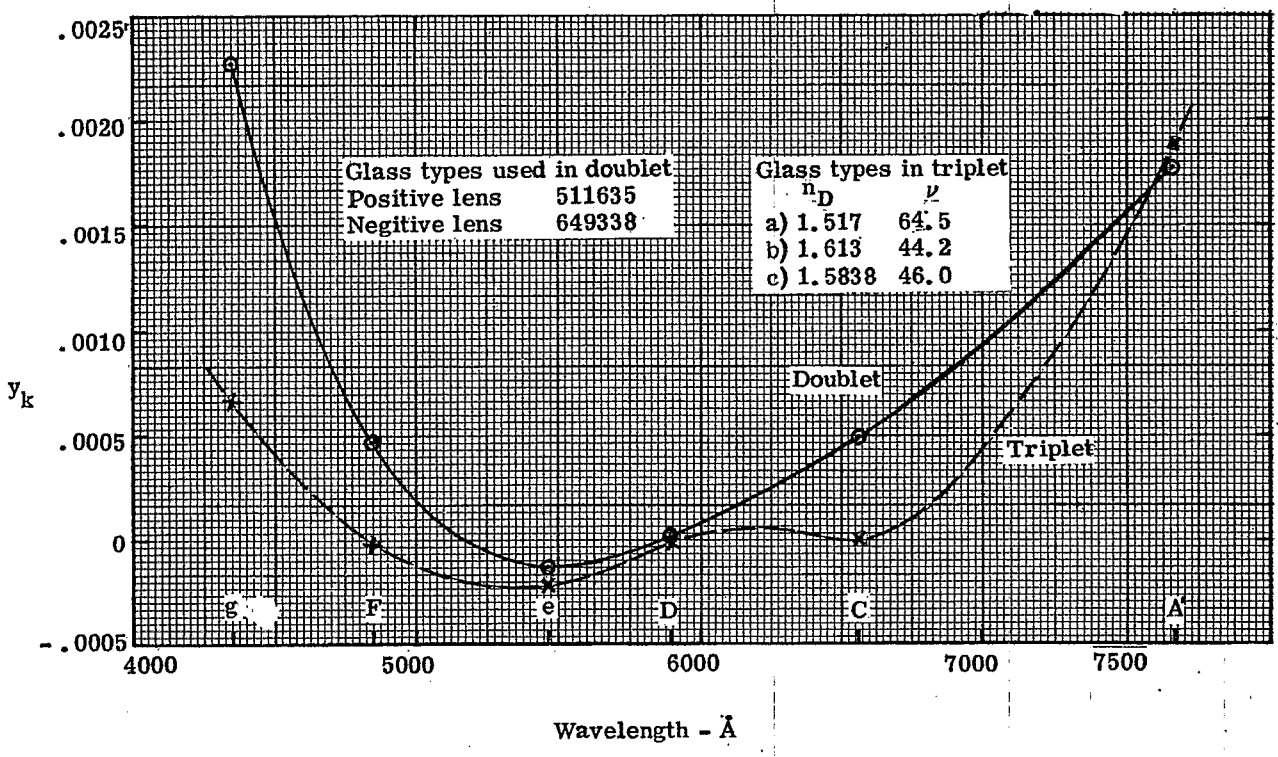

Figure 11.12 - Plot of y_k vs λ for a triplet corrected for secondary color.

Doublet	Triplet
$\phi_a = 0.21380$ $\phi_b = -0.1138$ $\phi = 0.1$	$\phi_a = 0.2812$ $\phi_b = -0.4747$ $\phi_c = 0.2935$ $\phi = 0.1$

Table 11.12- Comparison between powers in a triplet corrected for secondary color and an ordinary doublet.

11.4.4 Additional readings on secondary color. For further reading on secondary color, refer to the following articles:

(a) Three color achromats, R. E. Stephens, J. Opt. Soc. Am. 49, 398 (1959)

(b) Four-color achromats and superchromats, R. E. Stephens, J. Opt. Soc. Am. 50, 1016 (1960)

11.4.5 Sample design of a triplet corrected for secondary color.

11.4.5.1 A sample lens has been fully corrected for secondary color and ray traced. The glasses used in the design were all Schott glasses. The thin lens solution was given by R. E. Stephens in the second of the above papers. The thin lens glasses and powers were given as follows:

Glass	Power
F-1	0.338
KzFS-4	-0.721
PKS-1	0.483

These powers add up to 0.1. The focal length is therefore 10. The lens was corrected for an f-number of 12. The final lens specifications are shown in Table 11.13.

LENS SPECIFICATIONS

c	t	Glass
0.1989	0.1683	F-1
-0.0791	0.0175	Air
-0.1502	0.1400	KzFS-4
0.6180	0.0100	Air
0.6387	0.2964	PKS-1
-0.1272	9.2728	Air

RAY TRACE DATA

Y_1	$(Y_k)_D$	$(Y_k)_F$	$(Y_k)_C$
0.25	0.00000369	0.000092	0.000023
0.375	-0.000155	0.000074	-0.000164
0.500	-0.001056	-0.000574	-0.001137

Table 11.13 - Three lens system corrected for secondary color.

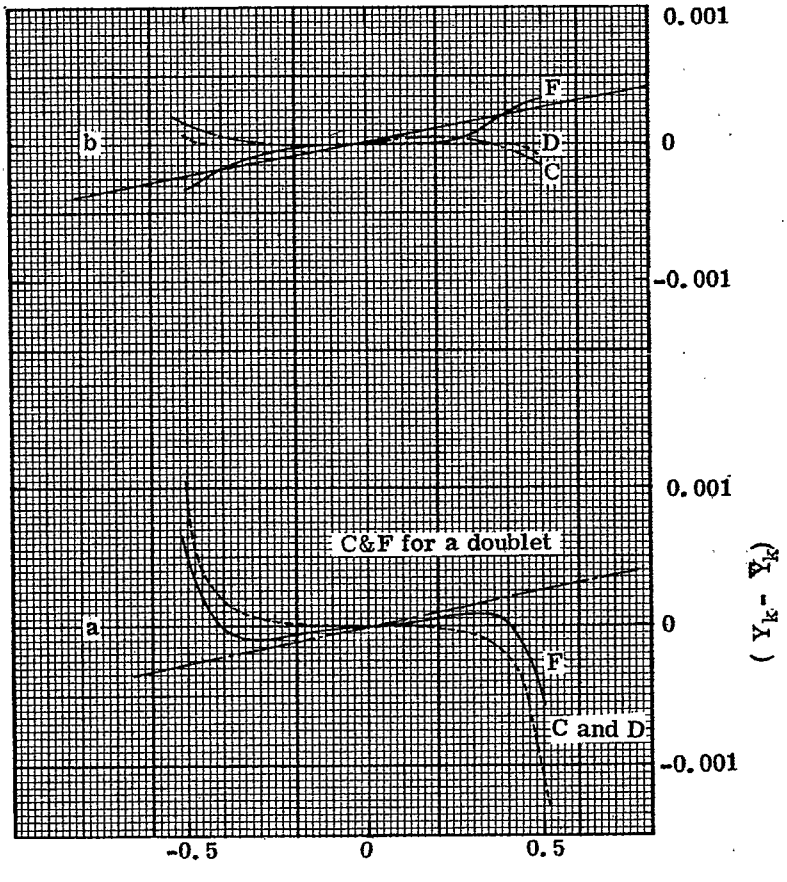

Figure 11.13 - Meridional ray plot at 0°, for triplet.

The meridional ray plot for this lens is shown in Figure 11.13a. It is plotted on the same scale as the doublet shown in Figure 11.3. These data show that the triplet corrected for secondary color has to be made to a much larger f-number than the doublet. One can see that the curves are stronger than the doublet, and the higher order spherical aberration is large. The straight dashed line in Figure 11.13a shows the best possible aberration curves for F and C light in a simple doublet. The curves for the triplet out to a value of $Y_1 = 0.4$ show that some advantage is gained by using the triplet. Beyond $Y_1 = 0.4$ there is no gain at all, for the high order spherical aberration is so heavily under-corrected. If the lens had been stopped down to a value of $Y_1 = 0.3$ it could have been corrected with a smaller residual aberration. The lens would then be corrected with approximately one third the aberration in a simple doublet. This would give an f-number of 16.7.

11.4.5.2 Other solutions. The triplet described in Table 11.13 is not a completely optimized solution. The higher order aberrations might have been further reduced by adjusting the air spaces. One must also consider other orientations of the lenses. To illustrate this effect a solution was corrected with the PKS-1 as the first element, and F-1 as the final element. This solution is shown in Table 11.14. This shows some improvement over the first solution shown. This lens could probably be used at $f/11$. This lens is better corrected than the one with F-1 in front. It is not, however, certain that this is a characteristic of the lens. The second system was designed much more carefully than the first one. Many, many solutions were found for the second design. The solutions were found automatically for varying amounts of primary and secondary color, and finally, the zonal spherical aberration was reduced by adjusting the air space between the second and third lens. The second solution is, we believe, nearly as good a solution as it is possible to design with this combination of glass; but we are not sure, for there are many things that should be studied. For example, the axial color should probably be made slightly more negative. This would lower the F light curve slightly and raise the C light curve. The two curves would therefore cross further out in the aperture.

LENS SPECIFICATIONS

c	t	Glass
0.5334	0.3180	PKS-1
-0.3322	0.0100	Air
-0.2792	0.1400	KzFS-4
0.7079	0.1000	Air
0.5469	0.1969	F-1
-0.1723	9.018	Air

RAY TRACE DATA

Y_1	$(Y_k)_D$	$(Y_k)_F$	$(Y_k)_C$
0.25	0.0000021	0.0000127	0.0000517
0.375	0.0000028	0.0001495	0.0000265
0.500	-0.000085	0.0003700	-0.0001531

Table 11.14- Three lens system corrected for secondary color.

The meridional ray plot is shown in Figure 11.13b.

11.4.5.3 The amount of computing that went into the above designs is beyond the comprehension of anyone not familiar with the problem. We found 16 automatic third order solutions. Usually it took a minimum of four iterations. For each solution a fifth order and 9 rays were traced. Only one out of five possible thicknesses was used as a variable. Before one could say he really had an optimum solution it would be necessary to check the effectiveness of varying the thickness, trying the negative lens out front and use other glasses. Thanks to the modern computer it is beginning to become practical to do this at a reasonable cost. When we realize how limited our present approaches are to the problem, we can look forward to promising solutions in the future.

11.4.6 Evaluation of lens from optical path. The gain in image quality is however, misleading. This is an example of why one must always remember to consider the physical optics of the problem. Figure 11.13 shows that if the perfect doublet is stopped down to $f/16.7$ the C and F light would have a transverse aberration of 0.00015, with respect to the D light focus. If we assume the focal length is 10 cm then this corresponds to a transverse aberration of 0.00015 cm. There is a relation between the transverse aberration and optical path difference for shift of focus. The equation is

$$OPD = Y_k \cdot \frac{Y_1}{2f'}$$

where Y_k is the transverse aberration for the ray entering the lens at Y_1. Inserting the above aberration into this equation shows that the OPD in the simple doublet is 0.038 wavelengths. Now if the Rayleigh tolerance of $\lambda/4$ is assumed, this means an $f/16.7$ doublet with a focal length of 10 cm has so little secondary spectrum it will never be noticed. Its focal length could be scaled up 0.25/0.038 times the 10 cm focal length. This amounts to a focal length of 65.8 cm. Therefore, there is no point whatsoever in designing a lens to reduce the secondary spectrum, when the focal length is less than 65.8 cm , if it has to be stopped down to $f/16.7$. The above triplet therefore would not show any advantage until scaled to focal lengths longer than 65.8 cm. To realize a two to one gain over a doublet, it will have to be scaled to 131.6 cm focal length. At $f/16.7$ this would be a lens 7.9 cm in diameter. This is getting to be a fairly expensive size lens in which to use the unusual glass KzFS-4.

11.5 SUMMARY

One can now see the relation between a doublet and a triplet corrected for secondary color. One can design a doublet with two types of glasses and split the positive lens into two and make the system a triplet. Then it is necessary to find two glasses with the same values of P* and P**. Since there are only very few glasses removed from the $\tilde{P}$ versus ν line this means that relatively few glasses are available for the positive lens. By using a third glass type it is possible to use a much larger selection of glasses. In order to find an optimum solution it is necessary to study many combinations of glass. One must completely correct the lens and ray trace the solution before deciding what glass choices are most suitable. There will be variation of spherical aberration with wavelength. This aberration may become so large that all the advantage of using the special glasses to correct the first order effects may be completely lost.

12 LENS RELAY SYSTEMS

12.1 INTRODUCTION

12.1.1 Lens relay systems of the type mentioned in Section 7 (Paragraph 7.5 and Figures 7.5 and 7.6) are described in more detail here.

12.1.2 Relay systems are used for two purposes: to provide the proper orientation of the image, and to transfer the light from one region to another. Sometimes the distance between the object and the final image may be large and, in addition, the diameter of the lenses must not become excessive. These conditions may require a series of relay lenses resulting in a system called a periscope.

12.2 THE BASIC LENS PROBLEM OF A RELAY SYSTEM

12.2.1 Suppose a relay system is needed to transfer light from an object plane to an image plane. The two planes are separated by the distance D, Figure 12.1. The magnification should be -1.

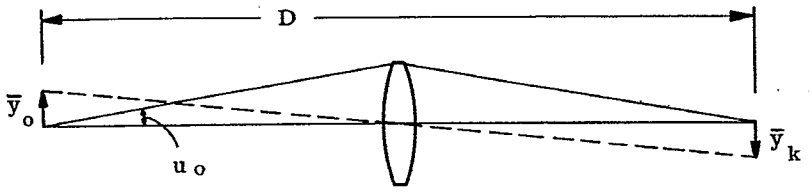

Figure 12.1 - A single-relay-system.

12.2.2 The diameter of the objective will be determined by the angle u_o. The type of lens to use for the objective depends upon the image quality required. For the moment, however, assume that the relay lens will consist of two telescope objectives of the type described in Section 11. The objectives could be placed so that the light would be parallel between them. One could start with any of the lenses shown in Tables 11.3, 11.5, 11.6 or 11.7.

12.3 A VISUAL SYSTEM, NUMERICAL EXAMPLE

12.3.1 To evaluate the visual performance with telescope objectives, first suppose that the system is a visual system, with a 10X eyepiece (see Section 14) used to view the image.

12.3.2 In Section 11.1.3 the effect of the Petzval curvature was described. Equation 8-(28) gives the value of P for a thin lens as $-\phi/n$. The value of P for the relay lens shown in Figure 12.1 would then be $-\frac{4}{Dn_e}$, where n_e is the effective index of the doublets used for the relay lens. The 10X eyepiece could be any of those described in Section 14. For this example, the very common Erfle eyepiece shown in Figure 14.19 will be used. According to Table 14.7, the lens will have a value of P = -0.2125 in reciprocal cm.

12.3.3 From the data shown in Section 11 on doublets, it is evident that the doublets could be used at $f/3.5$. If they could be 10 cm in diameter, each doublet could have a focal length of 35 cm, and the distance D would be approximately 70 cm. The value of P for the relay lens would then be -0.038.

12.3.4 This is only 18% of the Petzval contribution introduced by the eyepiece. It is, therefore, probably negligible as long as the field of view is maintained within the field of the eyepiece. The data in Figure 14.21 show that this eyepiece can cover about 28^o half field with a negative distortion of approximately 8%. The maximum image height is therefore 1.32 cm. This means that the maximum object height will be 1.32 cm.

12.3.5 The use of other types of lenses for relay objectives is considered here. If two triplet objectives of the type designed in Section 10 were used, the value of n_e in the equation $P = -\phi/n_e$ could be raised to about 3.0 or 4.0. With a value of $n_e = 4.0$, the P value of the relay lens would be -0.014. This would be completely negligible compared to the value introduced by the eyepiece. On the other hand, the triplet would not be as well corrected on the axis as the doublets. It is usually not a good idea to attempt to correct the Petzval curvature of the relay lenses until they start to introduce a contribution which is one half, or at most equal to, that of the eyepiece.

12.4 SECONDARY COLOR IN A RELAY SYSTEM

12.4.1 In paragraph 6.10.8.3 it was indicated that telescope lenses made out of ordinary glass have an amount of secondary color given by the expression

$$TAch_{F-D} = \frac{y_1}{2200} .$$

12.4.2 The relay lens in the sample problem in Figure 12.1 would have secondary color given by the equation

$$TAch_{F-D} = \frac{2y_1}{2200} = \frac{u_o D}{2200} . \qquad (1)$$

12.4.3 Equation (1) shows that the secondary blur at the focal plane of the eyepiece increases as u_o or D is increased. In the sample problem, if $u_o = 0.14$ and $D = 70$ cm., the radius of the secondary blur $TAch_{F-D}$ is 0.005 cm. With the 10X eyepiece, this would subtend an angle of 0.002 radians. This is 6.6 minutes, which is definitely noticeable but usually tolerated. Any more than this is objectionable.

12.4.4 Secondary color is usually a serious problem in relay systems. If the distance D must be maintained, then the secondary color can most easily be reduced by making u_o smaller. A value of $u_o = 0.14$ means that the exit pupil diameter will be 7 mm. This is desirable for maximum light transmission, but it could be reduced to 2 mm without impairing the observer's resolution. This would then cut down the secondary color to 2.2 minutes.

12.4.5 The secondary color can be reduced by separating the two doublets. As long as there is parallel light between the two lenses, the space between the lenses can be considered free space. If this distance is d, the secondary color is given by the equation

$$TAch_{F-D} = \frac{u_o (D-d)}{2200} . \qquad (2)$$

12.4.6 As d is made larger, the focal lengths of the lenses are reduced. They therefore introduce more field curvature. It is a fairly general rule that any step taken to reduce secondary color without sacrificing clear aperture will result in more field curvature.

12.5 FURTHER DETAILS ON DESIGN OF DOUBLETS AS RELAY LENSES

For a unit power relay system, there are advantages in using two identical doublets with parallel light between them. Since the doublets are usually air-spaced, this means there are eight glass air surfaces. In principle it is possible to combine the positive elements of the doublets into a single lens surrounded by two negative lenses. One could also combine the two negative lenses and surround the combination with two positive elements. One can see what would be involved in doing this by considering the solutions shown in Table 11.3. In these solutions, the curvature facing the parallel light c_1 is about 0.16. In order to make the positive element in the combined doublets a single lens, it would be necessary to bend these solutions until $c_1 = 0$. Take, for example, Case No. 10 in Table 11.3. If the lens should be bent to make $c_1 = 0$, the remaining curvatures would be $c_2 = -0.4798$, $c_3 = -0.4694$, and $c_4 = -0.2341$. The doublet would no longer be corrected for spherical aberration or coma. The spherical aberration, at least to the third order, could be corrected by adjusting the curvature differences between c_2 and c_3. The coma would, however, be far from corrected. By facing this with an identical doublet, the two plane surfaces could be contacted. This means the positive lens could be made into a single equiconvex lens. The spherical aberration of the doublets would add, but the coma would subtract, to zero. This argument shows that a triplet relay lens is possible, but it also shows that it will probably

have considerably more higher order spherical aberration than the two doublets. The use of a triplet of this type could be recommended only when the zonal spherical aberration is tolerable.

12.6 DOUBLE-RELAY SYSTEMS

12.6.1 Often in relay systems one is limited in the diameter of lens which may be used as, for example, when the lens must be confined to a given diameter. In the single-relay example described in 12.3.3, the relay was allowed to have a diameter of 10 cm. Suppose there was a limitation to a 5-cm. diameter for all lenses. In order to maintain $u_o = 0.14$, it would be necessary to use a double-lens relay system as illustrated in Figure 12.2.

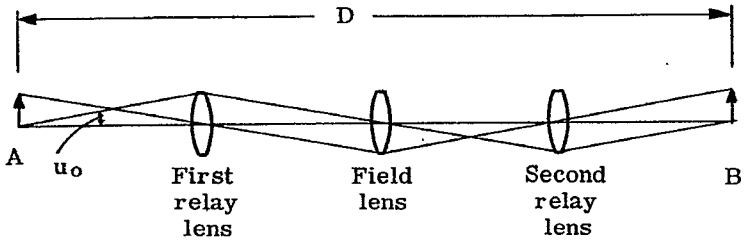

Figure 12.2 - A double-relay system.

12.6.2 In the double-relay lens system, the first and second relay lenses must have just one-half the focal length of the single-relay lens. They will, therefore, each add twice the Petzval contribution.

12.6.3 The two relay lenses will not introduce any more secondary color. Each relay transfers by the distance D/2, so that each has half the secondary color; but they add, so the total comes out the same. Equation (1) still applies for a double relay system.

12.6.4 Note that in Figure 12.2 an extra lens has been added in the intermediate focal plane. This is called a field lens. Its function is to image the chief ray passing through the center of the first relay lens at the center of the second relay lens. This field lens has a focal length equal to D/8. It will also introduce negative field curvature equal to 8/Dn.

12.6.5 One can see then that doubling up the relay system in order to reduce the diameter of the lenses has introduced Petzval field curvature. The relay lenses introduce four times as much field curvature, and the field lens adds as much as one of the relays. The double-relay lens, therefore, introduces six times as much field curvature as the single-relay system of equal length and numerical aperture. The secondary color is not changed.

12.6.6 Reducing the field of view. One can argue that there is little to be gained in reducing the field of view. The eyepiece is designed for, and capable of, viewing an object height of 1.32 cm. It is true that the relay lenses are going to make the image at the end of the field more blurred, but to introduce a stop at the field lens would merely mean a slightly smaller field lens. The savings in cost would be negligible. If one decides to use doublet relay lenses, nothing is lost in using the full field of the eyepiece. It is better to see the wide field, even if it is blurred, than to stop it down. As a rule, the field of a visual instrument should not be reduced if the extra field can be obtained with no increase in cost and size of instrument.

12.6.7 Relay lenses corrected for field curvature. If the problem demands improved quality at the edge of the field, it is necessary to abandon the doublet relay lenses and use a lens with reduced field curvature. Triplets as described in Section 10 may be used if one does not try to increase n_e beyond 4. If this is not enough, a double Gauss lens is recommended.

12.6.8 Field lenses corrected for field curvature. It is possible to introduce compound field lenses, such as triplets, to reduce the Petzval curvature of the field lens. If the field lens is located between the two unit power relay systems, it must be symmetrical. It will have to perform for a finite conjugate, and the region of solution will be quite different from the lenses described in Section 10. One can think of the lens as basically two inverted telephoto objectives with parallel light between them. The lens can be roughed out by first designing one side. One should avoid placing a lens surface directly in the intermediate focal plane, for it will eventually collect dust.

12.7 SUMMARY

12.7.1 Relay systems are inherently limited by problems of field curvature and secondary color. One should always try to use as few relays as possible, until glass weight and cost become a problem.

12.7.2 If it is necessary to use more than one relay, the same rules apply. The relay and field lenses should be kept as large as practicable. The size of the relay or field lenses should never be reduced needlessly.

12.7.3 The secondary color depends on the over-all distance of relay and the value of u_o. If the secondary color becomes serious, it is necessary either to accept it, reduce u_o, or resort to special lens materials.

12.7.4 Whenever attempts are made to correct the field curvature, more secondary color is introduced. See Figure 6.21.

12.7.5 Doublet relay lenses are usually prefered to other more complicated types. They represent a good compromise between simplicity, cost, number of surfaces, and reasonable image quality. It is possible rapidly to reach a point of diminishing returns in trying to reduce field curvature: the result will be a design with increased secondary color and chromatic variation of aberrations.